Design of Filter Banks for Subband Coding Systems

Alexandros Alexandrou

Department of Electrical Engineering
McGill University
Montreal, Quebec

June 1985

A thesis submitted to the
Faculty of Graduate Studies and Research
in partial fulfillment of the requirements for
the degree of Masters of Electrical Engineering

Abstract

The performance of subband coders relies on the ability of analysis and reconstruction filter banks to provide good isolation between contiguous frequency bands of speech signals. In general, analysis/reconstruction filter banks introduce, to some degree, aliasing, amplitude distortion and phase distortion to the reconstructed signal. These impairments as well as the overall system delay and implementation complexity are the major issues in the design of filter banks for subband coding systems.

This study presents a detailed discussion of the different filter families that deal with the above issues. The discussion includes linear phase quadrature mirror (QMF) filters, IIR-QMF filters, Pseudo-QMF filters and nonlinear phase time-reversed QMF filters. Emphasis is given to nonlinear phase time-reversed QMF filters since they can be designed to remove all three types of distortion from the reconstructed signal. These filters are designed using the McClellan-Parks algorithm. Experimental results show that the amplitude distortion introduced by time-reversed QMF filters when implemented with finite precision arithmetic is negligible.

Sommaire

La performance des codeurs à sous-bandes de fréquence dépend de la qualité de la banque de filtres d'analyse et de reconstruction pour permettre une bonne isolation des bandes de fréquences adjacentes du signal de parole. En général, la banque de filtres d'analyse/reconstruction introduit, à un certain degré, un recouvrement de spectre, de même que des distortions d'amplitude et de phase, sur le signal reconstruit. Les trois types de distortion, en plus du délai global et de la complexité d'implantation du système, sont les problèmes majeurs à traiter dans la construction des banques de filtres pour les systèmes de codage à sous-bande.

Cette étude présente une discussion détaillée des différentes familles de filtres qui traitent les différents problèmes pré-cités. Cette discussion englobera les filtres miroirs à phase lineaire (QMF), les filtres IIR-QMF, les filtres Pseudo-QMF et les filtres QMF temporellement renversés à phase non-linéaire. L'emphase sera porté sur le dernier type de filtres puisqu'ils peuvent être construits de façon à éliminer les trois types de distortion. La construction de ces filtres est faite selon l'algorithme de McClellan-Parks. Les résultats expérimentaux montrent que pour les filtres QMF temporellement renversés on obtient un taux de distortion d'amplitude négligeable lorsque celui-ci est implementé avec une précision mathématique finie.

Acknowledgements

I wish to thank my advisor Dr. Peter Kabal for his technical guidance, encouragement and understanding as well as for his valuable suggestions in improving the presentation.

Table of Contents

Abstract i
Sommaire ii
Acknowledgments iii
Table of Contents iv
List of Figures vii
List of Tables ix

Chapter 1 Introduction 1

Chapter 2 Continuous—Discrete-Time Signals 8

2.1 Introduction 8
2.2 Sampling of Continuous-time Signals 9
2.3 Discrete-Time Signals–Sequences 11
2.3.1 Z-Transform 12
2.3.2 Sub-Sampling 13
2.3.3 Interpolation—Rate increase 14
2.4 Subband Analysis 15
2.4.1 Reversibility 16
2.4.2 Information Rate 17
2.4.3 Fractional-Band Filters 18

Chapter 3 Quadrature Mirror Filters (QMF) 22

3.1 Introduction 22
3.2 Half-Band Filters 23
3.3 Quadrature Mirror Filters (QMF) 24
3.4 Linear Phase QMF Filters 28
3.5 Design of Linear Phase QMF filters 30
3.5.1 Optimization criteria 31
3.5.2 Search Algorithm 33
3.5.3 New Design Technique for QMF filters 33
3.6 Implementation of a Two band QMF Subband System 34
3.7 Tree-Structured Subband Systems 37
3.8 Parallel QMF Filter Banks 41
3.9 Odd Length Linear Phase QMF Filters 46

Chapter 4 Recursive and Pseudo-QMF Filters 51

4.1 Introduction 51

4.2 IIR-QMF Filters 52

4.3 Pseudo-QMF Filter Banks 63

Chapter 5 Exact Reconstruction Filter Banks 71

5.1 Introduction 71

5.2 Time-Reversed Filters 73

5.3 Time-Reversed Filters in Subband Systems 74

5.4 Reversibility 76

5.5 Subband Filter Design 78

5.5.1 Decomposition of $F_0(z)$ 79

5.5.2 Transformation of filter characteristics 83

5.5.3 Constraints on the values of $f_0(n)$ 84

5.5.4 Design of $F_0(z)$—Windowing 87

5.5.5 Optimal (Minimax Error) Design of $F_0(z)$ 89

5.5.6 Extraction of the coefficients $h_0(n)$ 91

5.5.7 Reoptimization of the coefficients $h_0(n)$ 95

5.5.8 Extraction of the Coefficients $h_1(n)$, $g_0(n)$ and $g_1(n)$ 97

5.5.9 Summary of the Filter Design Procedure 97

5.6 Implementation of the Subband System 98

Chapter 6 Design Details for Exact Reconstruction Filter Banks 101

6.1 Introduction 101

6.2 McClellan-Parks Algorithm 102

6.3 Design of Antisymmetric Functions with McClellan-Parks Algorithm 108

6.4 Design of Antisymmetric Functions for Exact Reconstruction Systems with McClellan-Parks Algorithm 110

6.5 An Alternative Approach to the Design of Antisymmetric Functions 115

Chapter 7 Performance of Exact Reconstruction Filter Banks 120

7.1 Introduction 120

7.2 Equiripple Time-Reversed Filters 122

7.3 Non-Equiripple Time-Reversed Filters 124

7.4 The Effect of Weighting on Filter Designs 126
7.5 Performance of Time-Reversed QMF Filters in subband Systems 131

Chapter 8 Conclusions 132

Appendix A Filter Design Examples 135

References 169

List of Figures

1.1 Subband Coding System 2

2.1 Subband Analysis System 16

2.2 Sub-sampling in a subband analysis system 17

2.3 Subband analysis system with fractional filters 20

3.1 Two band subband system 23

3.2 Quadrature Mirror Filters 25

3.3 Optimization system-Block diagram 32

3.4 Efficient implementation of the analysis of a two band subband system with linear phase QMF filters. 35

3.5 Efficient implementation of the reconstruction of a two band subband system with linear phase QMF filters 37

3.6 Tree-structured four subband system 38

3.7 Tree-structured three band system 40

3.8 Multiband subband system 42

3.9 Equivalent sub-sampling/linear-filtering operations for the tree-structure/parallel-structure transformation 43

3.10 Subband system for odd length linear phase filters 48

3.11 Implementation of the analysis/reconstruction of a two band system with odd length filters 49

4.1 A typical zero-diagram for the response $P(z)$ 55

4.2 Zero-diagram for a typical system response $R(z)$ 56

4.3 Two band subband system with equalizers 59

4.4 Subband system with parallel filter banks 64

4.5 Frequency responses for the prototype and the bandpass filters of a typical pseudo-QMF filter bank 65

5.1 Zero-plot of a lowpass linear phase decomposable response 82

5.2 Frequency response of a lowpass decomposable response 83

5.3 Frequency response of an antisymmetric function 85

5.4 Frequency response of an offset antisymmetric function 86

5.5 Frequency characteristics of a decomposable response $F_0(z)$ obtained from a 63-tap rectangular response 88

5.6 Zero-plot for maximum/minimum phase filters 93

5.7 Implementation of the Analysis Filter Bank 98
5.8 Implementation of the Reconstruction Filter Bank 99
5.9 Subband system with unequal width subbands 99
6.1 Flowchart of the McClellan-Parks algorithm 106
6.2 Flowchart of the Remez exchange algorithm 108
6.3 Flowchart of the modified Remez exchange algorithm 113
6.4 32-tap equiripple filter designed by the modified Remez exchange algorithm 114
6.5 32-tap non-equiripple filter designed by the modified Remez exchange algorithm 114
6.6 32-tap filter designed by specifying the location of its maxima 118
7.1 Performance charts for equiripple time-reversed QMF filters 123
7.2 Performance charts for non-equiripple time-reversed QMF filters obtained by using Eq. (7.5) 125
7.3 Performance charts for non-equiripple time-reversed QMF filters obtained by using Eq. (7.7) 127
7.4 Performance charts of equal-length time-reversed QMF filters with different weightings 128
7.5 Performance charts of equal-width W_t time-reversed QMF filters with different weightings 130

List of Tables

4.1 Conditions on l and i for the terms in Eq. (4.36) that do not cancel 67

5.1 Zero-patterns of a typical linear phase response versus a decomposable response 81

Chapter 1 Introduction

Subband coding (SBC) is a frequency domain coding technique in which the input signal is decomposed into a number of subbands so that each of these frequency bands can be encoded separately. This technique was originally proposed by Crochiere, Webber and Flanagan [1] as a means to reduce the effect of quantizing noise due to coding and therefore to improve the quality of speech coding systems. Encoding in subbands offers several advantages that can be effectively used to achieve noise reduction. The main advantages of this approach are the following:

- The quantizing noise that is generated in a particular subband is limited to that band in the reconstruction, without being allowed to spread to other bands where there may be less signal energy.

- Bit resources can be allocated in such a way so that the number of quantizer levels and hence the reconstruction error variance can be separately controlled in each band. As a result, the shape of the quantizing noise spectrum can be controlled as a function of frequency. This property is very important especially when certain parts of the spectrum of the encoded signal appear to be more important than others, i.e. speech signals where the low-frequency bands must be preserved with more accuracy than high-frequency bands, given limited bit resources.

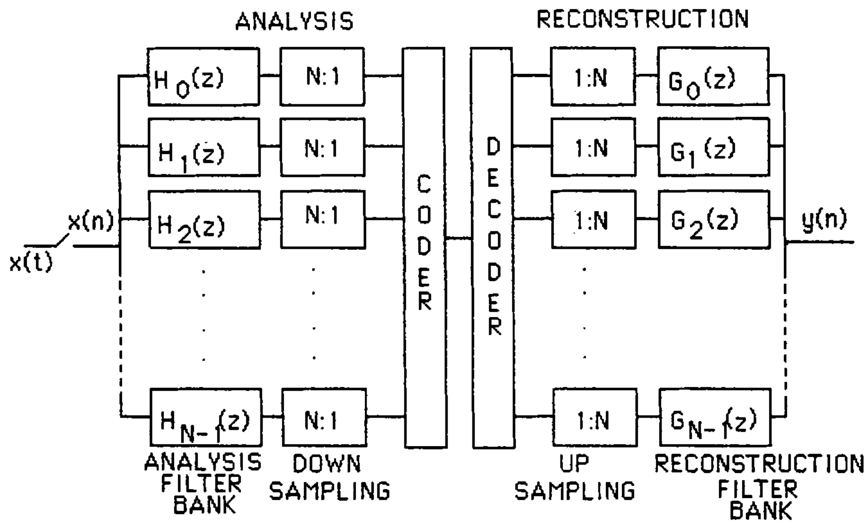

Fig. 1.1 Subband Coding System

In the subband coding system shown in Fig. 1.1, the input signal, after being sampled at its Nyquist rate, is divided into channels by first being passed through a bank of bandpass filters. The output of each filter is decimated to a rate determined by the bandwidth of the channel and then each of these channel outputs are encoded separately using adaptive pulse code modulation (APCM) or adaptive differential pulse code modulation (ADPCM) coders. At the receiver the signals, after being decoded, are interpolated back to the original sampling rate by a bank of interpolation filters and then are summed to reconstruct the input signal.

It is important that in subband coding systems the individual channel signals be decimated in such a way that the number of samples coded and transmitted does not exceed the number of samples in the original signal since this number is necessary and sufficient for the recovery of the original signal (Papoulis [2]). Under this constraint and in the absence of the channel coders, the overall system response indicates the quality of the system. Ideally, the filtering part of the system must be reversible [3], i.e. the overall system response must be a pure delay so that the input signal can be perfectly reconstructed at the receiver. However, in general reversibility can not be achieved and subband coding systems suffer from three different types of distortion, interband aliasing, amplitude distortion and phase distortion. Clearly the quality of the reconstructed signal can be no better than the quality of the system response. On top of that, the quality of the reconstructed signal degrades further, if coders are introduced to the channels.

Over the past several years, a number of subband coding systems have been introduced in an attempt to minimize or remove the three types of distortion mentioned above as well as to minimize the overall number of computations needed for the implementation of these systems. The original subband coding system which was presented by Crochiere, Webber and Flanagan [1], used finite impulse response (FIR) filters and the overall response of the system suffered from aliasing and amplitude distortion as well as distortion due to coding. In a later work presented by Crochiere [4], infinite impulse response (IIR) elliptic filters were used. These filters introduce, to some degree, phase distortion as well. Croisier, Esteban and Galand [5] in their work managed to remove the interband aliasing by introducing the concept of quadrature mirror filters (QMF) to realize a two band splitting analysis/reconstruction system. The input signal could be divided into more subbands by using this two band splitting system in a tree-structure. It was also shown that if equal length, linear phase, finite impulse response (FIR) quadrature mirror filters (QMF) are used, phase distortion is also eliminated leaving only the amplitude distortion.

The amplitude distortion can not be removed by using linear phase FIR-QMF subband splitting, except for the trivial case in which the resulting filters have no frequency selectivity. Johnston [6] though, by using an iterative approach, designed a number of linear phase FIR filters which produce minimum amplitude distortion in the overall system response. A new design approach which uses the same criteria as Johnston's was later presented by Jain and Crochiere [7].

The tree-structured QMF band-splitting with linear phase FIR filters allows some reduction to the computation load due to some similarities between the coefficients of the highpass and the lowpass filters of the two band system. This approach also results in subbands with nonsimilar frequency characteristics with respect to their transition bands and stopbands. A technique, first presented by Rothweiler [8] and Nussbaumer [9],[10] introduced a new approach for splitting the signal into subbands. This technique uses a new set of bandpass filters (known as Pseudo-QMF filters) which are derived by frequency translating a single prototype lowpass filter. It assumes that only the aliasing between adjacent bands is important and is to be removed. With this technique, the resulting subbands have similar frequency characteristics with respect to their transition bands and stopbands. Also, the implementation complexity of the system can be reduced considerably by using a polyphase network and an FFT to implement the analysis/reconstruction filter banks. The fact that this technique does not attempt to remove all the inter-band aliasing, is not that important since simulation results [10] proved that the performance of systems implementing this technique is comparable to that of the conventional tree-structured QMF systems.

A subband coding system that divides the input signal into N equal-width sub-bands using tree structured QMF band-splitting can be also realized by using a *parallel QMF filter bank* (Nussbaumer and Galand [11]). This filter bank has its N bandpass filters derived directly from the QMF filters of the equivalent tree structure and has the same characteristics with respect to perfect aliasing cancellation in decimation/interpolation operations and overall system response. Although the realization of a subband coding system with parallel QMF filter banks is less efficient than with tree structured QMF band-splitting in terms of computation load [11], parallel QMF filter banks appear to be more attractive for practical implementations. The computation load can be reduced to the tree technique's level, by truncating the impulse response of the bandpass filters, while keeping the residual aliasing noise due to imperfect cancellation of aliasing terms as well as the band-pass ripple and the stopband rejection below the acceptable upper bounds. Parallel QMF filter banks provide a smaller group delay, require less memory for signal storage, and have simplified or reduced house-keeping operations (pointer updating and delay shift lines).

As mentioned before, the ideal subband coding system is the one that allows no interband aliasing and has an overall analysis/reconstruction transfer function equivalent to a pure delay. Although Johnston [6] managed to design linear phase QMF filters which resulted in minimum amplitude distortion and no phase distortion or interband aliasing, the issue of completely removing the amplitude distortion or designing the ideal (reversible) system with none of the three types of distortion present was not discussed in any of the previously mentioned studies. Barnwell, in his analytical study on subband coding systems [12], showed that it is possible to remove the interband aliasing among the channels and have an overall analysis/reconstruction transfer function with either no phase distortion or no amplitude distortion. With the filters he used, it was shown that it was not possible to remove both phase and amplitude distortion at the same time. To remove the phase distortion, the method first introduced by Esteban and Galand [13] with linear phase FIR-QMF filters was used. To remove the amplitude distortion all-pole equalizers were introduced which lead to the design of IIR-QMF filters. The introduction of IIR filters can reduce the computation load while at the same time improving the quality of the system's performance due to the absence of amplitude distortion. However, Barnwell showed experimentally that IIR filters can be effective only when are used in the outermost splits of a tree decimation structure. Systems which meet this condition, were found to have slightly better quality and a slightly improved computational complexity than linear phase FIR-based systems.

In a recent work by Smith and Barnwell [14], the conditions for the ideal (reversible) system were developed and the general method for designing high quality analysis/reconstruction filters was given. The conditions developed, lead us to a new family of quadrature mirror filters with finite impulse response but nonlinear phase. For a particular channel, the reconstruction filter has an impulse response which is the time-reversal of the impulse response of the analysis filter. Also the impulse response of the analysis and reconstruction filters in cascade must obey certain conditions which will be discussed in a later chapter.

Smith and Barnwell, as it is evident in their work [14], designed the system and developed the conditions for reversibility using noncausal filters for the analysis and the reconstruction of the input signal. Although in many cases, analytical results obtained by using noncausal filters are the same as by using causal ones, in this particular case, due to the relationship between the highpass and the lowpass filters, the conditions prove to be slightly different. Taking the basic idea from the work of Smith and Barnwell but using causal filters, we present new conditions for a reversible causal system. Based on these conditions, we then develop a filter design procedure that makes use of a modified version of the McClellan-Parks algorithm [15] to design equiripple as well as non-equiripple filters. Charts showing the performance of these filters in isolating frequency bands are also presented and discussed. Finally, we perform experiments to observe the effects when finite precision arithmetic is used to implement these filters.

Chapter 2 Continuous—Discrete-Time Signals

2.1 Introduction

A *signal* can be defined as a function that conveys information generally about the state or behaviour of a physical system and in mathematical terms is represented as a function of one or more independent variables. Our interest is concentrated on signals with one independent variable (discrete or continuous), which by convention we refer to as *time*.

Since the independent variable can be either continuous or discrete, we can distinguish between signals which are *continuous-time* and *discrete-time*. Continuous-time signals are signals which are defined at a continuum of times and therefore are represented by continuous variable functions, whereas discrete-time signals are signals which are defined at discrete times and are represented by discrete variable functions, i.e. sequences of numbers. As we will see in Section 2.2, it is possible for a discrete-time signal to convey the same information as a continuous-time one provided that certain bandlimitedness conditions ho d.

In addition to the fact that time can be either continuous or discrete the amplitude of the signal may be either continuous or discrete. Signals that are continuous in time and amplitude are called *analog signals,* where signals that are discrete in time and amplitude are called *digital signals*. Similarly, signal processing systems may be classified as *continuous-time systems* if both the input and output signals are continuous-time, *discrete-time systems* if both the input and the output signals are discrete-time, *analog systems* if both the input and the output signals are analog and *digital systems* if both the input and the output signals are digital.

2.2 Sampling of Continuous-time Signals

It is possible for a discrete-time signal to convey the same information as a continuous-time one, provided that certain conditions hold. That means, it is theoretically possible to convert a continuous-time signal to a discrete-time one and then convert it back to the original continuous one without loss of information. The conditions which can be found in [16] are briefly discussed in this section.

Consider the analog signal $x_a(t)$ that has a *Fourier transform* $X_a(f)$ such that

$$X_a(f) = \int_{-\infty}^{+\infty} x_a(t)e^{-j2\pi ft}\,dt \tag{2.1}$$

$$x_a(t) = \int_{-\infty}^{+\infty} X_a(f)e^{j2\pi ft}\,df \tag{2.2}$$

If the signal $x_a(t)$ is periodically sampled with *sampling period* T, it results in a sampled signal $x_s(t)$ that is given by the equation

$$x_s(t) = \sum_{n=-\infty}^{+\infty} x_a(nT)\delta(t-nT) \tag{2.3}$$

where $\delta(t)$ is the unit impulse function. The Fourier transform of $x_s(t)$ is given by the equation

$$X_s(f) = \frac{1}{T} \sum_{r=-\infty}^{+\infty} X_a(f + \frac{r}{T}) \tag{2.4}$$

An alternate expression for $X_s(f)$ derived from Eq. (2.3) and the definition of the Fourier transform given by Eq. (2.1), is

$$X_s(f) = \sum_{n=-\infty}^{+\infty} x_a(nT) e^{-j2\pi fnT} \tag{2.5}$$

To recover $X_a(f)$ from $X_s(f)$ (reconstruction of the original signal from its samples), we have to operate on $X_s(f)$ in such a way so as to eliminate the $X_a(f+\frac{r}{T})$ for $r \neq 0$ terms, leaving only the $X_a(f)$ term. This can be done only when there is no overlap between the $X_a(f)$ and the $X_a(f + \frac{r}{T})$, $r \neq 0$ terms. The conditions for no overlap are:

$$X_a(f) = 0 \qquad |f| > f_{\max} \tag{2.6.a}$$

$$f_s = \frac{1}{T} > 2f_{\max} \tag{2.6.b}$$

i.e. the signal must be band-limited and the sampling rate f_s must be greater than twice the maximum frequency ($f_{\max}$).

Given the above conditions, $X_a(f)$ can be recovered by using an ideal lowpass filter with a cutoff frequency f_c that satisfies the inequality,

$$f_{\max} \leq f_c \leq f_s - f_{\max} \tag{2.7}$$

The minimum sampling rate that can be used without loss of information, is equal to twice the maximum frequency ($2f_{\max}$). If the sampling rate is less than $2f_{\max}$, the recovered signal suffers from *aliasing.*

Referring to Eq. (2.4), we can note that if the above conditions are true, the frequency characteristics of $x_a(t)$ can be determined by examining the characteristics of $x_s(t)$ in the range $0 \leq f \leq f_{\max}$.

2.3 Discrete-Time Signals–Sequences

Discrete-time system theory is concerned with the processing of signals that are represented by sequences of numbers. The notation we use for a sequence of numbers x is $[x(n)]$ where, n takes on integer values and $x(n)$ denotes the nth number (or sample) in the sequence.

A sequence $[x(n)]$ has a *Fourier Transform* $X(e^{j\omega})$ [16] which is given by the equation

$$X(e^{j\omega}) = \sum_{n=-\infty}^{+\infty} x(n)e^{-j\omega n} \tag{2.8}$$

where ω is called the *radial frequency.* The Fourier transform $X(e^{j\omega})$ is a continuous periodic function in ω with period equal to 2π.

The sequence $[x(n)]$ can be derived from $X(e^{j\omega})$ by taking the *inverse Fourier transform* which is defined as,

$$x(n) = \frac{1}{2\pi}\int_{-\pi}^{+\pi} X(e^{j\omega})e^{j\omega n}d\omega \tag{2.9}$$

Often discrete-time signals are derived from continuous-time signals by periodic sampling. We consider again the continuous-time signal $x_a(t)$ which is sampled with sampling period T to produce the impulse train $x_s(t)$. We also consider the sequence $[x(n)]$ derived from $x_a(t)$ such as,

$$x(n) = x_a(nT) \tag{2.10}$$

From Eq. (2.5) and the definition of Fourier transform for discrete-time signals (2.8), we find that,

$$X_s(f) = X(e^{j2\pi fT}) \tag{2.11}$$

Therefore, it is possible to relate the radial frequency ω of a discrete-time system to the frequency f of a continuous-time system through the relationship,

$$\omega = 2\pi fT \tag{2.12}$$

We can see that the sampling rate $f_s = 1/T$ corresponds to the radial frequency $\omega = 2\pi$. If the minimum sampling rate ($f_s = 2f_{\max}$) is used, then the maximum frequency $f_{\max}$ corresponds to the radial frequency $\omega = \pi$.

2.3.1 Z-Transform

The z-transform of a sequence $[x(n)]$ is defined as,

$$X(z) = \sum_{n=-\infty}^{+\infty} x(n) z^{-n} \tag{2.13}$$

where z is a complex variable. The *unit delay* z^{-1} represents a delay of one sample and if the sequence $[x(n)]$ is derived by sampling a continuous-time signal, it corresponds to a time delay equal to the sampling period T. The z-transform can be considered as a generalization of the Fourier transform since the Fourier transform $X(e^{j\omega})$ can be derived from $X(z)$, if $z = e^{j\omega}$. On the complex z-plane, $X(e^{j\omega})$ is derived by evaluating $X(z)$ on the *unit circle*, i.e. $|z| = 1$.

2.3.2 Sub-Sampling

The operation of *sub-sampling* a sequence can be interpreted as resampling a sequence. In mathematical terms, the sub-sampled sequence $[x_s(n)]$ is defined, in terms of the sequence $[x(n)]$ as,

$$x_s(n) = x(nR + r) \tag{2.14}$$

where R is the *sub-sampling ratio* and takes only integer values and r is an *offset* normally taking values $0 \leq r \leq R - 1$. We should note that the operation of sub-sampling in discrete-time signals corresponds to an increase of the sampling period T to RT in continuous-time signals.

It is desirable to express the z-transform $X_s(z)$ of the sub-sampled sequence $[x_s(n)]$ in terms of $X(z)$, R and r. The expression for the simple case where $r = 0$ can be found in problem 2.21 of [16]. The derivation of the formula for the general case where $r \neq 0$ is taken from [3]. The final expression is given below.

$$X_s(z) = \frac{1}{R} \sum_{l=0}^{R-1} z^{\frac{r}{R}} e^{-j(\frac{2\pi}{R})rl} X(z^{\frac{1}{R}} e^{-j(\frac{2\pi}{R})l}) \tag{2.15}$$

The Fourier transform $X_s(e^{j\omega})$ can be derived by allowing the substitution $z = e^{j\omega}$ in Eq. (2.15) which gives

$$X_s(e^{j\omega}) = \frac{1}{R} \sum_{l=0}^{R-1} e^{j(\omega - 2\pi l)\frac{r}{R}} X(e^{j(\omega - 2\pi l)\frac{1}{R}}) \tag{2.16}$$

We should note that the unit delay z^{-1} in the z-transform of the sub-sampled sequence $X_s(z)$ corresponds to a time delay of RT and the ω in the Fourier transform $X_s(e^{j\omega})$ corresponds to a frequency $f = \dfrac{\omega}{2\pi RT}$ in continuous-time signals.

From Eq. (2.16), we can observe that the frequency response of the sub-sampled sequence $X_s(e^{j\omega})$ is the sum of frequency translations of the response of the original sequence $X(e^{j\omega})$. We would like to establish the conditions under which the original sequence $X(e^{j\omega})$ can be reconstructed from the sub-sampled sequence $X_s(e^{j\omega})$. For an alias-free reconstruction, no overlapping must occur between the $X(e^{j\frac{\omega}{R}})$ term and the $X(e^{j(\omega-2\pi l)\frac{1}{R}})$ for $l \neq 0$ terms of Eq. (2.16), i.e.

$$X(e^{j\frac{\omega}{R}})X(e^{j(\omega-2\pi l)\frac{1}{R}}) = 0 \tag{2.17.a}$$

or

$$X(e^{j\omega})X(e^{j(\omega-\frac{2\pi l}{R})}) = 0 \tag{2.17.b}$$

for $0 < l \leq R-1$.

Equation (2.17.b) is true when $X(e^{j\omega})$ is defined as,

$$X(e^{j\omega}) \begin{cases} \neq 0 & \frac{(k-1)\pi}{R} \leq \omega \leq \frac{k\pi}{R} \\ = 0 & \text{elsewhere} \end{cases} \tag{2.18}$$

for $0 \leq \omega \leq \pi$ and $k = 1, \ldots, R$. These conditions correspond to the ideal case and are the required conditions for a perfectly alias-free reconstruction.

2.3.3 Interpolation—Rate increase

Interpolation involves inserting new samples between existing samples of a sequence with values derived from the values of the existing samples. This operation can be viewed as occuring in two steps. First the number of samples (sampling rate) is increased by a factor of R by inserting $R-1$ zero valued samples between the samples of the original sequence. The new sequence is then processed to modify the values of the $R-1$ intermediate sample values. The processing considered here is *linear filtering.*

We consider the original sequence $[x_s(n)]$ and the sequence $[x_f(n)]$ to be the sequence after $R-1$ null samples are inserted between the existing ones. We express $x_f(n)$ in terms of $x_s(n)$ as follows,

$$x_f(n) = \begin{cases} x_s(\frac{n-r}{R}) & \text{for } n = mR + r \quad (m \text{ integer}) \\ 0 & \text{elsewhere} \end{cases} \tag{2.19}$$

where R is the interpolation rate and r is an offset. The z-transform $X_f(z)$ of $x_f(n)$ becomes,

$$X_f(z) = z^{-r} X_s(z^R) \tag{2.20}$$

and the Fourier transform becomes,

$$X_f(e^{j\omega}) = e^{-j\omega r} X_s(e^{j\omega R}) \tag{2.21}$$

Finally, the interpolated sequence $[x_i(n)]$ is obtained by filtering $x_f(n)$ with a filter $H(z)$.

$$X_i(z) = z^{-r} X_s(z^R) H(z) \tag{2.22}$$

2.4 Subband Analysis

The purpose of subband analysis is to split the signal into a number of different frequency bands which will be transmitted separately. This can be generally achieved by using a bank of bandpass filters with different centre frequencies. The

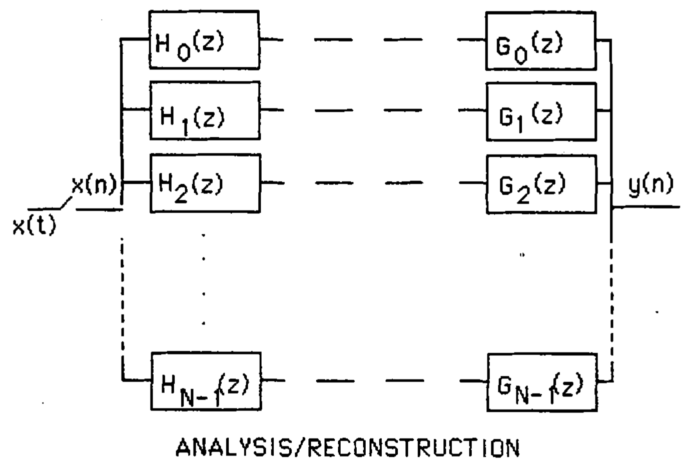

Fig. 2.1 Subband Analysis System

configuration of Fig. 2.1 considers a simple subband analysis system with N narrow band filters. In the case of subband coding where each band is coded individually the narrow band filters of the system are essentially non-overlapping.

2.4.1 Reversibility

Our concern is whether the signals at the outputs of the filters contain all the information of the input signal. If true, we should be able to reconstruct the original signal from this information. Reversible systems are the systems which allow perfect reconstruction of the input signal which means that they must have overall response equivalent to a pure delay. In the simple arrangement of Fig. 2.1 reversibility can be achieved only if

$$\sum_{i=0}^{N-1} H_i(z)G_i(z) = G_a z^{-k} \tag{2.23}$$

where G_a is a gain. In the discussions to follow any gain $G_a \neq 0$ will be acceptable since it can be easily removed with a simple scaling of all the output filter coefficients by $1/G_a$.

2.4.2 Information Rate

Considering again the simple subband system of Fig. 2.1, we observe an increase of the overall sampling rate by a factor of N. This means that the outputs of the analysis filter bank contain redundant information concerning the input signal. It is possible to remove the redundant information by sub-sampling the output of each subband with a sub-sampling ratio defined by the ratio of the input signal's bandwidth to the subband's bandwidth.

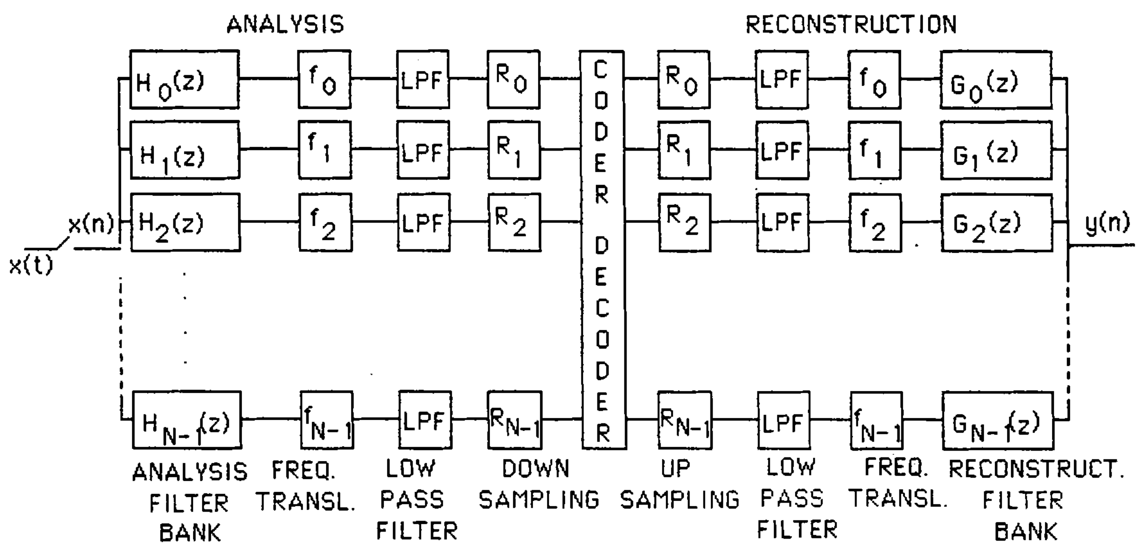

Fig. 2.2 Sub-sampling in a subband analysis system

A subband system which uses sub-sampling of the subbands to remove the redundant information is shown in Fig. 2.2. The input signal is passed through a filter bank to produce N bandpass signals. Each of those signals is frequency translated and filtered to produce a lowpass signal and then sub-sampled according to its bandwidth. In general, frequency translation is required prior to sub-sampling in order to avoid any aliasing due to overlapping of the original and the frequency translated signals which result from the sub-sampling operation. The translation frequency of a particular subband that can be used for an alias-free and minimum bandwidth lowpass signal, is the frequency of the upper or lower edge of this particular subband. Filtering is required after the frequency translation to remove the highpass components that resulted from the frequency translation operation. At the receiver, the subbands are interpolated back to the original sampling rate and frequency translated to their initial positions. Bandpass filtering is required to remove all the external frequency components and then the subbands are combined together to reconstruct the original signal.

2.4.3 Fractional-Band Filters

One case of interest involves a uniform structure with the same sub-sampling ratio in each subband ($R_k = N$). Clearly the nominal bandwidth of the subbands must be the same and equal to $1/N$ of the signal's bandwidth. The sub-sampling ratio is assured to take on integer values only. For a particular subband, if the ratio of the bandwidth of the signal to the bandwidth of the subband (which defines the sub-sampling ratio), is not an integer number, then the next larger integer number is taken to be the sub-sampling ratio. The use of this method usually results in an overall sampling rate which is greater than the sampling rate of the input signal unless equal bandwidth subbands are used which result in a system with no increase in the overall sampling rate.

In such a system, the bandwidth of the kth subband $k = 0, 1 \ldots, N-1$ is given by

$$\frac{k\pi}{N} \leq \omega \leq \frac{(k+1)\pi}{N} \tag{2.24}$$

The translation frequency ω_k can be either the lower edge frequency $k\pi/N$ or the upper edge frequency $(k+1)\pi/N$ since both frequencies can produce an alias-free minimum bandwidth lowpass signal.

If the translation frequencies are considered according to the formula,

$$\omega_k = \begin{cases} \frac{k\pi}{N} & \text{for } k \text{ even} \\ \frac{(k+1)\pi}{N} & \text{for } k \text{ odd} \end{cases} \tag{2.25}$$

the frequency translation operation at the transmitter is not required at all. This is due to the fact that in a frequency translation operation, the samples are multiplied by $\cos(\omega_k n)$. The constraint imposed on the translation frequencies ω_k by Eq. (2.25) makes the samples selected by the sub-sampler to be always multiplied by unity.

The above result can be also obtained from Eq. (2.18). The bandwidths of the subbands of an equal-bandwidth subband system completely satisfy Eq. (2.18) if $R = N$. Therefore, the subband signals can be sub-sampled without the requirement of previously being frequency translated into lowpass signals. Under the same conditions, the receiver can be also simplified. Instead of interpolating with a lowpass filter and then frequency translating, the two operations can be combined. In this case, each of the sub-sampled signals is interpolated with the appropriate bandpass filter.

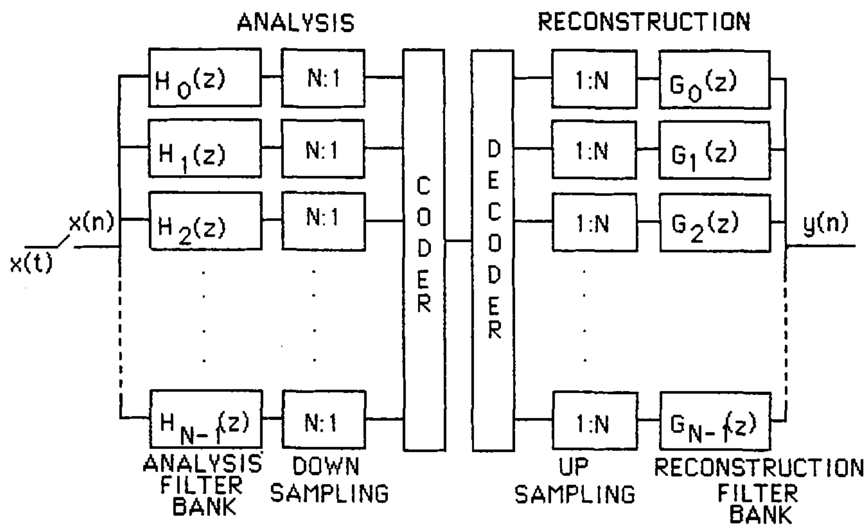

Fig. 2.3 Subband analysis system with fractional filters

The result of the above discussion is the simplified subband analysis system shown in Fig. 2.3. The overall response of this system with input signal $X(z)$ and output signal $Y(z)$ is derived using Eq. (2.15), Eq. (2.20) and Eq. (2.22).

$$Y(z) = \frac{1}{N} \sum_{i=0}^{N-1} \sum_{l=0}^{N-1} X(ze^{-j(\frac{2\pi}{N})l}) H_i(ze^{-j(\frac{2\pi}{N})l}) G_i(z) \tag{2.26}$$

where $H_i(z)$ and $G_i(z)$ are the filters of the i'th subband on the transmitting and receiving side respectively. It is expected that $H_i(z)$ and $G_i(z)$ have similar frequency characteristics in terms of their passband and stopband.

If reversibility is to be achieved as described by the equation

$$Y(z) = z^{-k} X(z) \ , \tag{2.27}$$

the following conditions must be obeyed.

$$\frac{1}{N} \sum_{i=0}^{N-1} H_i(ze^{-j(\frac{2\pi}{N})l}) G_i(z) = \begin{cases} 0 & \text{for } l \neq 0 \\ z^{-k} & \text{for } l = 0 \end{cases} \tag{2.28}$$

The $l \neq 0$ terms are the aliasing terms which must be eliminated. A simple system which obeys the above conditions is the *ideal* system where the filter Fourier transforms are defined as,

$$|H_i(e^{j\omega})|, |G_i(e^{j\omega})| = \begin{cases} 1 & \frac{i\pi}{N} \leq \omega \leq \frac{(i+1)\pi}{N} \\ 0 & \text{elsewhere} \end{cases} \tag{2.29}$$

for $i = 0, 1 \ldots, N-1$ and $0 < \omega < \pi$.

Filters with such frequency characteristics can not be exactly realized but only approximated. As a result, subband systems generally suffer from three different types of distortion, aliasing due to nonperfect cancellation of the aliasing terms (the $l \neq 0$ terms of Eq. (2.26)), amplitude distortion and phase distortion due to the fact that the $l = 0$ term of Eq. (2.28) is not equal to a perfect delay as indicated for a reversible system.

In the following chapters we will discuss the means to remove or minimize any of the three types of distortion.

Chapter 3 Quadrature Mirror Filters (QMF)

3.1 Introduction

Subband systems, as mentioned in Chapter 1, were first introduced by Crochiere, Webber and Flanagan [1] as a means to reduce the effect of quantizing noise due to coding. Ideally, these systems should not introduce any distortion to the input signal in the absence of the individual channel coders. The conditions on the analysis and the reconstruction filters for a distortionless reconstruction of the input signal are given by Eq. (2.28). Except for special cases, these conditions cannot be completely satisfied and the reconstructed signal suffers, to some degree, from three different types of distortion, aliasing, amplitude and phase distortion. Aliasing is due to the nonperfect cancellation of the aliasing terms generated by the sub-sampling operation whereas amplitude and phase distortion are due to the frequency and phase characteristics of the filters used for the analysis and the reconstruction of the input signal.

In the original subband coding systems reported in [1],[4], the analysis/reconstruction filters used were either linear phase finite impulse response (FIR) or infinite impulse response (IIR) elliptic filters. Systems with linear phase FIR filters introduce only aliasing and amplitude distortion to the input signal whereas systems with IIR filters introduce phase distortion as well. Croisier, Esteban and Galand [5],[13] managed to remove the aliasing introduced by a two band subband system by using a special kind of half-band filters known as quadrature mirror filters (QMF). It was also shown that if equal length linear phase filters are used, the overall system response has linear phase and hence the reconstructed signal does not suffer phase distortion. The key points of the QMF technique are discussed in this chapter.

3.2 Half-Band Filters

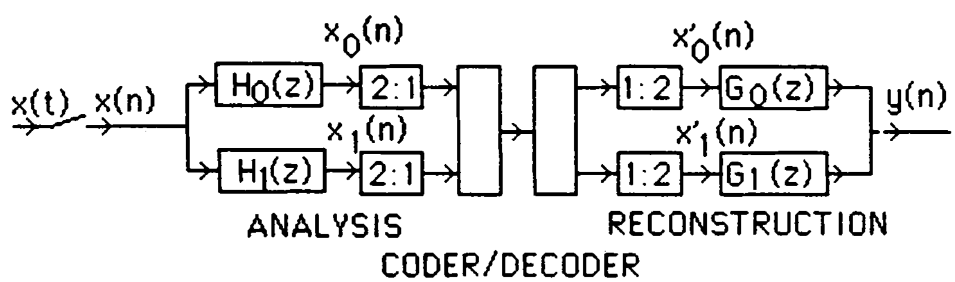

Fig. 3.1 Two band subband system

The subband system shown in Fig. 3.1 is the simplest form of the general system shown earlier in Fig. 2.3 which uses fractional-band filters. The filters here are called *half-band filters* since they divide the input signal into two equal-width bands. Although simple, this system is very important since it can be used as a building block in a tree structure to divide the signal into more subbands.

The overall response of the system can be derived from Eq. (2.26). For $N = 2$,

$$
\begin{aligned}
Y(z) =& \frac{1}{2}\sum_{i=0}^{1}\sum_{l=0}^{1} X(ze^{-j\pi l})H_i(ze^{-j\pi l})G_i(z) \\
=& \frac{1}{2}X(z)\Big\{H_0(z)G_0(z) + H_1(z)G_1(z)\Big\} \\
&+ \frac{1}{2}X(-z)\Big\{H_0(-z)G_0(z) + H_1(-z)G_1(z)\Big\}
\end{aligned}
\tag{3.1}
$$

The second term represents aliasing. Aliasing is eliminated if the following condition holds,

$$H_0(-z)G_0(z) + H_1(-z)G_1(z) = 0 \tag{3.2.a}$$

or

$$\frac{H_0(-z)}{H_1(-z)} = -\frac{G_1(z)}{G_0(z)} \tag{3.2.b}$$

A simple way satisfy this condition is by allowing

$$G_0(z) = H_1(-z) \tag{3.3.a}$$

and

$$G_1(z) = -H_0(-z) \tag{3.3.b}$$

which results in an overall response

$$Y(z) = \frac{1}{2}\Big\{H_0(z)H_1(-z) - H_0(-z)H_1(z)\Big\}X(z) \tag{3.4}$$

3.3 Quadrature Mirror Filters (QMF)

Consider the half-band filters with frequency responses as shown in stylized fashion in Fig. 3.2. By closely examining these responses, we observe that one is the

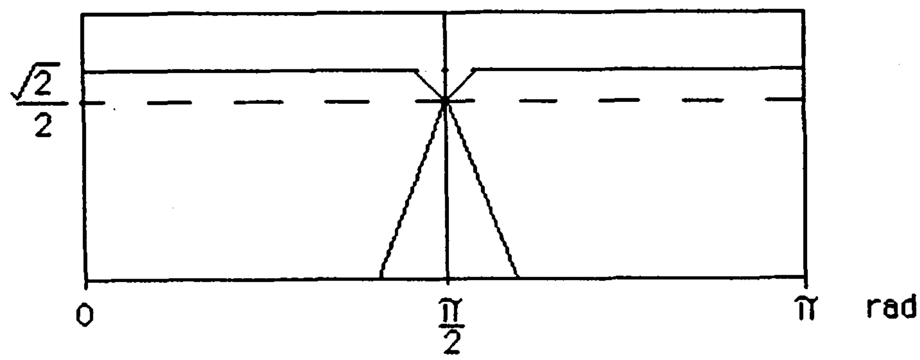

Fig. 3.2 Quadrature Mirror Filters

mirror image of the other with respect to $\omega = \pi/2$ which is the cutoff frequency of both the highpass and the lowpass filters. It can also be observed that the response of the highpass filter can be derived by frequency translating the frequency response of the lowpass filter by $\omega = \pi$, i.e.

$$|H_1(e^{j\omega})| = |H_0(e^{j(\omega-\pi)})| \tag{3.5}$$

Half-band filters with real coefficients that satisfy Eq. (3.5), also satisfy the equation,

$$|H_0(e^{j(\frac{\pi}{2}-\omega)})| = |H_1(e^{j(\frac{\pi}{2}+\omega)})| \tag{3.6}$$

This shows that they are symmetric about $\omega = \pi/2$. These filters are known as *quadrature mirror filters* or *QMF filters.*

Equation (3.5) imposes no constraints on the phase characteristics of the filters. One family of half-band filters that satisfy Eq. (3.5) requires that,

$$H_1(z) = H_0(-z) \tag{3.7}$$

These filters can be used in the subband system of Fig. 3.1. For an alias-free reconstruction, the following conditions which are derived from Eq. (3.3.a) and

Eq. (3.3.b) must hold,

$$H_1(z) = H_0(-z) \tag{3.8.a}$$

$$G_0(z) = H_0(z) \tag{3.8.b}$$

and

$$G_1(z) = -H_0(-z) \tag{3.8.c}$$

This results in an overall response

$$Y(z) = \frac{1}{2}\left\{{H_0}^2(z) - {H_0}^2(-z)\right\}X(z) \tag{3.9}$$

Consider the conditions under which the system is reversible, i.e.

$$\frac{1}{2}\left\{{H_0}^2(z) - {H_0}^2(-z)\right\} = G_a z^{-k} \tag{3.10}$$

where G_a is the overall system gain. The left-hand side of the equation can be expanded to

$$\frac{1}{2}\left\{{H_0}^2(z) - {H_0}^2(-z)\right\} = \frac{1}{2}\left\{H_0(z) + H_0(-z)\right\}\left\{H_0(z) - H_0(-z)\right\} \tag{3.11}$$

By definition, the z-transforms of the causal filters $H_0(z)$ and $H_0(-z)$ can be written as,

$$H_0(z) = \sum_{n=0}^{\infty} h_0(n) z^{-n} \tag{3.12.a}$$

$$H_0(-z) = \sum_{n=0}^{\infty} (-1)^n h_0(n) z^{-n} \tag{3.12.b}$$

where $h_0(n)$ is the nth filter coefficient. The first part of Eq. (3.11) can be written as,

$$\begin{aligned} H_0(z) + H_0(-z) &= \sum_{n=0}^{\infty} \left\{1 + (-1)^n\right\} h_0(n) z^{-n} \\ &= 2 \sum_{n \text{ even}} h_0(n) z^{-n} \end{aligned} \tag{3.13}$$

the second part as,

$$
\begin{aligned}
H_0(z) - H_0(-z) &= \sum_{n=0}^{\infty}\Big\{1-(-1)^n\Big\}h_0(n)z^{-n} \\
&= 2\sum_{n \text{ odd}} h_0(n)z^{-n}
\end{aligned}
\tag{3.14}
$$

and the overall response as,

$$
\begin{aligned}
{H_0}^2(z) - {H_0}^2(-z) =& 4\sum_{n \text{ even}}\sum_{u \text{ odd}} h_0(n)h_0(u)z^{-(u+n)} \\
=& 4h_0(0)h_0(1)z^{-1} \\
&+ 4\Big\{h_0(0)h_0(3) + h_0(2)h_0(1)\Big\}z^{-3} \\
&+ 4\Big\{h_0(0)h_0(5) + h_0(2)h_0(3) + h_0(4)h_0(1)\Big\}z^{-5} \\
&+ 4\Big\{h_0(0)h_0(7) + h_0(2)h_0(5) \\
&+ h_0(4)h_0(3) + h_0(6)h_0(1)\Big\}z^{-7} \\
&\dots
\end{aligned}
\tag{3.15}
$$

For reversibility, only one of the above factors should be nonzero, otherwise the signal will suffer distortion. Clearly, if the filter $H_0(z)$ has even or odd numbered coefficients only, the overall system response is zero. On the other hand, if more than two coefficients are nonzero, more than one of the above factors is nonzero and the signal suffers distortion. Therefore, for a reversible system, $H_0(z)$ must have the form,

$$H_0(z) = Az^{-p}(1 + Bz^{-q}) \tag{3.16}$$

where, q is an odd integer and p is any integer. Filters of the above form do not have good frequency selectivity. Therefore, it is expected that if we use quadrature mirror filters that satisfy Eq. (3.8) but which do not satisfy Eq. (3.16), the reconstructed signal will suffer from amplitude and possibly phase distortion.

3.4 Linear Phase QMF Filters

It is possible, as shown in [13], to design a subband system with QMF filters as in Eq. (3.8) that allows only amplitude distortion using linear phase finite impulse response (FIR) filters. The design of these filters will be such that the amplitude distortion is minimized. Obviously, linear phase systems which allow the presence of nulls in the overall system response should not be used.

A causal finite impulse response (FIR) filter $H_0(z)$ is defined as,

$$H_0(z) = \sum_{n=0}^{N-1} h_0(n) z^{-n} \tag{3.17}$$

for $N < \infty$. Given that $h_0(0) \neq 0$ and $h_0(N-1) \neq 0$, $H_0(z)$ has linear phase characteristics if

$$h_0(n) = h_0(N-1-n) \tag{3.18}$$

For a linear phase FIR filter, the frequency response $H_0(e^{j\omega})$ can be written as,

$$H_0(e^{j\omega}) = H_0(\omega) e^{-j\frac{(N-1)}{2}\omega} \tag{3.19}$$

where

$$H_0(\omega) = |H_0(e^{j\omega})| \tag{3.20}$$

Note the distinction in terms of argument between the frequency response $H_0(e^{j\omega})$ and its absolute value $H_0(\omega)$.

The output $Y(e^{j\omega})$ can be written as,

$$\begin{aligned} Y(e^{j\omega}) &= \frac{1}{2}\left\{ {H_0}^2(e^{j\omega}) - {H_0}^2(e^{j(\omega-\pi)}) \right\} X(e^{j\omega}) \\ &= \frac{1}{2}\left\{ {H_0}^2(\omega) e^{-j\omega(N-1)} - {H_0}^2(\omega-\pi) e^{-j(\omega-\pi)(N-1)} \right\} X(e^{j\omega}) \\ &= \frac{1}{2}\left\{ {H_0}^2(\omega) - {H_0}^2(\omega-\pi) e^{j\pi(N-1)} \right\} e^{-j\omega(N-1)} X(e^{j\omega}) \end{aligned} \tag{3.21}$$

We consider here two cases, even length and odd length filters. For even length filters (N even), Eq. (3.21) becomes,

$$Y(e^{j\omega}) = \frac{1}{2}\Big\{{H_0}^2(\omega) + {H_0}^2(\omega - \pi)\Big\}e^{-j\omega(N-1)}X(e^{j\omega}) \tag{3.22}$$

A reversible system must have,

$${H_0}^2(\omega) + {H_0}^2(\omega - \pi) = 1 \tag{3.23}$$

but from the discussion in Section 3.3 this is not exactly possible.

The error function $E_r(\omega)$ which is defined as

$$E_r(\omega) = 1 - \Big\{{H_0}^2(\omega) + {H_0}^2(\omega - \pi)\Big\} \tag{3.24}$$

gives us a measure of the level of distortion as function of the radial frequency ω. Minimization of this function will be a major consideration in the filter design, especially when the two subband system is used in a tree-structure analysis/reconstruction to divide the signal into more than two subbands.

For odd length filters, Eq. (3.21) becomes,

$$Y(e^{j\omega}) = \frac{1}{2}\Big\{{H_0}^2(\omega) - {H_0}^2(\omega - \pi)\Big\}e^{-j\omega(N-1)}X(e^{j\omega}) \tag{3.25}$$

For $\omega = \frac{\pi}{2}$ we get,

$$Y(e^{j\frac{\pi}{2}}) = \frac{1}{2}\Big\{{H_0}^2(\frac{\pi}{2}) - {H_0}^2(-\frac{\pi}{2})\Big\}e^{-j\frac{\pi}{2}(N-1)}X(e^{j\frac{\pi}{2}}) \tag{3.26}$$

since $H_0(z)$ has real coefficients, $H_0(\frac{\pi}{2}) = H_0(-\frac{\pi}{2})$ which makes $Y(e^{j\frac{\pi}{2}}) = 0$. Odd length filters can not be used in configurations like the one in Fig. 3.1 since they allow the existence of nulls in the overall system response. A slightly modified system though, which will be considered later in this chapter, can utilize odd length linear phase filters without the overall system response containing any nulls.

3.5 Design of Linear Phase QMF filters

The fact that linear phase QMF filters allow complete cancellation of the aliasing terms when used in a subband system gives us some flexibility in designing these filters. Generally, band-splitting filter banks which do not allow complete cancellation of the aliasing terms have to have filters with very narrow transition bands, so that the overlapping between the subbands and therefore the aliasing is kept small. In order to achieve that, high order filters have to be used which makes the implementation of the subband systems complicated. Also, the use of filters which do not overlap results in an overall system response with spectral gaps.

By using linear phase QMF filters, the subband systems become less complicated. This is due to the fact that the aliasing terms are eliminated and the width of the transition bands of the filters is not as important. Therefore, lower order filters with wider transition bands can be used and the spectral gaps can be also avoided. Referring to Eq. (3.23), in order to avoid the spectral gap, it is required that the response of the filter must be very close to -3 dB $(1/\sqrt{2})$ at $\omega = \pi/2$.

Although some commonly used filters (equiripple, Hamming, Hanning) can have acceptable performance when used in a subband system, the filters that have attracted special attention, are those designed by Johnston [6]. To design these filters, Johnston established two criteria.

1. The ripple in the system response described by the error function $E_r(\omega)$ in Eq. (3.24).

2. The stopband rejection of the individual filter.

The first criterion refers to the amount of distortion imposed by the system on the input signal. In a subband system, the subbands must be isolated from each other so that the noise that is generated from coding a particular subband is not allowed to spread over to the other subbands. This leads us to the second criterion which can be considered as a measure of the leakage between the subbands.

The filters we are interested in, have an even number of coefficients and are symmetric. If the number of filter coefficients is N, these constraints reduce the number of variables by 2 yielding $N/2$ variables to be searched. In order to obtain the optimum values for the filter coefficients, an optimization metric that expresses the above criteria as a single function of these coefficients must be first constructed. A search algorithm will then determine the optimum values that minimize the constructed metric.

3.5.1 Optimization criteria

The following formula which is the same formula used by Johnston, can be used to combine the two criteria into a single optimization metric E,

$$E = E_{rp} + \alpha E_s(f_{SB}) \tag{3.27}$$

where

$$E_{rp} = \int_0^{\pi} E_r^{\,2}(\omega)d\omega$$
$$= 2\int_0^{\frac{\pi}{2}} \left\{ H_0^{\,2}(\omega) + H_0^{\,2}(\omega-\pi) - 1 \right\}^2 d\omega$$

$$E_s(f_{SB}) = \int_{f_{SB}}^{\pi} H_0^{\,2}(\omega)d\omega$$

α is the stopband weighting and f_{SB} is the stopband edge. E_{rp} corresponds to the ripple "energy" and E_s is the stopband energy for the filter $H_0(z)$. Since the filter $H_0(z)$ has an even number of coefficients, $H_0(\omega)$ can be expressed in terms of the filter coefficients $h_0(n)$ as

$$H_0(\omega) = 2\sum_{n=0}^{N/2-1} h_0(n)\cos\left\{\omega\left(\frac{N-1}{2} - n\right)\right\} \tag{3.28}$$

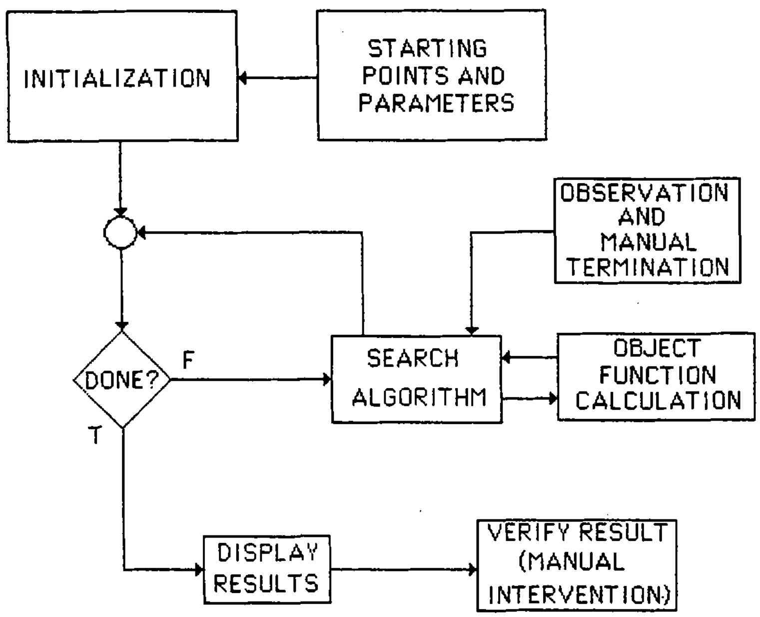

Fig. 3.3 Optimization system-Block diagram

3.5.2 Search Algorithm

The Hooke and Jeaves Algorithm [17] is a relatively unsophisticated search algorithm that attempts to minimize a single *objective function* of several variables. It was used by Johnston in the optimization system shown in Fig. 3.3 for the filter design.

Due to the use of a simple search method such as that of Hooke and Jeaves, the starting position as well as the step size are important in some cases. It is possible that the search will get trapped in local minima or fail to converge at all, if the step size is inappropriate.

Since the Hooke and Jeaves method does not guarantee termination in a global minimum, the suggested procedure is to consider a starting position well away from the desired solution The search should be repeated with different carefully selected starting positions and step sizes to assure a successful optimization.

3.5.3 New Design Technique for QMF filters

A new design technique for QMF filters was introduced by Jain and Crochiere [7]. This design which uses the same optimization criteria as Johnston's, converges to the optimum solution without any manual intervention or repeated trials with different starting points. A description of the design algorithm as well as the performance charts that allow the designer to select the appropriate weighting function α and the filter length N so that the filters will have the desired frequency characteristics, are presented in the same study.

3.6 Implementation of a Two band QMF Subband System

The use of linear phase QMF filters in subband systems, apart from the alias-free reconstruction, offers some computational advantages as well. Referring to Fig. 3.1, the signals $x_0(n)$ and $x_1(n)$ represent respectively the low and high half-bands of input signal $x(n)$ with z-transforms $X_0(z)$ and $X_1(z)$ equal to

$$X_0(z) = H_0(z)X(z) \tag{3.29.a}$$

$$X_1(z) = H_1(z)X(z) \tag{3.29.b}$$

Since $H_1(z) = H_0(-z)$, the values of $x_0(n)$ and $x_1(n)$ can be expressed in terms of $h_0(n)$ and $x(n)$ as

$$x_0(n) = \sum_{k=0}^{N-1} h_0(k)x(n-k) \tag{3.30.a}$$

$$x_1(n) = \sum_{k=0}^{N-1} (-1)^k h_0(k)x(n-k) \tag{3.30.b}$$

If the values of $x_0(n)$ and $x_1(n)$ are computed separately, $2N$ multiplications and $2(N-1)$ additions will be required for every sub-sampled sample. The load though, can be considerably reduced, if we take advantage of the similarity between the computations required for both signals. Consider the functions $x_e(n)$ and $x_d(n)$ defined as

$$x_e(n) = \sum_{k=0}^{N/2-1} h_0(2k)x(n-2k) \tag{3.31.a}$$

$$x_d(n) = \sum_{k=0}^{N/2-1} h_0(2k+1)x(n-2k-1) \tag{3.31.b}$$

The values of $x_0(n)$ and $x_1(n)$ can be determined in terms of $x_e(n)$ and $x_d(n)$ as

$$x_0(n) = x_e(n) + x_d(n) \tag{3.32.a}$$

$$x_1(n) = x_e(n) - x_d(n) \tag{3.32.b}$$

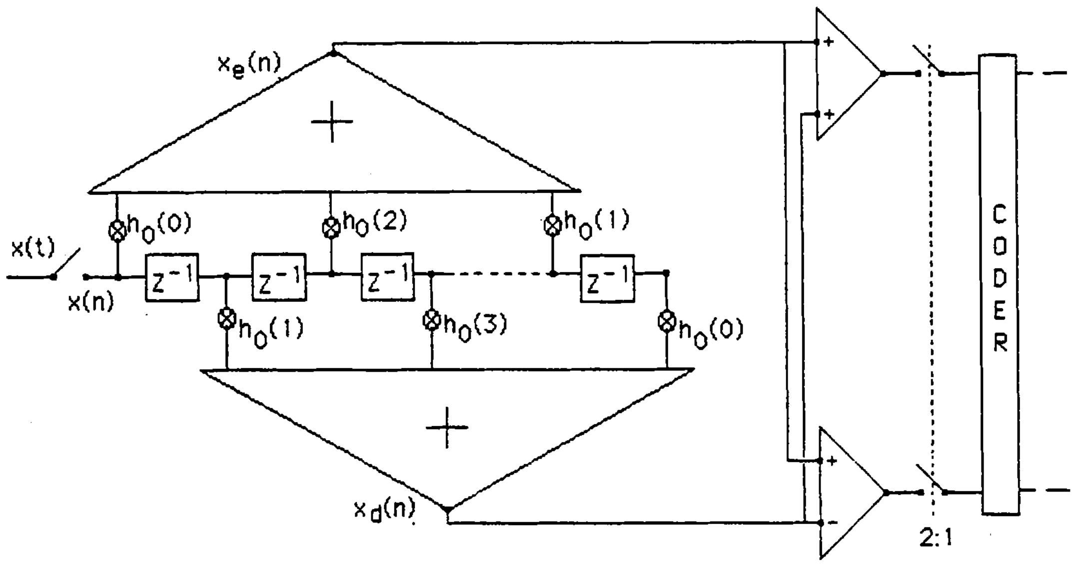

Fig. 3.4 Efficient implementation of the analysis of a two band subband system with linear phase QMF filters.

To compute the values of $x_e(n)$ and $x_d(n)$, we need $N/2$ multiplications and $N/2-1$ additions for each. This implies that the computation load can be reduced to N multiplications and N additions for every two input samples, if the computation of $x_e(n)$ and $x_d(n)$ is used as an intermediate step. The implementation of the analysis of the subband system is illustrated in Fig. 3.4.

The reconstruction of the signal can be also done in a computationally efficient way. Referring again to Fig. 3.1, the signals $x'_0(n)$ and $x'_1(n)$ are obtained after null samples are inserted between the samples of the decoded signal. The z-transform of the output signal $Y(z)$ is given in terms of the z-transforms of the above signals as

$$Y(z) = G_0(z)X_0'(z) + G_1(z)X_1'(z)$$
$$= H_0(z)X_0'(z) - H_0(-z)X_1'(z) \tag{3.33}$$

We consider the inverse z-transform of the above equation to obtain the relationship between the coefficients $y(n)$, $x_0'(n)$ and $x_1'(n)$,

$$y(n) = \sum_{k=0}^{N-1} h_0(k)\Big\{x_0'(n-k) + (-1)^{k+1}x_1'(n-k)\Big\} \tag{3.34}$$

By introducing the functions $x_d'(n)$ and $x_e'(n)$ to be the sum and the difference of the signals $x_0'(n)$ and $x_1'(n)$ respectively,

$$x_e'(n) = x_0'(n) - x_1'(n) \tag{3.35.a}$$

$$x_d'(n) = x_0'(n) + x_1'(n) \tag{3.35.b}$$

the output signal $y(n)$ can be expressed as,

$$\begin{aligned} y(n) = &\sum_{k=0}^{N/2-1} h_0(2k)x_e'(n-2k) \\ &+ \sum_{k=0}^{N/2-1} h_0(2k+1)x_d'(n-2k-1) \end{aligned} \tag{3.36}$$

Both $x_e'(n)$ and $x_d'(n)$ are zero for odd values of n, being the sum and the difference of zero-valued samples and the above equation can be written as

$$y(n) = \begin{cases} \displaystyle\sum_{k=0}^{N/2-1} h_0(2k)x_e'(n-2k) & \text{for } n \text{ even} \\ \displaystyle\sum_{k=0}^{N/2-1} h_0(2k+1)x_d'(n-2k-1) & \text{for } n \text{ odd} \end{cases} \tag{3.37}$$

The implementation of the reconstruction part of the system becomes more efficient if the computation of $x_e'(n)$ and $x_d'(n)$ is used as an intermediate step. To compute $x_d'(n)$ and $x_e'(n)$, two additions are required for every nonzero sample.

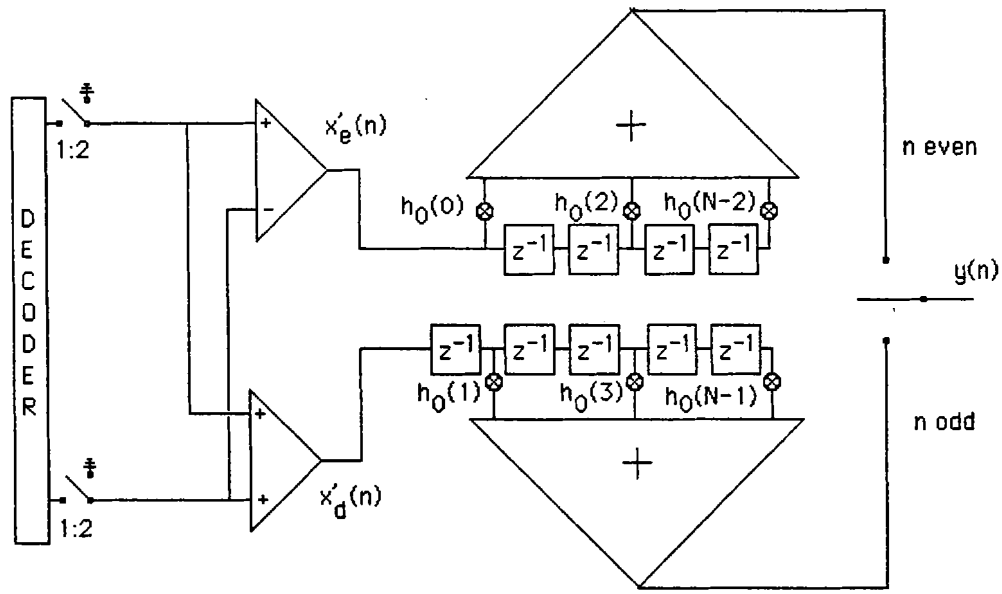

Fig. 3.5 Efficient implementation of the reconstruction of a two band subband system with linear phase QMF filters

To compute the output signal $y(n)$ by means of Eq. (3.37), $N/2$ multiplications and $N/2-1$ additions are required for every sample. Therefore, the number of calculations can be reduced to $N/2$ additions and $N/2$ multiplications per output sample. This can be implemented as shown in Fig. 3.5.

3.7 Tree-Structured Subband Systems

In the previously described implementation, the input signal $x(n)$ was decomposed into two subbands in which sampling rate was reduced to 1/2 of its original value. This decomposition can be extended to more than two subbands by applying the same decomposition process to each of these two subbands as to the input signal $x(n)$. The resulting system, as illustrated in Fig. 3.6, has four subbands each with a sampling rate reduced to 1/4 of the sampling rate of the input signal. Obviously,

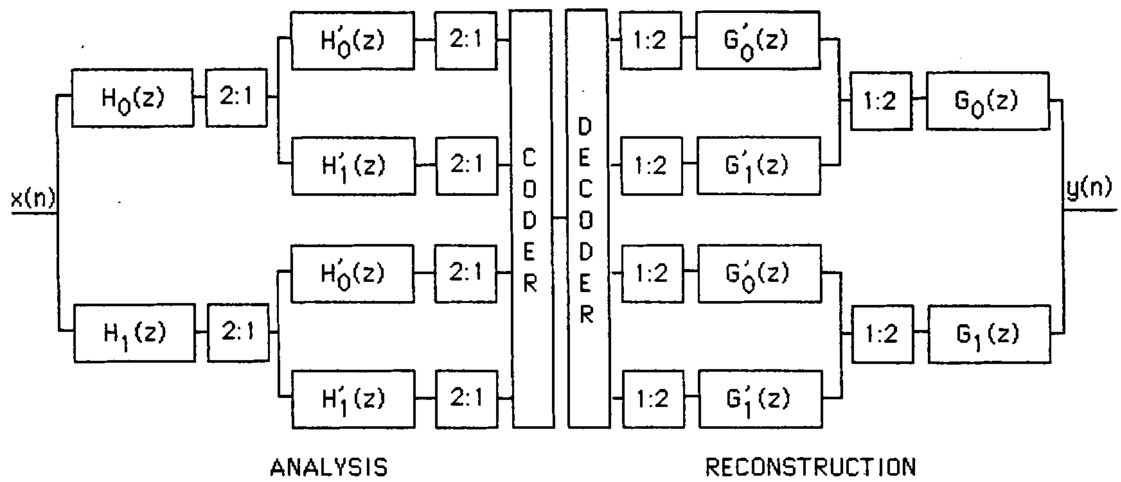

Fig. 3.6 Tree-structured four subband system

this decomposition can be extended to 8 and in general 2^p subbands by repeating the same decomposition process p times. At each of the p stages of the decomposition process, the number of two band systems required, is equal to 2^{p-1} and the total number of two band systems is equal to $2^p - 1$.

The process of reconstructing the input signal can be considered as the "mirror image" of the decomposition process. For the four subband system in Fig. 3.6, the reconstruction is done in two stages. First, the two lowpass and the two highpass signals are combined together to form only two signals which are finally used to reconstruct the input signal.

The choice of the analysis and reconstruction filters is limited by the alias-free requirement. Although, the frequency characteristics of the filters might differ from stage to stage they must be the same within a particular stage. For example, the lowpass half-band filters $H_0(z)$ and $H_0'(z)$ used respectively for the first and second stage of the system in Fig. 3.6, might be different, but both lowpass filters of the second stage must be the same. Also, both groups $H_0(z)$, $H_1(z)$, $G_0(z)$, $G_1(z)$ and $H_0'(z)$, $H_1'(z)$, $G_0'(z)$, $G_1'(z)$ must satisfy the alias-free reconstruction conditions set by Eq. (3.8). Under these conditions, the overall system response $R(z)$ is given by the equation

$$R(z) = \frac{1}{4} R_1(z) R_2(z^2) \tag{3.38.a}$$

where

$$R_1(z) = {H_0}^2(z) - {H_0}^2(-z) \tag{3.38.b}$$

and

$$R_2(z) = {H_0'}^2(z) - {H_0'}^2(-z) \tag{3.38.c}$$

The results can be extended to cover systems with p stages (2^p subbands) with an overall response $R(z)$ given by

$$R(z) = \left(\frac{1}{2}\right)^p R_1(z) R_2(z^2) R_3(z^4) \dots R_p(z^{2^{p-1}}) \tag{3.39}$$

where $\frac{1}{2} R_k(z)$ is the overall response of the two band system used for the kth stage.

Exact reconstruction cannot be achieved, if linear phase QMF filters are used. To show this, all we have to show is that the overall system response $R(z)$ cannot be equal to a pure delay. Obviously, if $R(z) = z^{-k}$, its zero-pole diagram will have k poles and no zeros. Referring to Eq. (3.39), $R(z)$ is the product of the z-transforms $R_k(z)$ for $k = 1, 2, \dots, p$. Except for trivial cases, any z-transform $R_k(z)$, being the overall response of a linear phase QMF two band system, does have zeros somewhere on the z-plane which implies that $R(z)$ cannot be a zero-free transform. Therefore, $R(z) \neq z^{-k}$ and exact reconstruction cannot be achieved. On the other hand, although it is possible for the amplitude distortion to accumulate, it will always be between a maximum and a minimum bound set respectively by the sum of all the maximum and all the minimum values of distortion (in dB) that occur at the individual stages.

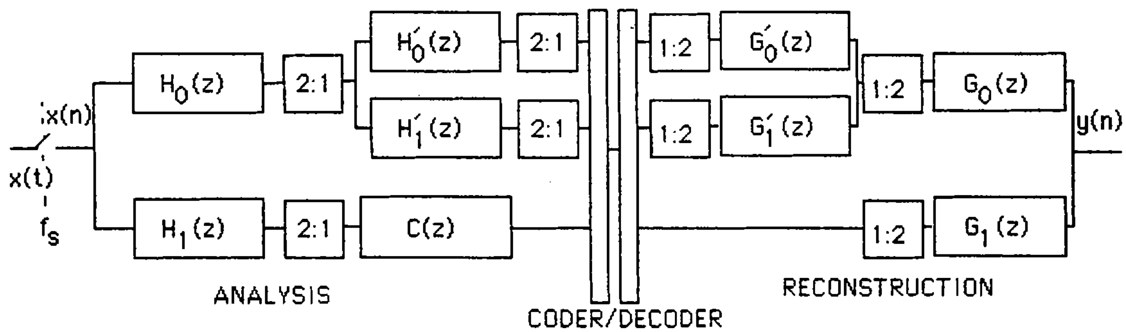

Fig. 3.7 Tree-structured three band system

It is sometimes desirable to have subbands with unequal bandwidths. In these cases the tree decomposition is done partly on some branches so as to produce subbands with bandwidths multiples of the basic bandwidth. For example, a three band system can be implemented with a two stage tree-structure as illustrated in Fig. 3.7. Note that one of the subbands has twice the bandwidth of the other two. In this case, alias-free reconstruction can be achieved only if a filter $C(z)$ equal to

$$C(z) = \frac{1}{2}\left\{H_0'^2(z) - H_0'^2(-z)\right\} \tag{3.40}$$

is used to compensate for the distortion imposed on the lowpass half-band due to the extra splitting.

3.8 Parallel QMF Filter Banks

In the previous section, we have discussed the decomposition of a signal into a number of subbands by means of a tree-structure scheme which allows an alias-free reconstruction. The tree-structure scheme can be easily replaced by another one that utilizes parallel filter banks for both the analysis and the reconstruction. This new scheme which is illustrated in Fig. 3.8 was used by Esteban and Galand [18] and by Galand and Nussbaumer[11] as a simple way to practically implement a subband coding system.

The bandpass filters of the filter banks, when derived from the equivalent QMF tree-structures retain their alias-free reconstruction property and for this reason the filter banks are called parallel QMF filter banks. Obviously, the number of equal-width subbands that can be allowed is restricted to powers of 2.

To establish a relationship between the bandpass filters of the QMF filter banks and the half-band filters of the equivalent tree-structures, we introduce a slightly different notation than the one previously used. We define $F_k(z)$ and $F_k'(z)$ the kth filters of the analysis and the reconstruction filter banks respectively. $H_i(z)$, $H_i(-z)$ are the low and highpass filters used for the i'th stage of the analysis part of the tree-structure and $H_i(z)$ and $-H_i(-z)$ are the filters for the i'th stage of the reconstruction part of the tree-structure. The total number of subbands N is equal to

$$N = 2^p \tag{3.41}$$

where p is the number of stages of the equivalent tree-structure.

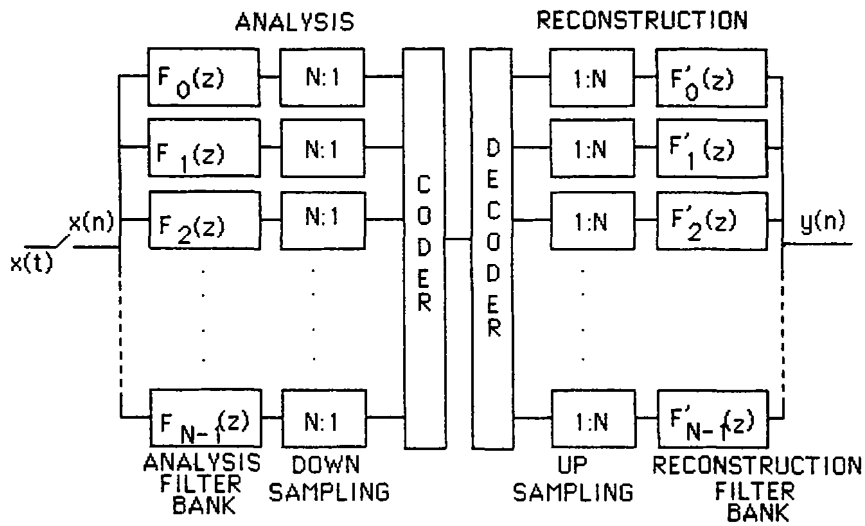

a) Parallel QMF structure

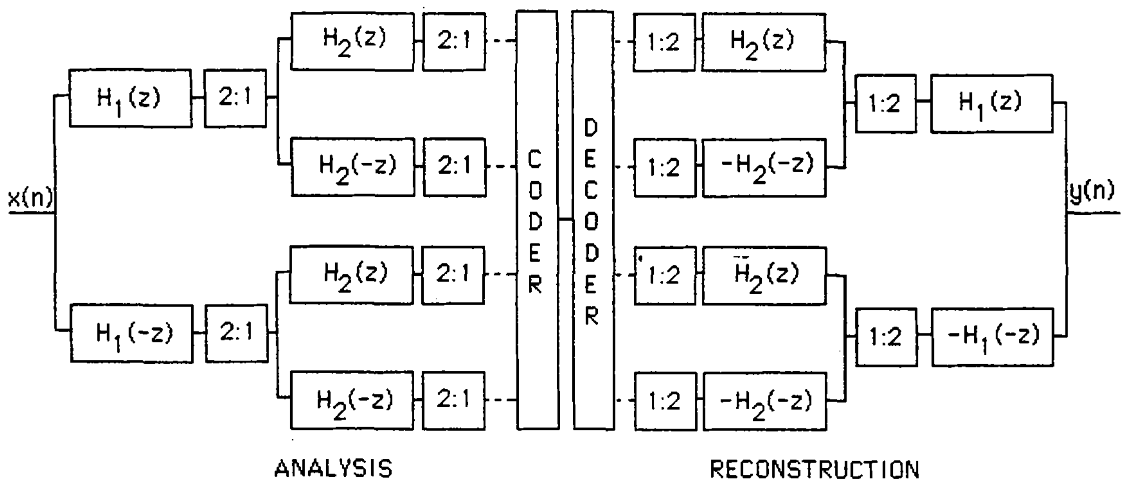

b) Equivalent tree-structure

Fig. 3.8 Multiband subband system

It can be shown that the two sub-sampling/linear-filtering operations shown in Fig. 3.9.a are equivalent. This equivalence can be used to transform the analysis part of the tree-structure scheme into its parallel form. Similarly, the equivalence between the two sub-sampling/linear-filtering operations shown in Fig. 3.9.b can be used to transform the reconstruction part of the tree-structure scheme into its parallel form. Using these equivalent operations, the following relationships between

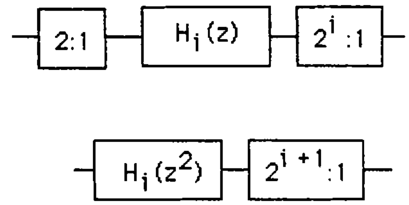

a) For the analysis part

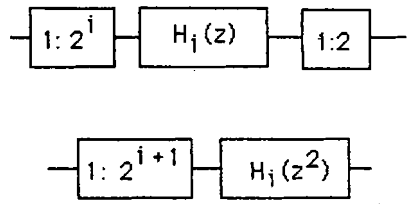

b) For the reconstruction part

Fig. 3.9 Equivalent sub-sampling/linear-filtering operations for the tree-structure/parallel-structure transformation

$F_k(z)$, $F_k'(z)$, $k = 0, 1, \ldots, N-1$ and $H_i(z)$, $i = 1, 2, \ldots, p$ are derived.

$$F_k(z) = \prod_{i=1}^{p} H_i(s_i z^{2^{i-1}}) \tag{3.42.a}$$

$$F_k'(z) = N c_k F_k(z) \tag{3.41.b}$$

where N is a gain normalization factor and s_i and c_k indicate the signs which can be determined by the following procedure. For s_i, we express the value of k of the filter $F_k(z)$ in its binary form considering only p digits. Counting from left to right, we find the i'th bit b_i and determine the value of s_i according to the formula,

$$s_i = \begin{cases} +1 & \text{for } b_i = 0 \\ -1 & \text{for } b_i = 1 \end{cases} \tag{3.43}$$

For example, to find the expression for $F_5(z)$ when the number of stages $p = 3$, we express 5 in binary using only 3 bits and obtain the values of b_i. Since $5 = (101)_2$ $(b_1 = 1, b_2 = 0, b_3 = 1)$, then $s_1 = -1$, $s_2 = +1$ and $s_3 = -1$ and

$$F_5(z) = H_1(-z)H_2(z^2)H_3(-z^4)$$

To find c_k, we consider the value of d_k such as

$$d_k = b_1 \oplus b_2 \oplus \ldots b_p \tag{3.44}$$

and c_k is given by the formula

$$c_k = \begin{cases} +1 & \text{for } d_k = 0 \\ -1 & \text{for } d_k = 1 \end{cases} \tag{3.45}$$

For the same example, $d_5 = 0$ therefore, $c_5 = +1$ and $F_5'(z) = NF_5(z)$.

The process of generating the filters $F_k(z)$ from the half-band filters of an equivalent tree-structure, guarantees that

$$F_{N-1-k}(z) = F_k(-z) \tag{3.46}$$

This can be proved by considering the numbers k and $N-1-k$ in their binary form. Since $N = 2^p$, k and $N-1-k$ are 1's complement of each other, meaning that everywhere k has a 0 which corresponds to a positive sign, $N-1-k$ has a 1 which corresponds to a negative sign. For the previous example, the 1's complement of $5 = (101)_2$ is $2 = (010)_2$ and

$$F_2(z) = H_1(z)H_2(-z^2)H_3(z^4)$$

which makes $F_2(z) = F_5(-z)$.

By considering the inverse z-transform of Eq. (3.46), we obtain the following relationship

$$f_{N-1-k}(n) = (-1)^n f_k(n) \tag{3.47}$$

that can be used for a more efficient implementation of the parallel QMF filter banks.

Referring to Section 3.6, the analysis of a two band system is done with N multiplications and N additions for every two input samples. If the sampling rate used is equal to f_s, a real time implementation will require $f_s N/2$ multiplications and $f_s N/2$ additions per second. For the i'th stage of the tree-structure implementation, the sampling rate of the input signal is $f_s/2^{i-1}$. If the order of the filter $H_i(z)$ is M_i, the number of computations required is equal to $M_i/2$ multiplications and $M_i/2$ additions for every two band system. This makes the overall computation rate of the particular stage equal to $f_s M_i/2$ multiplications and $f_s M_1/2$ additions per second. Therefore, the overall computation rate for the analysis is equal to $f_s(M_1 + M_2 \ldots + M_p)/2$ multiplications and additions per second.

For the equivalent parallel QMF structure, the order L of the bandpass filters, is given by the equation

$$L = 1 + \sum_{i=1}^{p}(M_i - 1)2^{i-1} \tag{3.48}$$

where M_i is the order of $H_i(z)$. The overall computation rate can be reduced to $f_s L/2$ multiplications and additions per second if the relationship among the filter coefficients described by Eq. (3.47), is properly used. Clearly, the value of L is much greater than the sum of the values M_i which implies that the computation load will increase considerably with the parallel filter banks.

Generally speaking, the tree-structure scheme offers the most computationally efficient way of implementing a subband system. Its main disadvantages though, are that the different stages of the tree-structure must operate at different sampling rates and delay lines must be established and updated for the original input signal as well as for all the other input signals to the intermediate stages. The housekeeping operations are simplified when parallel QMF filter banks are used. Although longer, there is only one delay line of the original signal to be updated and only one sampling rate.

The parallel implementation of the subband system can be simplified by truncating the impulse response of the bandpass filters. Truncation of the impulse response can be costly in terms of aliasing since the alias-free reconstruction condition will not in general be satisfied after truncation. In addition, the overall frequency characteristics of the system and frequency characteristics of the bandpass filters may be degraded. For a specific application, once the acceptable bounds for the above three factors are established, the filters' impulse responses can be appropriately truncated and reoptimized. Clearly, the truncation will reduce the overall group delay imposed by the system as well as the memory and the overall number of computations. More detailed discussions on specific applications of truncated parallel QMF filter banks can be found in [18],[11].

3.9 Odd Length Linear Phase QMF Filters

The discussion in Section 3.4 has shown that odd length filters cannot be used in configurations like the one in Fig. 3.1, since they introduce nulls into the overall system response. If we examine Eq. (3.25) and Eq. (3.26), we observe that the null exists because of the phase characteristics rather than the frequency characteristics of the filters. Therefore, we might be able to remove the null by inserting equalizers that change the phase characteristics without changing the frequency characteristics. The simplest equalizer is a pure delay.

Consider again the lowpass half-band filter $H_0(z)$ and the other three filters of the subband system which are defined in terms of $H_0(z)$ as,

$$H_1(z) = z^{-k} H_0(-z) \tag{3.49.a}$$

$$G_0(z) = (-1)^{k+1} z^{-k} H_0(z) \tag{3.49.b}$$

$$G_1(z) = H_0(-z) \tag{3.49.c}$$

where k is an integer. The conditions for an alias-free reconstruction which are given by Eq. (3.2.a), are satisfied and the overall response becomes,

$$Y(z) = \frac{1}{2}\Big\{{H_0}^2(z)(-1)^{k+1} + {H_0}^2(-z)\Big\} z^{-k} X(z) \tag{3.50}$$

Using linear phase filters with N coefficients the overall frequency response $Y(e^{j\omega})$ becomes,

$$Y(e^{j\omega}) = \frac{1}{2}\Big\{{H_0}^2(\omega)(-1)^{k+1} + {H_0}^2(\omega-\pi)e^{j\pi(N-1)}\Big\} e^{-j\omega(k+N-1)} X(e^{j\omega}) \tag{3.51}$$

We evaluate $Y(e^{j\omega})$ at $\omega = \pi/2$,

$$Y(e^{j\frac{\pi}{2}}) = \frac{1}{2}\Big\{{H_0}^2(\tfrac{\pi}{2})(-1)^{k+1} + {H_0}^2(-\tfrac{\pi}{2})e^{-j\pi(N-1)}\Big\} e^{-j\frac{\pi}{2}(k+N-1)} X(e^{j\frac{\pi}{2}}) \tag{3.52}$$

Since $H_0(\frac{\pi}{2}) = H_0(-\frac{\pi}{2})$, we find that if both k and N are even or both k and N are odd, the overall response is null-free.

For a null-free response and odd length filters the overall delay is minimum if $k = 1$. Under these conditions, Eq. (3.49) becomes,

$$H_1(z) = z^{-1} H_0(-z) \tag{3.53.a}$$

$$G_0(z) = z^{-1} H_0(z) \tag{3.53.b}$$

$$G_1(z) = H_0(-z) \tag{3.53.c}$$

and the overall response

$$Y(z) = \frac{1}{2}\left\{ H_0{}^2(z) + H_0{}^2(-z) \right\} z^{-1} X(z) \tag{3.54}$$

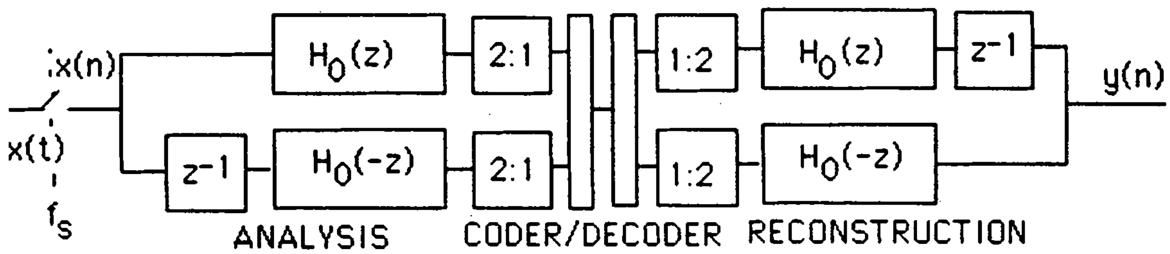

Fig. 3.10 Subband system for odd length linear phase filters

The subband system with filters described by Eq. (3.53) is shown in Fig. 3.10, where the unit delay z^{-1} is shown as a separate operation.

One family of odd length half-band filters that has some interesting properties can be derived by windowing the response of the ideal half-band filter.

$$h_0(n) = h\left(n - \frac{N-1}{2}\right) \tag{3.55.a}$$

where

$$h(n) = \beta \; w(n) \frac{\sin(\pi n/2)}{\pi n/2} \quad \text{for } n = -\frac{N-1}{2}, \ldots, \frac{N-1}{2} \tag{3.55.b}$$

$w(n)$ is a window function and β is the gain normalization factor.

These filters discussed in [19], have $h(n) = 0$ for n even, with $n \neq 0$. This means that almost half of the filter coefficients are zero and therefore the complexity of

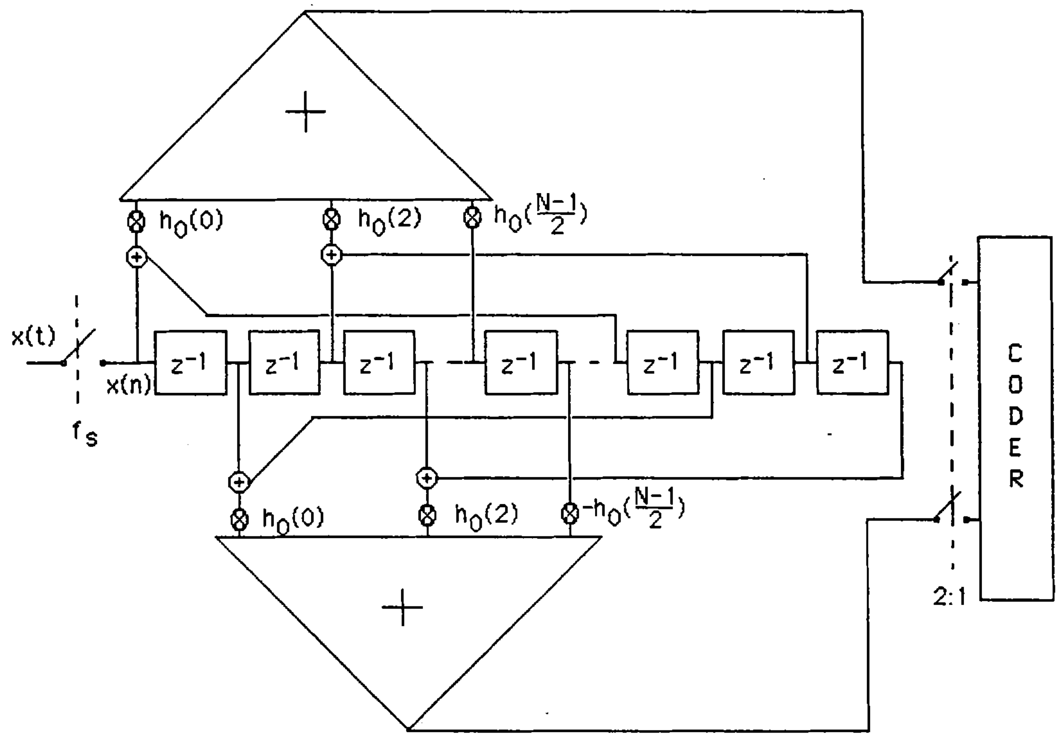

a) Analysis

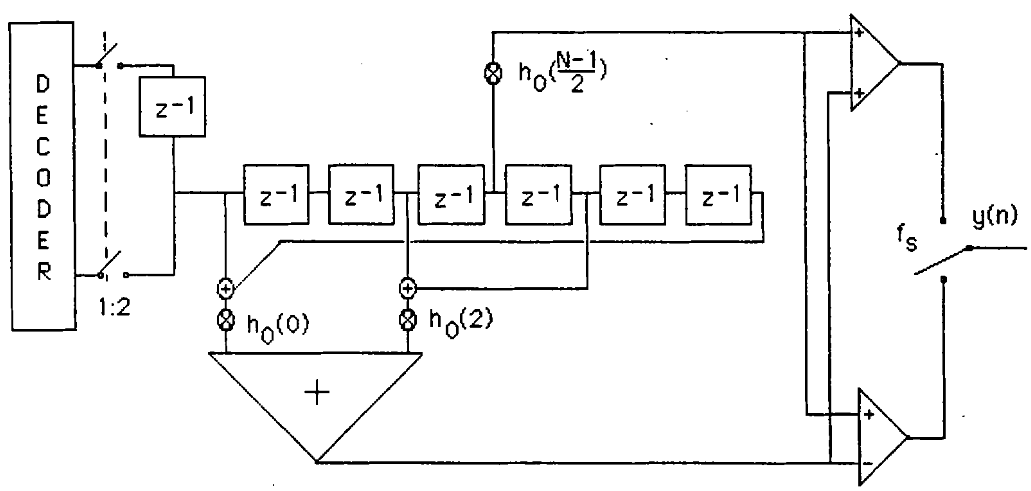

b) Reconstruction

Fig. 3.11 Implementation of the analysis/reconstruction of a two band system with odd length filters the system can be reduced. Figure 3.11 shows an efficient way to implement the analysis and the reconstruction of a two band system with odd length window designed filters. In order to implement an N-tap filter, $(N+3)/4$ multiplications and $(N-1)/4$ additions are required for every second input, which implies that the load is almost half of the load using even length QMF filters. A major drawback though, is that these filters, independently of the shape of the window $w(n)$, have a gain of -6 dB $(1/2)$ at $\omega = \pi/2$ which also makes the overall gain equal to -6 dB at that frequency. Equalization procedures can be used to modify the overall system response, provided that the system remains less complex than systems with even length filters.

Chapter 4 Recursive and Pseudo-QMF Filters

4.1 Introduction

Two major topics related to the design of the analysis and the reconstruction filters of subband coding systems, are to be discussed in this chapter. The first one is based on the work presented by Barnwell [12] and deals with a new family of QMF filters with infinite impulse response (IIR). Unlike the linear phase FIR filters discussed in the previous chapter, the IIR filters can be designed to introduce only phase distortion to the reconstructed signal. For certain applications, where the conservation of the frequency characteristics of the signal is much more important than the conservation of linear phase, the use of IIR filter might be a better alternative.

The second topic of this chapter deals with a new approach to the analysis/reconstruction problem presented by Rothweiler [8] and Nussbaumer [9],[10]. The conventional parallel QMF filter bank is replaced by the so called pseudo-QMF filter bank. Unlike the parallel QMF filter bank which has its filters determined from the half-band filters of the equivalent tree-structure, the pseudo-QMF bank has its bandpass filters derived by frequency translating a single prototype lowpass filter. The "pseudo" name comes from the fact that the new type of filter banks can remove the aliasing due to adjacent bands only.

4.2 IIR-QMF Filters

The idea of designing IIR filters that could be used in a subband system without causing any amplitude distortion or aliasing, was based on the following facts.

1. IIR filters can be considered as the cascade of two filters. One is an all-zero filter which can have linear phase characteristics and the other is an all-pole filter with its poles inside the unit circle for stability.

2. Linear phase filters can provide good isolation between the subbands but cause amplitude distortion when used in a subband system.

3. All-pole filters can be used to equalize any response that does not have zeros on the unit circle.

According to the above, the design of the IIR-QMF filters can be considered as the design of an all-pole equalizer which will remove the amplitude distortion caused by the linear phase QMF filters. Our discussion on IIR-QMF filters is based on results obtained in the previous chapter as part of the discussion on linear phase QMF filters.

First consider the two band system shown in Fig. 3.1 which utilizes even-length linear phase FIR filters. The conditions for an alias-free reconstruction given by Eq. (3.8) are:

$$H_1(z) = H_0(-z) \tag{4.1.a}$$

$$G_0(z) = H_0(z) \tag{4.1.b}$$

$$G_1(z) = -H_0(-z) \tag{4.1.c}$$

where $H_0(z)$ is the lowpass half-band filter. Under the above conditions, the reconstructed signal $Y(z)$ is given by the formula

$$Y(z) = \frac{1}{2}\left\{{H_0}^2(z) - {H_0}^2(-z)\right\}X(z) \tag{4.2}$$

We define the z-transform $F(z)$ to be the cascade of the two lowpass filters

$$\begin{aligned} F(z) &= H_0(z)G_0(z) \\ &= {H_0}^2(z) \end{aligned} \tag{4.3}$$

and the z-transform $R(z)$ to be the overall response of the system (multiplied by 2) such as

$$\begin{aligned} R(z) &= 2\frac{Y(z)}{X(z)} \\ &= {H_0}^2(z) - {H_0}^2(-z) \end{aligned} \tag{4.4}$$

Since $H_0(z)$ has linear phase characteristics $R(z)$ and $F(z)$ also have linear phase characteristics.

The system response $R(z)$ can be expressed in terms of $F(z)$ as

$$R(z) = F(z) - F(-z) \tag{4.5}$$

We also obtain the coefficients of $R(z)$, by considering the inverse z-transform of Eq. (4.5)

$$r(n) = \left\{1 - (-1)^n\right\}f(n) \tag{4.6}$$

where $f(n) = h_0(n) * h_0(n)$. From the above equation, it is clear that

$$r(n) = \begin{cases} 0 & \text{for } n \text{ even} \\ 2f(n) & \text{for } n \text{ odd} \end{cases} \tag{4.7}$$

Our intention is to find an expression for $R(z)$ in terms of its zeros. For this reason, we introduce the z-transform $P(z)$ whose coefficients $p(n)$ are defined as

$$p(n) = 2f(2n+1) \tag{4.8}$$

The system response $R(z)$ can be written in terms of $P(z)$ as

$$R(z) = z^{-1}P(z^2) \tag{4.9}$$

If the lowpass filter $H_0(z)$ has N (even) coefficients, then $F(z)$ will have $2N-1$ (odd) coefficients and $P(z)$ will have $N-1$ (odd) coefficients. $P(z)$ is expected to have an odd-length impulse response because if it was an even-length one, at least one of its zeros would have been on the unit circle ($z=-1$) and the system response $R(z)$ would have had a spectral null at $\omega = \pi/2$.

We like to express the response $P(z)$ in terms of its zeros. $P(z)$, being an odd-length linear phase response, has its complex zeros z_m in groups of four (z_m, z_m^*, $1/z_m, 1/z_m^*$) where z_m^* is the complex conjugate of z_m and its real zeros z_r in groups of two ($z_r, 1/z_r$). In order to include both types of zero-patterns in our expression, we make the assumption that $P(z)$ has a single pair of real zeros, therefore,

$$P(z) = G_a z^{-(4M+2)}(z-z_r)(z-\frac{1}{z_r})\prod_{m=1}^{M}(z-z_m)(z-z_m^*)(z-\frac{1}{z_m})(z-\frac{1}{z_m^*}) \tag{4.10}$$

where M represents the total number of groups with complex zeros and $G_a = p(0)$. Figure 4.1 shows the zero diagram of a typical response $P(z)$.

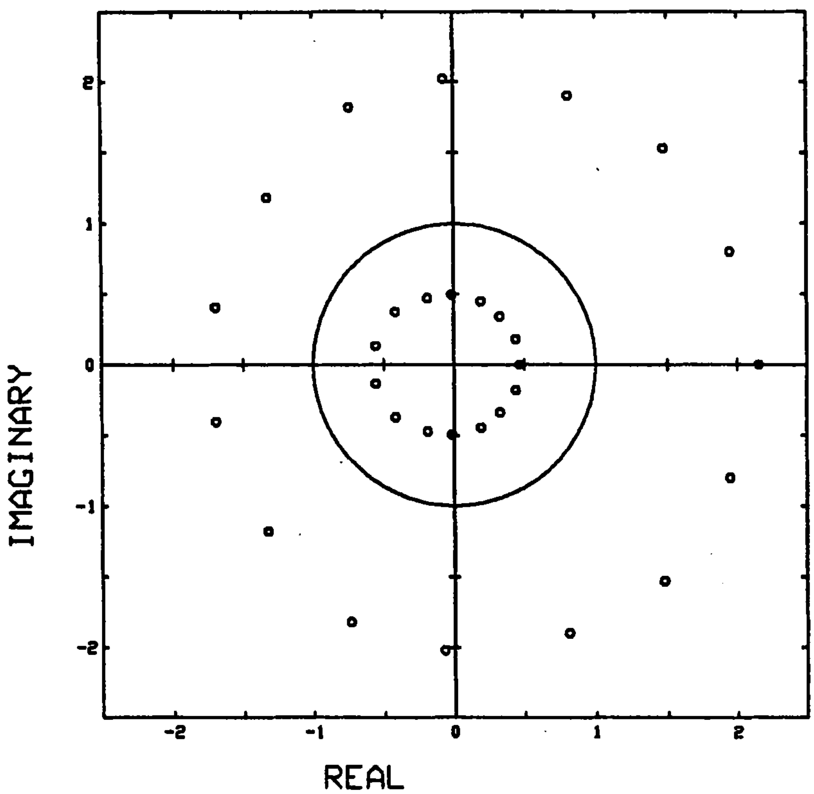

Fig. 4.1 A typical zero-diagram for the response $\tilde{P}(z)$

Referring to Eq. (4.9), the relationship between $R(z)$ and $P(z)$ makes the complex zeros of $R(z)$ to appear in groups of eight ($z_m, -z_m, z_m^*, -z_m^*, 1/z_m, -1/z_m, 1/z_m^*, -1/z_m^*$) and its real zeros in groups of four ($z_r, -z_r, 1/z_r, -1/z_r$). $R(z)$ can be expressed in terms of its zeros as

$$R(z) = G_a z^{-(8M+5)}(z - z_r)(z + z_r)(z - \frac{1}{z_r})(z + \frac{1}{z_r})$$
$$\prod_{m=1}^{M}(z - z_m)(z + z_m)(z - z_m^*)(z + z_m^*)(z - \frac{1}{z_m})(z + \frac{1}{z_m})(z - \frac{1}{z_m^*})(z + \frac{1}{z_m^*}) \tag{4.11}$$

with a typical zero diagram shown in Fig. 4.2.

An all-zero response cannot have flat frequency characteristics. Clearly, if we like to have a response with such characteristics, an all-pole stable equalizer $Q(z)$

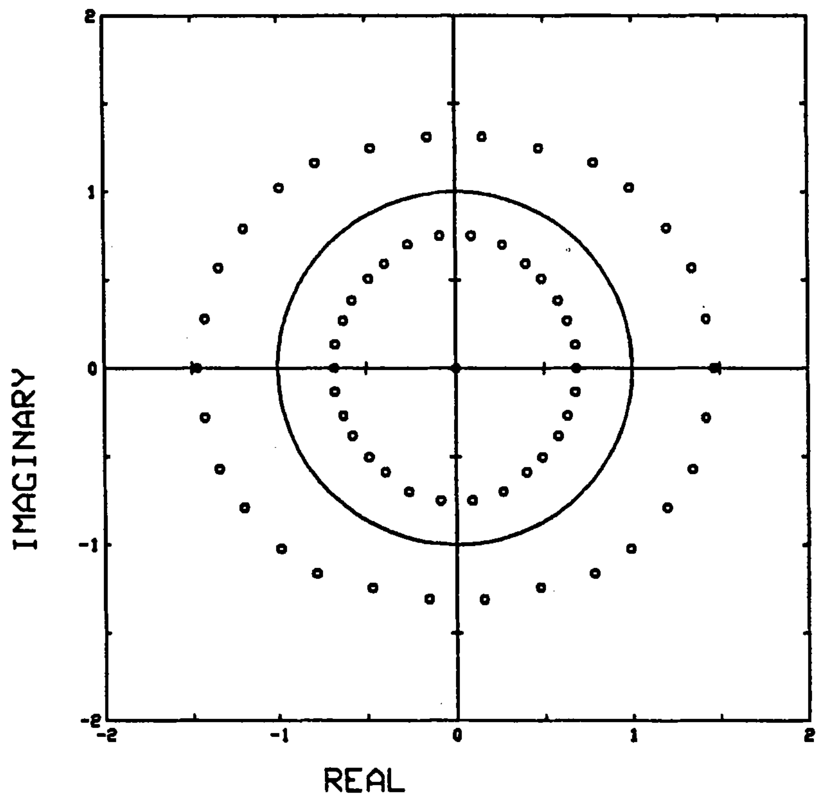

Fig. 4.2 Zero-diagram for a typical system response $R(z)$

must be introduced which will satisfy the following equation.

$$|R(e^{j\omega})Q(e^{j\omega})| = 1 \tag{4.12}$$

In order to design the equalizer $Q(z)$, we consider the system response $R(z)$ as the cascade of two responses, one with minimum phase characteristics $B(z)$ and one maximum phase characteristics $B'(z)$ such as

$$R(z) = G_a z^{-1} B(z) B'(z) \tag{4.13}$$

With no loss of generality, we assume that the zeros z_r and z_m, $m = 1, \ldots, M$ of $R(z)$ occur inside the unit circle. The minimum phase response $B(z)$ has its zeros inside the unit circle and can be expressed as

$$B(z) = z^{-(4M+2)}(z - z_r)(z + z_r) \prod_{m=1}^{M} (z - z_m)(z + z_m)(z - z_m^*)(z + z_m^*) \quad (4.14)$$

The maximum phase response has its zeros outside the unit circle and can be expressed as

$$B'(z) = z^{-(4M+2)}(z - \frac{1}{z_r})(z + \frac{1}{z_r}) \prod_{m=1}^{M} (z - \frac{1}{z_m})(z + \frac{1}{z_m})(z - \frac{1}{z_m^*})(z + \frac{1}{z_m^*}) \quad (4.15)$$

The two responses $B(z)$ and $B'(z)$ are related to each other through the equation

$$B'(z) = G_b z^{-(4M+2)} B(z^{-1}) \quad (4.16)$$

where

$$G_b = -{z_r}^2 \prod_{m=1}^{M} |z_m|^4$$

The equalizer $Q(z)$ can be considered as the cascade of the responses $A(z)$ and $A'(z)$ which equalize $B(z)$ and $B'(z)$ respectively, i.e.

$$Q(z) = \frac{1}{G_a} A(z) A'(z) \quad (4.17)$$

and

$$|B(e^{j\omega})A(e^{j\omega})| = 1 \quad (4.18)$$

$$|B'(e^{j\omega})A'(e^{j\omega})| = 1 \quad (4.19)$$

Consider first the minimum phase response $B(z)$. Since all its zeros occur inside the unit circle, we can define the response $A(z)$ to be its inverse

$$A(z) = \frac{1}{B(z)} \quad (4.20)$$

Clearly, $A(z)$ is stable since it has its poles inside the unit circle. Also, Eq. (4.18) is satisfied.

For the maximum phase response $B'(z)$, since its zeros occur outside the unit circle, its inverse is unstable and it cannot be used as an equalizing response. To obtain the response $A'(z)$, we introduce the one-pole one-zero allpass filter $E_k(z)$ which is defined as

$$E_k(z) = \frac{|z_k|(z - \frac{1}{z_k})}{(z - z_k)} \tag{4.21}$$

$E_k(z)$ is stable only when its pole is inside the unit circle ($|z_k| < 1$) which according to the above definition implies that its zero must be outside the unit circle. The cascade of any number of these one-pole one-zero allpass filters that satisfy Eq. (4.21) have flat frequency characteristics, i.e.

$$\prod_k |E_k(e^{j\omega})| = 1 \tag{4.22}$$

An interesting interpretation that can be given to the above results, is that every zero $1/z_k$ that occurs outside the unit circle can be equalized by a pole z_k inside the unit circle. Therefore, the equalizing response $A'(z)$ must have the form

$$A'(z) = \frac{{z_r}^2 \prod_{m=1}^{M} |z_m|^4}{z^{-(4M+2)}(z - z_r)(z + z_r) \prod_{m=1}^{M} (z - z_m)(z + z_m)(z - z_m^*)(z + z_m^*)} \tag{4.23}$$

Referring to Eq. (4.14), the denominator of the above expression is the definition of the minimum phase response $B(z)$. The response $A'(z)$ can be written as

$$A'(z) = G_b \frac{1}{B(z)} \tag{4.24}$$

If we ignore the gain normalization factors, we can observe that the equalizing responses $A(z)$ and $A'(z)$ are identical.

The equalizer $Q(z)$, being the cascade of $A(z)$ and $A'(z)$ can be expressed in terms of $B(z)$ as

$$Q(z) = \frac{G_b}{G_a} \frac{1}{B^2(z)} \tag{4.25}$$

and can be considered as a single linear filtering operation or as two or more linear filtering operations in cascade. Since the system is designed to remove all the aliasing terms, $Q(z)$ can be implemented at any point prior to the sub-sampling operation or after the interpolation operation. In general, we like the computation load of the system to be evenly distributed among the transmitter and the receiver. If $Q(z)$ is considered as a single filtering operation, it will have to be implemented either at the transmitter prior to sub-sampling or at the receiver after the interpolation, causing an uneven distribution of the computation load. Equation (4.17) can give us a better alternative. Ignoring the gain factors, $Q(z)$ can be considered as the cascade of two all-pole filters $A(z)$ and $A'(z)$ one which can be implemented at the transmitter and one at the receiver. Since these two filters are identical, the computation load is evenly distributed.

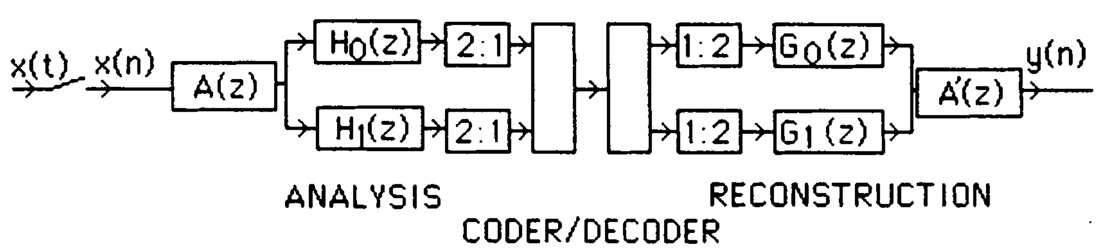

Fig. 4.3 Two band subband system with equalizers

A system which uses equalizers to obtain a flat frequency response is shown in Fig. 4.3. The equalization is done partly by the the filter $A(z)$ at the transmitter and partly by the filter $A'(z)$ at the receiver. One concern though, is how the equalizing filter at the transmitter affects the stopband characteristics of the analysis filters which determine the performance of the system in terms of isolating the two subbands. By evaluating Eq. (4.12) and Eq. (4.17) on the unit circle, the response of the filter $A(e^{j\omega})$ can be expressed in terms of the overall system response $R(e^{j\omega})$ as

$$|A(e^{j\omega})| = G_c \frac{1}{\sqrt{|R(e^{j\omega})|}} \tag{4.26}$$

where G_c is a gain factor. Since $R(e^{j\omega})$ is a non frequency selective function, the filter response $A(e^{j\omega})$ is also non frequency selective, oscillating about the unity-gain line. Obviously, $A(e^{j\omega})$ being a non-perfectly flat response will alter the characteristics of the filters but by no more than the size of its ripples. For a typical linear phase QMF system, the size of the ripple of the overall response is not more than 3 dB and usually much less. This makes the size of the ripple of $A(e^{j\omega})$ approximately 1.5 dB. A typical value for the stopband rejection is 40 dB which implies that by having the equalizing filter at the transmitter, the performance of the system in isolating the subbands although it might improve, will undergo small changes.

The IIR-QMF filters $H_0'(z)$, $H_1'(z)$, $G_0'(z)$, $G_1'(z)$ that can be used in the conventional two band system shown in Fig. 3.1 are obtained using the following equations

$$H_0'(z) = A(z)H_0(z) \tag{4.27.a}$$

$$H_1'(z) = A(z)H_1(z) \tag{4.27.b}$$

$$G_0'(z) = A(z)G_0(z) \tag{4.27.c}$$

$$G_1'(z) = A(z)G_1(z) \tag{4.27.d}$$

Clearly, this system is equivalent to the one shown in Fig. 4.3 and its system response is expected to be flat.

The design procedure for IIR-QMF filters can be summarized into the following steps.

1. Obtain the linear phase filters $H_0(z)$, $H_1(z)$, $G_0(z)$, $G_1(z)$ that satisfy the QMF conditions (Eq. (4.1)) and have the appropriate frequency characteristics.

2. Find the transfer function $R(z)$ as described by Eq. (4.4).

3. Split $R(z)$ into a minimum and maximum phase response $B(z)$ and $B'(z)$ (Eq. (4.14) and Eq. (4.15)) and obtain the all-pole filter $A(z) = 1/B(z)$.

4. Obtain the IIR-QMF filters $H_0'(z)$, $H_1'(z)$, $G_0'(z)$ and $G_1'(z)$ as described by Eq. (4.27).

Referring to Eq. (4.14), the response $B(z)$ can be written in terms of its zeros in a slightly different form

$$B(z) = (1 - {z_r}^2 z^{-2}) \prod_{m=1}^{M} (1 - {z_m}^2 z^{-2})(1 - {z_m^*}^2 z^{-2}) \tag{4.28}$$

This implies that the equalizing filter $A(z)$, being the inverse of $B(z)$ as well as the

IIR-QMF filter $H_0'(z)$ can be expressed as

$$A(z) = \frac{1}{1 - \sum_{m=1}^{2M+1} a_m z^{-2m}} \tag{4.29}$$

$$H_0'(z) = \frac{\sum_{n=0}^{N-1} h_0(n) z^{-n}}{1 - \sum_{m=1}^{2M+1} a_m z^{-2m}} \tag{4.30}$$

where the values of a_m are derived from the zeros z_m and z_r and $h_0(n)$ are the coefficients of the linear phase filter $H_0(z)$. $H_0'(z)$, like any other IIR filter when implemented, requires two delay lines, one for the input samples and one for the output samples. According to the above expression, only every second of the delayed output samples is required to determine the value of the new output. Since the linear filtering operation is followed by a sub-sampling operation which removes all the odd output samples, the above expression indicates that only the even output samples need to be obtained and stored. Clearly, this property of the filters can be used for a computationally efficient implementation of the system.

It appears though, that the implementation complexity of the system is reduced, if the equalization operation is done separately, as shown in Fig. 4.3. Since the denominators of both the highpass and the lowpass filters $H_1'(z)$ and $H_0'(z)$ which correspond to the equalizing function $A(z)$ are the same, they can be implemented once for both filters. This reduces the complexity of the system.

The discussion on equalization can be extended to cover systems which use odd-length linear phase filters such as the one shown in Fig. 3.10. The procedure for designing equalizers for odd-length filters is the same with the one previously described for even-length ones. The only difference is the expression of the overall system response $R(z)$ which is given by the equation

$$R(z) = z^{-1}\Big\{{H_0}^2(z) + {H_0}^2(-z)\Big\} \tag{4.31}$$

where $H_0(z)$ represents an odd-length lowpass half-hand filter with linear-phase.

A special case of odd-length filters with some interesting properties are the ones which are derived by windowing the ideal lowpass half-band filter. A discussion in Section 3.9 has shown that these filters can be implemented in a very efficient way due to the fact that almost half of their coefficients are zeros. Their major disadvantage which is the existence of a -6 dB ripple in the overall response of the system can be eliminated in a very efficient way by using the all-pole equalizers.

According to the study in [12] which tested different subband coding systems with APCM and ADPCM coders on speech signals, the simulation results show that in general no dramatical changes in the system's performance are observed with either FIR or IIR filters. The introduction of IIR filters improves the frequency characteristics but inserts phase distortion to the signal which sometimes affects its quality. A simple rule that can be used to achieve some improvement in the system's performance, is to use IIR filters for the outer stages of tree-structures only. This way they insert only a small phase distortion to the signal with a slight improvement of the system's performance.

4.3 Pseudo-QMF Filter Banks

Consider the subband system shown in Fig. 4.4, where the analysis and the reconstruction of the input signal $x(n)$ is done by two filter banks. This structure is similar to the one shown in Fig. 3.8 for parallel QMF filter banks. As it was mentioned earlier, the difference between the two structures is the way the bandpass filters are obtained. For the new filter banks, which are referred to as "pseudo-QMF banks", all of the bandpass filters are derived by frequency translating a single prototype lowpass filter.

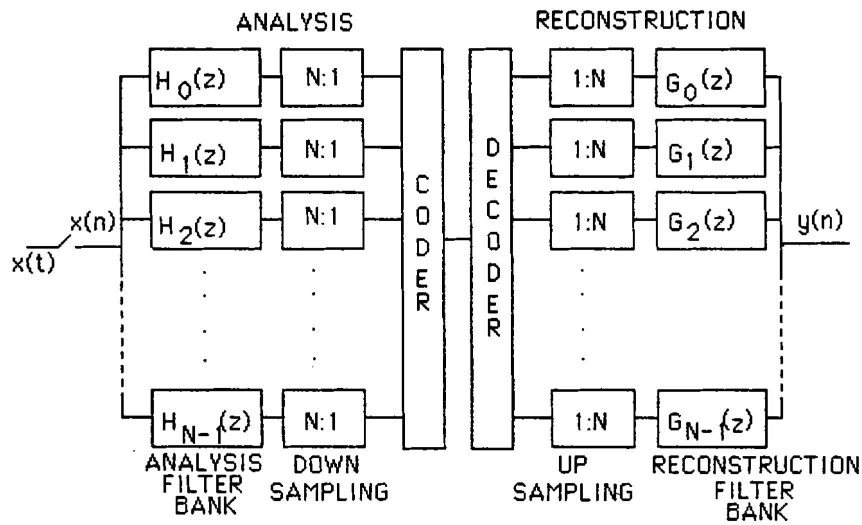

Fig. 4.4 Subband system with parallel filter banks

An idealized L-tap prototype filter $H(z)$ has its frequency response shown in Fig. 4.5. Its cutoff frequency ω_c is given by the formula

$$\omega_c = \frac{\pi}{2N} \tag{4.32}$$

where N is the number of equal-width subbands in the system. The bandpass filters of the analysis and the reconstruction are obtained by frequency translating $H(z)$ using respectively the functions $\cos(\omega_i n + \phi_i)$ and $\cos(\omega_i n + \theta_i)$ to weight the

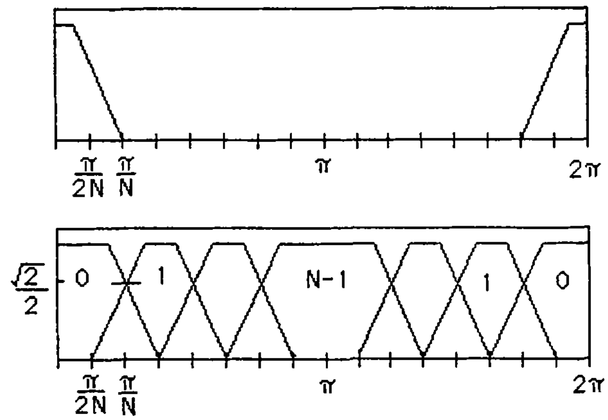

Fig. 4.5 Frequency responses for the prototype and the bandpass filters of a typical pseudo-QMF filter bank

coefficients $h(n)$ where ω_i is the translation frequency for the i'th filter given by

$$\omega_i = \frac{(2i+1)\pi}{2N} \tag{4.33}$$

and ϕ_i and θ_i are phase angles used respectively for the i'th analysis filter $H_i(z)$ and the i'th reconstruction filter $G_i(z)$ so as to remove the aliasing terms. Thus,

$$h_i(n) = h(n)\cos(\omega_i n + \phi_i) \tag{4.34.a}$$

$$g_i(n) = h(n)\cos(\omega_i n + \theta_i) \tag{4.34.b}$$

for $i = 0, 1, \ldots, N-1$.

Taking the z-transforms of the above equations,

$$H_i(z) = \frac{1}{2}\left\{e^{-j\phi_i} H(ze^{j\omega_i}) + e^{j\phi_i} H(ze^{-j\omega_i})\right\} \tag{4.35.a}$$

$$G_i(z) = \frac{1}{2}\left\{e^{-j\theta_i} H(ze^{j\omega_i}) + e^{j\theta_i} H(ze^{-j\omega_i})\right\} \tag{4.35.b}$$

Since these filters belong to the more general category of fractional-band filters, we obtain the z-transform of the output signal $Y(z)$ by using Eq. (2.26).

$$
\begin{aligned}
Y(z) &= \frac{1}{N}\sum_{i=0}^{N-1}\sum_{l=0}^{N-1} X(ze^{-j\frac{2\pi l}{N}})H_i(ze^{-j\frac{2\pi l}{N}})G_i(z) \\
&= \frac{1}{4N}\sum_{i=0}^{N-1}\sum_{l=0}^{N-1} X(ze^{-j\frac{2\pi l}{N}}) \\
&\qquad \Big\{e^{-j(\phi_i+\theta_i)}H(ze^{j(\omega_i-\frac{2\pi l}{N})})H(ze^{j\omega_i}) \\
&\qquad + e^{-j(\phi_i-\theta_i)}H(ze^{j(\omega_i-\frac{2\pi l}{N})})H(ze^{-j\omega_i}) \\
&\qquad + e^{j(\phi_i-\theta_i)}H(ze^{-j(\omega_i+\frac{2\pi l}{N})})H(ze^{j\omega_i}) \\
&\qquad + e^{j(\phi_i+\theta_i)}H(ze^{-j(\omega_i+\frac{2\pi l}{N})})H(ze^{-j\omega_i})\Big\}
\end{aligned}
\tag{4.36}
$$

For alias-free reconstruction, all the terms for which $l \neq 0$ must cancel. This condition is insured by eliminating the aliasing due to adjacent filters and designing the prototype lowpass filter $H(z)$ in such a way so that nonadjacent bandpass filters do not have overlapping responses.

$$
H(e^{j\alpha}) = 0 \quad |\alpha| > \frac{\pi}{N} \text{ given } |\alpha| < 2N \tag{4.37}
$$

Thus,

$$
H(e^{j\alpha})H(e^{j\beta}) = 0 \quad \frac{2\pi}{N} \le |\alpha - \beta| \le \frac{2\pi(N-1)}{N} \tag{4.38}
$$

The corresponding values of α and β for the four different sets of terms in Eq. (4.36) as well as the conditions for the terms that do not cancel are given in

	$H(ze^{j\alpha})$ α	$H(ze^{j\beta})$ β	$\alpha - \beta$	No cancellation condition
1	$\omega_i - \frac{2\pi l}{N}$	ω_i	$-\frac{2\pi l}{N}$	$l = 0$
2	$\omega_i - \frac{2\pi l}{N}$	$-\omega_i$	$\frac{\pi}{N}(2i - 2l + 1)$	$l = (i+1)_N,\ l = i$
3	$-\omega_i - \frac{2\pi l}{N}$	ω_i	$-\frac{\pi}{N}(2i + 2l + 1)$	$l = (-1-i)_N,\ l = (-i)_N$
4	$-\omega_i - \frac{2\pi l}{N}$	$-\omega_i$	$-\frac{2\pi l}{N}$	$l = 0$

Note: $\omega_i = \frac{\pi}{2N}(2i+1)$

Table 4.1 Conditions on l and i for the terms in Eq. (4.36) that do not cancel

Table 4.1. The output signal $Y(z)$ can be then expressed as

$$
\begin{aligned}
Y(z) = \frac{1}{4N}\Big\{ & \sum_{i=0}^{N-1} e^{-j(\phi_i+\theta_i)} H^2(ze^{j\omega_i}) + e^{j(\phi_i+\theta_i)} H^2(ze^{-j\omega_i}) \\
& + \sum_{i=0}^{N-2} e^{-j(\phi_i-\theta_i)} H(ze^{-j\omega_{i+1}}) H(ze^{-j\omega_i}) X(ze^{-j(\omega_i+\omega_{i+1})}) \\
& + \sum_{i=1}^{N-1} e^{-j(\phi_i-\theta_i)} H(ze^{-j\omega_{i-1}}) H(ze^{-j\omega_i}) X(ze^{-j(\omega_{i-1}+\omega_i)}) \\
& + \sum_{i=0}^{N-2} e^{j(\phi_i-\theta_i)} H(ze^{j\omega_{i+1}}) H(ze^{j\omega_i}) X(ze^{j(\omega_i+\omega_{i+1})}) \\
& + \sum_{i=1}^{N-1} e^{j(\phi_i-\theta_i)} H(ze^{j\omega_{i-1}}) H(ze^{j\omega_i}) X(ze^{j(\omega_{i-1}+\omega_i)})
\end{aligned} \tag{4.39}
$$

$$+e^{-j(\phi_0-\theta_0)} H(ze^{j\omega_0}) H(ze^{-j\omega_0}) X(z)$$

$$+e^{-j(\phi_{N-1}-\theta_{N-1})} H(ze^{j\omega_{N-1}}) H(ze^{-j\omega_{N-1}}) X(z)$$

$$+e^{j(\phi_0-\theta_0)} H(ze^{-j\omega_0}) H(e^{j\omega_0}) X(z)$$

$$+e^{j(\phi_{N-1}-\theta_{N-1})} H(ze^{-j\omega_{N-1}}) H(ze^{j\omega_{N-1}}) X(z) \Big\}$$

In order to remove the aliasing and have flat overall response, the following equations must be satisfied

$$\phi_{i+1} - \theta_{i+1} = \phi_i - \theta_i + (2k+1)\pi \tag{4.40.a}$$

$$\phi_i + \theta_i = 2k\pi \tag{4.40.b}$$

for $i = 0, 1, \ldots, N-1$.

One possible solution to the above set of equations that was suggested by Nussbaumer [10], can be obtained by allowing

$$\phi_i = -\frac{(2i+1)\pi}{4} \tag{4.41.a}$$

$$\theta_i = \frac{(2i+1)\pi}{4} \tag{4.41.b}$$

This yields the following reconstructed signal

$$Y(z) = \frac{1}{4N} X(z) \sum_{i=0}^{N-1} \Big\{ H^2(ze^{j\omega_i}) + H^2(ze^{-j\omega_i}) \Big\} \tag{4.42}$$

Thus, the overall system response $R(z)$ is given by

$$\begin{aligned} R(z) &= \frac{Y(z)}{X(z)} \\ &= \frac{1}{4N} \sum_{i=0}^{N-1} \Big\{ H^2(ze^{j\omega_i}) + H^2(ze^{-j\omega_i}) \Big\} \end{aligned} \tag{4.43}$$

To examine the frequency characteristics we evaluate $R(z)$ on the unit circle

$$R(e^{j\omega}) = \frac{1}{4N}\sum_{i=0}^{N-1}\left\{H^2(e^{j(\omega-\omega_i)}) + H^2(e^{j(\omega+\omega_i)})\right\}$$
$$= \frac{1}{4N}\sum_{i=0}^{N-1}\left\{e^{-j(L-1)(\omega-\omega_i)}H^2(\omega-\omega_i) + e^{-j(L-1)(\omega+\omega_i)}H^2(\omega+\omega_i)\right\} \tag{4.44}$$

where $H(\omega) = |H(e^{j\omega})|$. The length of the filter L must be chosen so as to avoid any spectral nulls due to the phase characteristics of $H(e^{j\omega})$. For $\omega = 0$ $(z = 1)$, only the $i = 0$ terms of the above equation contribute to the gain which becomes

$$R(1) = e^{j(L-1)\frac{\pi}{2N}}H^2(-\frac{\pi}{2N}) + e^{-j(L-1)\frac{\pi}{2N}}H^2(\frac{\pi}{2N}) \tag{4.45}$$

Clearly, L must be an odd number so as to avoid a spectral null at $\omega = 0$.

A flat frequency response can be established if the following condition is satisfied

$$\frac{1}{4N}\sum_{i=0}^{N-1}\left\{H^2(\omega-\omega_i) + H^2(\omega+\omega_i)\right\} = 1 \tag{4.46}$$

This implies that the frequency characteristics of the prototype filter must satisfy the equation

$$H(\omega) = \begin{cases} 1 & \text{for } |\omega| < \frac{\pi}{2N} \\ \frac{\sqrt{2}}{2} & \text{for } |\omega| = \frac{\pi}{2N} \\ 0 & \text{elsewhere} \end{cases} \tag{4.47}$$

in the region $|\omega| \leq \pi$. Clearly, the above conditions can not be exactly satisfied by a causal FIR filter. As a result, the reconstructed signal will suffer from amplitude distortion as well as aliasing due to non adjacent subbands. For this reason, the design of the prototype filter $H(z)$ should be based on minimizing the level of distortion due to the above two sources. A filter design method similar to the one used by Johnston to design half-band QMF filters [6] could be used, with the only difference being that the stopband rejection in the region $\pi/N < |\omega| < \pi$ should be more weighted than the stopband rejection in the region $\pi/2N < |\omega| < \pi/N$ so as to minimize the terms that cause aliasing.

It is possible to implement a pseudo-QMF filter bank with a polyphase network and an FFT by using only one half of the computations required for the previously discussed parallel QMF filter bank. The method that is described in [10],[9] takes advantage of the fact that all the filters are derived from a single prototype one. According to the first study, the results from simulation experiments that were conducted, show that with the pseudo-QMF banks, the original signal is nearly perfectly reconstructed at the receiver with maximum amplitude distortion equal to 0.2 dB. Also, the rejection of the main aliasing term is in excess of 40 dB when the prototype filter has 65 taps.

Chapter 5 Exact Reconstruction Filter Banks

5.1 Introduction

The work presented in this chapter is based on a recent paper by Smith and Barnwell [14], in which the basic steps to design a reversible subband system were shown. Smith and Barnwell developed the conditions for reversibility, using non-causal filters for the analysis and the reconstruction of the input signal. Causality is required though, if the system is to be actually designed and tested. Taking the basic idea from this paper but using causal filters, we develop new conditions for a reversible causal system which in turn are used to actually design systems. To satisfy these conditions, a new family of quadrature mirror filters is introduced with finite impulse response but nonlinear phase. One of its important characteristics, is that the impulse responses of the reconstruction filters are the time-reversals of the impulse responses of the analysis filters. For this reason these filters are called *time-reversed QMF filters.*

In Chapter 3, we have discussed the conditions on the analysis/reconstruction filters under which the aliasing introduced by a two band subband system can be removed. According to these conditions which are given by Eq. (3.3), two of the four analysis/reconstruction filters should be defined in terms of the other two. Given that the alias-free conditions are satisfied, the overall system response which is given by Eq. (3.4) has linear phase characteristics, if the nonaliasing terms of each individual channel have also linear phase characteristics.

Linear phase QMF filters satisfy the conditions for an alias-free linear phase system response since all four filters are defined in terms of a single linear phase prototype one. This constraint though, introduces amplitude distortion to the system response. The fact that each of the four filters is a linear phase filter, is a sufficient but not a necessary condition for the system to have linear phase response. This implies that it is possible to remove the additional constraint of linear phase filters and still have a system response with linear phase and possibly without any amplitude distortion.

The cascade of two time-reversed filters with arbitrary phase characteristics has always linear phase characteristics. By using time-reversed filters in a subband system, the nonaliasing terms of each individual channel have linear phase which is a necessary and sufficient condition for the system response to also have linear phase. However, since the linear phase constraint on the individual filters is not required, other constraints can be imposed on the filters which will remove the amplitude distortion from the system response as well.

5.2 Time-Reversed Filters

Consider the equal length finite impulse response filters $H_0(z)$ and $G_0(z)$ defined as

$$H_0(z) = \sum_{n=0}^{N-1} h_0(n) z^{-n} \tag{5.1.a}$$

$$G_0(z) = \sum_{n=0}^{N-1} g_0(n) z^{-n} \tag{5.1.b}$$

By definition, the two filters are time-reversals of each other if

$$g_0(n) = h_0(N-1-n) \quad \text{for } n = 0, ..., N-1 \tag{5.2}$$

giving

$$\begin{aligned} G_0(z) &= \sum_{n=0}^{N-1} h_0(N-1-n) z^{-n} \\ &= z^{-(N-1)} \sum_{n=0}^{N-1} h_0(N-1-n) z^{N-1-n} \end{aligned} \tag{5.3}$$

By making the substitution $u = N-1-n$ we get

$$\begin{aligned} G_0(z) &= z^{-(N-1)} \sum_{u=0}^{N-1} h_0(u) z^{u} \\ &= z^{-(N-1)} H_0(z^{-1}) \end{aligned} \tag{5.4}$$

We are interested on the frequency and phase characteristics of the two filters. The frequency response of the filter $H_0(z)$ is given by

$$\begin{aligned} H_0(e^{j\omega}) &= H_R(\omega) + jH_I(\omega) \\ &= H_0(\omega) e^{j\phi(\omega)} \end{aligned} \tag{5.5}$$

where,

$$H_R(\omega) = \mathrm{Re}\{H_0(e^{j\omega})\} \tag{5.6.a}$$

$$H_I(\omega) = \mathrm{Im}\{H_0(e^{j\omega})\} \tag{5.6.b}$$

$$H_0(\omega) = |H_0(e^{j\omega})| = \sqrt{H_R^2(\omega) + H_I^2(\omega)} \tag{5.6.c}$$

$$\phi(\omega) = \tan^{-1}\left\{\frac{H_I(\omega)}{H_R(\omega)}\right\} \tag{5.6.d}$$

Note again the distinction in terms of argument between the filter response $H_0(e^{j\omega})$ and its absolute value $H_0(\omega)$.

Using Eq. (5.4), we can express the frequency response of $G_0(z)$ in terms of $H_0(\omega)$ and $\phi(\omega)$. We assume that $H_0(z)$ has real coefficients. This makes $H_0(\omega)$ an *even* function and $\phi(\omega)$ an *odd* function. For $z = e^{j\omega}$,

$$\begin{aligned} G_0(e^{j\omega}) &= e^{-j\omega(N-1)} H_0(e^{-j\omega}) \\ &= H_0(-\omega) e^{j\{-\omega(N-1)+\phi(-\omega)\}} \\ &= H_0(\omega) e^{-j\{\omega(N-1)+\phi(\omega)\}} \end{aligned} \tag{5.7}$$

Equation (5.7) shows that both $H_0(z)$ and $G_0(z)$ have the same amplitude characteristics and the phase characteristics are mirror image to each other with respect to the line $\omega(N-1)/2$. The important fact about time-reversed filters is that, although the individual filters might not have linear phase characteristics, their cascade form has linear phase, i.e.

$$H_0(e^{j\omega}) G_0(e^{j\omega}) = H_0{}^2(\omega) e^{-j\omega(N-1)} \tag{5.8}$$

5.3 Time-Reversed Filters in Subband Systems

Consider again the two band subband system shown in Fig. 3.1. The overall response as given by Eq. (3.1) is equal to,

$$\begin{aligned} Y(z) =& \frac{1}{2}\Big\{H_0(z)G_0(z) + H_1(z)G_1(z)\Big\}X(z) \\ &+ \frac{1}{2}\Big\{H_0(-z)G_0(z) + H_1(-z)G_1(z)\Big\}X(-z) \\ =& \frac{1}{2}R(z)X(z) + \frac{1}{2}S(z)X(-z) \end{aligned} \tag{5.9}$$

where,

$$R(z) = H_0(z)G_0(z) + H_1(z)G_1(z) \tag{5.10.a}$$

$$S(z) = H_0(-z)G_0(z) + H_1(-z)G_1(z) \tag{5.10.b}$$

$H_0(z)$ is a lowpass FIR half-band filter with N coefficients. We define $G_0(z)$ to be the time-reversal of $H_0(z)$,

$$G_0(z) = z^{-(N-1)}H_0(z^{-1}) \tag{5.11.a}$$

To obtain an alias-free reconstruction, we allow the highpass filters $H_1(z)$ and $G_1(z)$ to be defined in terms of $H_0(z)$ as,

$$G_1(z) = H_0(-z) \tag{5.11.b}$$

$$H_1(z) = -(-z)^{-(N-1)}H_0(-z^{-1}) \tag{5.11.c}$$

Under these conditions, $S(z) = 0$ and is independent of the number of coefficients N. Also, the overall response becomes $\frac{1}{2}R(z)$, where

$$\begin{aligned} R(z) &= H_0(z)G_0(z) + H_1(z)G_1(z) \\ &= z^{-(N-1)}H_0(z)H_0(z^{-1}) - (-z)^{-(N-1)}H_0(-z)H_0(-z^{-1}) \\ &= z^{-(N-1)}\left\{H_0(z)H_0(z^{-1}) + (-1)^N H_0(-z)H_0(-z^{-1})\right\} \\ &= z^{-(N-1)}\left\{F_0(z) + (-1)^N F_0(-z)\right\} \end{aligned} \tag{5.12}$$

and

$$F_0(z) = H_0(z)H_0(z^{-1}) \tag{5.13}$$

The z-transform $F_0(z)$ which we will be referring to as the *cascade filter response* is defined as

$$F_0(z) = \sum_{n=-(N-1)}^{N-1} f_0(n) z^{-n} \tag{5.14}$$

where

$$\begin{aligned} f_0(n) &= h_0(n) * h_0(-n) \\ &= \sum_{u=0}^{N-1} h_0(u) h_0(u-n) \quad \text{for} \quad n = -(N-1), \ldots, N-1. \end{aligned}$$

Note that $F_0(z)$ has a zero phase frequency response, i.e. $f_0(n) = f_0(-n)$.

5.4 Reversibility

The reversibility (exact reconstruction) condition requires that

$$R(z) = z^{-k} \tag{5.15}$$

Referring to Eq. (5.12), since $F_0(z)$ is a zero phase response, this is possible only if

$$F_0(z) + (-1)^N F_0(-z) = 1 \tag{5.16}$$

which makes $k = N - 1$. The z-transform $F_0(-z)$ is defined in terms of $f_0(n)$ as

$$F_0(-z) = \sum_{n=-(N-1)}^{N-1} f_0(n)(-1)^n z^{-n} \tag{5.17}$$

To establish the conditions on $f_0(n)$, under which Eq. (5.16) is satisfied, the inverse z-transform of Eq. (5.16) is considered,

$$f_0(n) + (-1)^{N+n} f_0(-n) = \delta(n) \tag{5.18}$$

At this point, we can establish the values of N for which exact reconstruction can be achieved. For $n = 0$ we have,

$$f_0(0)\left\{1 + (-1)^N\right\} = 1 \tag{5.19}$$

Clearly, Eq. (5.19) and therefore Eq. (5.18) can be true only for *even* values of N. This implies that odd length time-reversed filters cannot be used for exact reconstruction. From now on, we will consider only even length time-reversed filters and the exact reconstruction Eq. (5.16) and Eq. (5.18) are simplified to

$$F_0(z) + F_0(-z) = 1 \tag{5.20}$$

and

$$f_0(n)\left\{1 + (-1)^n\right\} = \delta(n) \tag{5.21}$$

The conditions on $f_0(n)$ so that Eq. (5.21) is true are

$$f_0(n) = \begin{cases} 0 & \text{for } n \text{ even with } n \neq 0 \\ \frac{1}{2} & \text{for } n = 0 \end{cases} \tag{5.22}$$

given that $-(N-1) \leq n \leq N-1$.

Any cascade filter response with coefficients of the form

$$f_0(n) = w(n)\frac{\sin(\pi n/2)}{\pi n} \tag{5.23}$$

where $w(n)$ is a window function, will satisfy the conditions set by Eq. (5.22) for exact reconstruction. These conditions though, are not the only requirements for the design of a reversible subband system since, the cascade filter response $F_0(z)$ is defined by Eq. (5.13) as the product of two time-reversed filters. In order to design the subband system, we must be able to find a cascade filter response with odd numbered coefficients of such values that it can be decomposed into two time-reversed filters.

5.5 Subband Filter Design

The coefficients of the filters of a subband system can be expressed in terms of the coefficients of the filter $H_0(z)$, therefore, we must concentrate only on the design of a finite impulse response lowpass filter. In the design procedure, we must consider two things. First, the frequency characteristics of the filter in terms of the bandpass and stopband ripple, the transition band width and the filter length N. Second, the conditions the filter must satisfy for perfect reconstruction which were discussed in the previous section and are described by the equation

$$h_0(n) * h_0(-n) = w(n)\frac{\sin(\pi n/2)}{\pi n} \tag{5.24}$$

where, $h_0(n)$ is the nth coefficient of $H_0(z)$, the $*$ corresponds to a convolution operation, i.e.

$$h_0(n) * h_0(-n) = \sum_{n=0}^{N-1} h_0(u)h_0(u-n)$$

and $w(n)$ is a weighting function with nonzero values in the region $-(N-1) \leq n \leq (N-1)$ that are defined by the frequency characteristics of the filter.

The approach to the design of $H_0(z)$ is an indirect one. Instead of directly attempting the design of $H_0(z)$, we will design the cascade filter response $F_0(z)$ as a first step and then decompose it into two time-reversed filters.This approach requires the establishment of three major criteria.

1. The coefficients $f_0(n)$ of the cascade filter response $F_0(z)$ must satisfy Eq. (5.22).

2. $F_0(z)$ can be decomposed into two time-reversed filters according to Eq. (5.13).

3. The frequency characteristics of $F_0(z)$ as well as its length must be such, so that the decomposed filters will have the specified frequency characteristics and length.

5.5.1 Decomposition of $F_0(z)$

To establish the conditions under which $F_0(z)$ can be decomposed into two time-reversed filters, we consider the zeros and the poles of the z-transform of the filter. $H_0(z)$ is an $N-1$ degree polynomial and can be written in terms of its zeros and poles as

$$\begin{aligned} H_0(z) &= \sum_{n=0}^{N-1} h_0(n) z^{-n} \\ &= G_a z^{-(N-1)} \prod_{m=1}^{N-1} (z - z_m) \end{aligned} \tag{5.25}$$

where $G_a = h_0(0)$ and z_m is the mth zero. $H_0(z)$ has $N-1$ poles at $z=0$ and $N-1$ zeros. Since the coefficients $h_0(n)$ are real, the zeros z_m appear in complex conjugate pairs. Also, it is required that N should be an even number which means that the number of zeros should be odd and at least one zero (in general an odd number of zeros) must be real. For simplicity, we assume that $H_0(z)$ has only one real zero which we refer to as z_r. Equation (5.25) can be written in terms of its zeros in conjugate pairs as

$$H_0(z) = G_a z^{-(N-1)} (z - z_r) \prod_{m=0}^{N/2-1} (z - z_m)(z - z_m^*) \tag{5.26}$$

where z_m^* is the complex conjugate of z_m.

The time-reversed filter $H_0(z^{-1})$ can be written as

$$\begin{aligned} H_0(z^{-1}) &= G_a z^{N-1}(z^{-1} - z_r) \prod_{m=0}^{N/2-1} (z^{-1} - z_m)(z^{-1} - z_m^*) \\ &= G_b(z - \frac{1}{z_r}) \prod_{m=0}^{N/2-1} (z - \frac{1}{z_m})(z - \frac{1}{z_m^*}) \end{aligned} \tag{5.27}$$

where $G_b = h_0(N-1)$. Referring to Eq. (5.13), the cascade filter response $F_0(z)$ can be written in terms of the filter zeros z_m as

$$\begin{aligned} F_0(z) &= H_0(z)H_0(z^{-1}) \\ &= G_a G_b z^{-(N-1)}(z - z_r)(z - \frac{1}{z_r}) \prod_{m=0}^{N/2-1} (z - z_m)(z - z_m^*)(z - \frac{1}{z_m})(z - \frac{1}{z_m^*}) \end{aligned} \tag{5.28}$$

According to Eq. (5.28), $F_0(z)$ can be decomposed into two time-reversed filters, if the complex roots z_m appear in groups of four $(z_m, z_m^*, 1/z_m, 1/z_m^*)$ and the real roots z_r appear in groups of two $(z_r, 1/z_r)$.

A response that appears to meet these requirements is the linear phase one. In general, a linear phase response has its zeros in groups of four $(z_m, z_m^*, 1/z_m, 1/z_m^*)$ for $|z_m| \neq 1$, in groups of two (z_m, z_m^*) for $|z_m| = 1$, in groups of two $(z_m, 1/z_m)$ for z_m real with $|z_m| \neq 1$ and in groups of one for $z_m = \pm 1$. According to the Table 5.1, which considers the properties of a typical linear phase response versus the properties of a decomposable response in terms of zero-patterns, the linear phase filter that meets the requirements of Eq. (5.28) has,

1. Double zeros on the unit circle ($|z| = 1$), so that all the complex pairs appear in groups of four.

Position of zeros z_m	Typical linear phase response		Decomposable response		Comments
	zeros per group	Locations	zeros per group	Locations	
$\|z_m\| \neq 1$ z_m complex	4	$z_m,\ z_m^*$ $\frac{1}{z_m},\ \frac{1}{z_m^*}$	4	$z_m,\ z_m^*$ $\frac{1}{z_m},\ \frac{1}{z_m^*}$	
$\|z_m\| \neq 1$ z_m real	2	$z_m, \frac{1}{z_m}$	2	$z_m, \frac{1}{z_m}$	
$\|z_m\| = 1$ z_m complex	2	z_m, z_m^*	2 double	z_m, z_m^*	$\frac{1}{z_m} = z_m^*$ $\frac{1}{z_m^*} = z_m$
$\|z_m\| = 1$ z_m real	1	1 or -1	1 double	-1	for lowpass response

Table 5.1 Zero-patterns of a typical linear phase response versus a decomposable response

2. Double zero at $z = -1$. Note that $F_0(z)$ has no zeros at $z = 1$ since it has lowpass characteristics.

3. No restrictions regarding the real value zeros and the complex ones which are not on the unit circle.

In general, we can state that a linear phase response is decomposable only if the zeros on the unit circle are double. A zero-plot of a lowpass linear phase response that has double zeros on the unit circle is shown in Fig. 5.1.

The requirement of double zeros on the unit circle will have certain implications

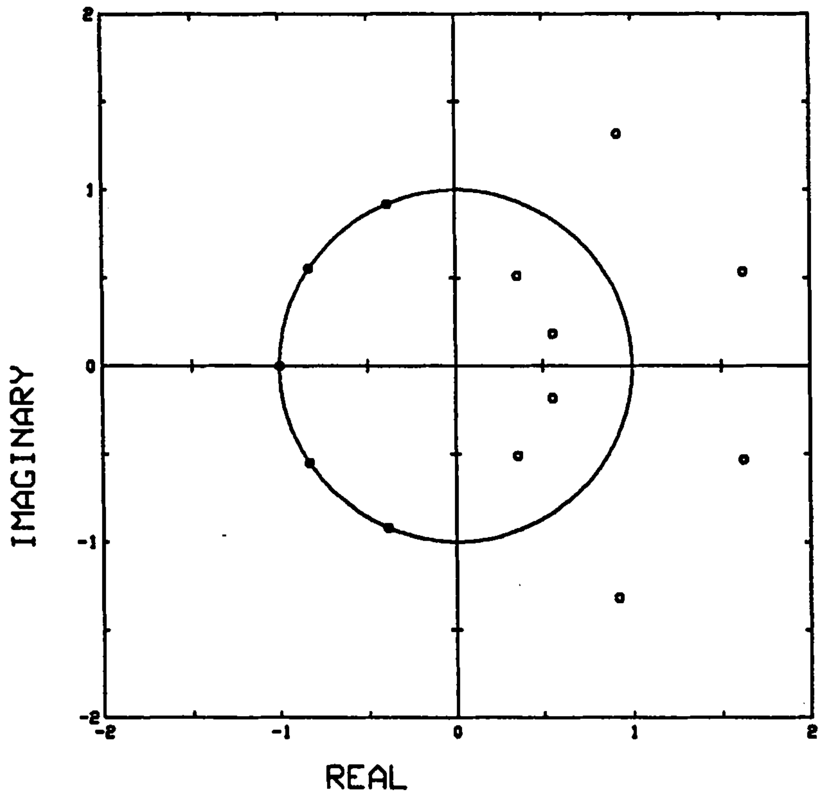

Fig. 5.1 Zero-plot of a lowpass linear phase decomposable response

on the frequency characteristics of $F_0(z)$. For $z = e^{j\omega}$,

$$
\begin{aligned}
F_0(e^{j\omega}) &= H_0(e^{j\omega})H_0(e^{-j\omega}) \\
&= H_0(\omega)e^{j\phi(\omega)}H_0(\omega)e^{-j\phi(\omega)} \qquad (5.29) \\
&= {H_0}^2(\omega)
\end{aligned}
$$

Assume that a zero occurs at $\omega = \omega_k$ such as, $H_0(\omega_k) = 0$ as well as $F_0(e^{j\omega_k}) = 0$. We define $F_0'(e^{j\omega})$ as the first derivative of $F_0(e^{j\omega})$ with respect to ω and is equal to

$$
\begin{aligned}
F_0'(e^{j\omega}) &= \frac{d\{F_0(e^{j\omega})\}}{d\omega} \\
&= 2H_0(\omega)\frac{d\{H_0(\omega)\}}{d\omega}
\end{aligned}
\qquad (5.30)
$$

Since $H_0(\omega_k) = 0$, the first derivative $F_0'(e^{j\omega_k}) = 0$. A typical lowpass frequency

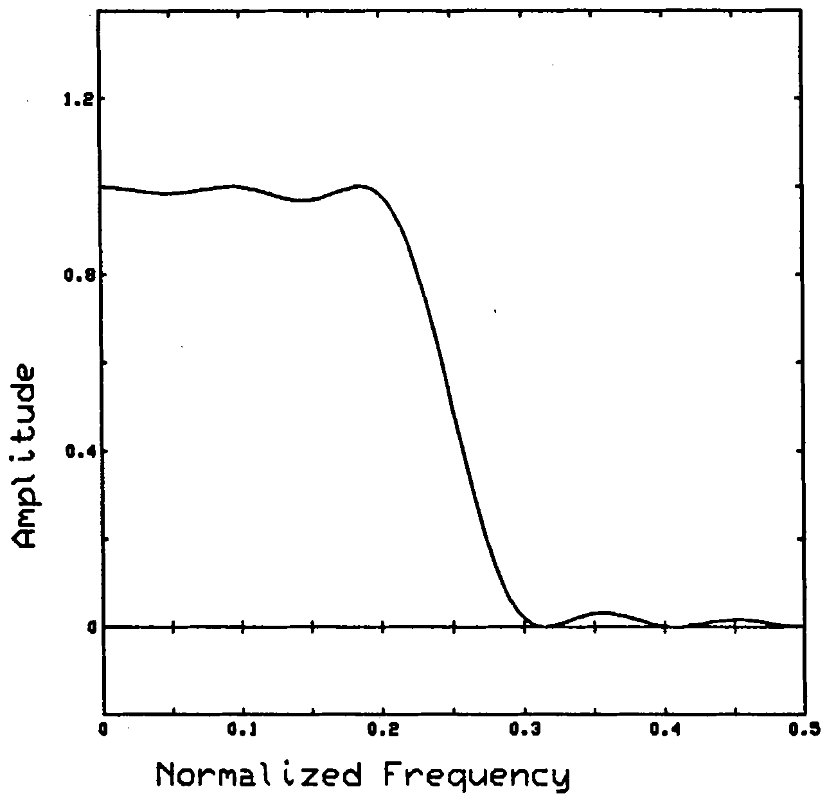

Fig. 5.2 Frequency response of a lowpass decomposable response

response which has double zeros on the unit circle, is shown in Fig. 5.2. As a result of the double zeros, the ω-axis is tangent to response curve at the points where the double zeros occur. Due to the fact that all the zeros on the unit circle are double, the response curve never crosses the ω-axis.

5.5.2 Transformation of filter characteristics

The design of $F_0(z)$ is an intermediate stage to the design of the filter $H_0(z)$ and for this reason the characteristics of $F_0(z)$ must be specified in terms of the characteristics of $H_0(z)$. If the number of coefficients in $F_0(z)$ is L and the number of coefficients in $H_0(z)$ is N, then

$$L = 2N - 1 \tag{5.31}$$

since $F_0(z)$ is the cascade of $H_0(z)$ and $H_0(z^{-1})$.

The transformation of the frequency characteristics can be established using Eq. (5.29). Since $F_0(e^{j\omega}) = {H_0}^2(\omega)$, the transformation is straight forward. For example, if the stopband rejection is A dB, then $F_0(z)$ must be designed with stopband rejection of $2A$ dB.

We should note here, that the requirements for exact reconstruction impose certain constraints on the frequency characteristics of the filters which should be violated. For example, the gain at $\omega = \pi/2$ which should be -3 dB and the bandpass ripple which, as we will show in the next section, should be the same as the stopband ripple.

5.5.3 Constraints on the values of $f_0(n)$

The conditions on the values of the coefficients $f_0(n)$ for exact reconstruction are given by Eq. (5.22). Obviously, the fact that all the even numbered coefficients have specified values, i.e.

$$f_0(2n) = \begin{cases} \frac{1}{2} & \text{for } n = 0 \\ 0 & \text{for } n \neq 0 \end{cases} \tag{5.32}$$

will affect the frequency characteristics of $F_0(z)$. In order to establish a design procedure for $F_0(z)$, it is important to know how the above conditions affect its frequency characteristics. For this reason, we consider the zero phase response

$V(z)$ with coefficients that satisfy the equation,

$$v(n) = f_0(n) - \frac{1}{2}\delta(n) \tag{5.33}$$

Clearly $v(2n) = 0$ and the frequency response $V(\omega)$ can be written as

$$V(\omega) = 2 \sum_{k=0}^{N/2-1} f_0(2k+1)\cos\{(2k+1)\omega\} \tag{5.34}$$

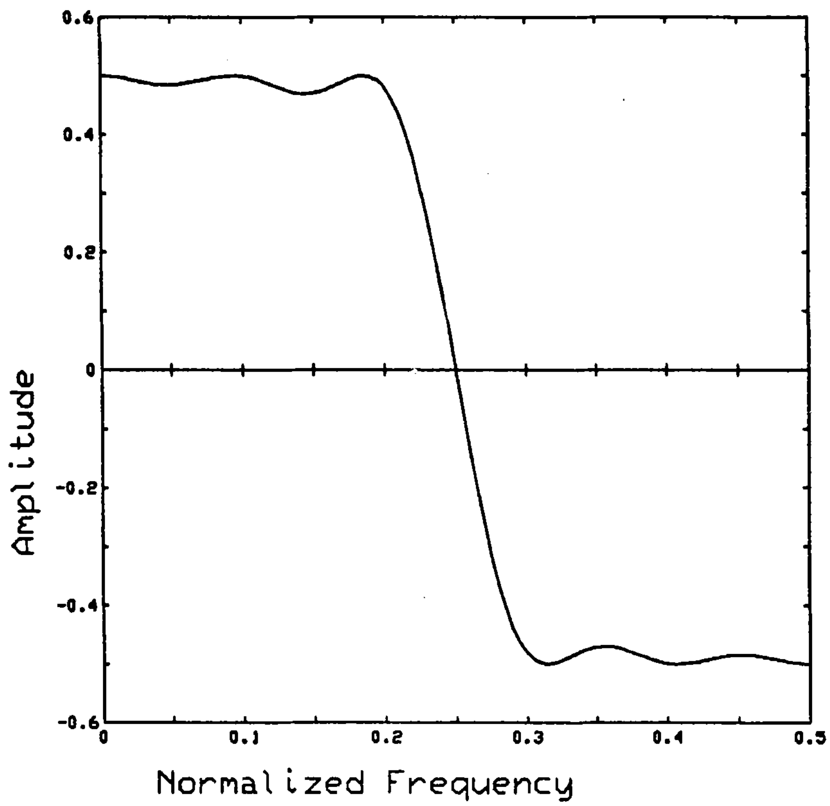

Fig. 5.3 Frequency response of an antisymmetric function

Due to the fact that $V(\omega)$ is the sum of cosines of odd multiples of the frequency ω, it is easy to show that it is antisymmetric about $\omega = \pi/2$, i.e.

$$V(\frac{\pi}{2} + \omega) = -V(\frac{\pi}{2} - \omega) \tag{5.35}$$

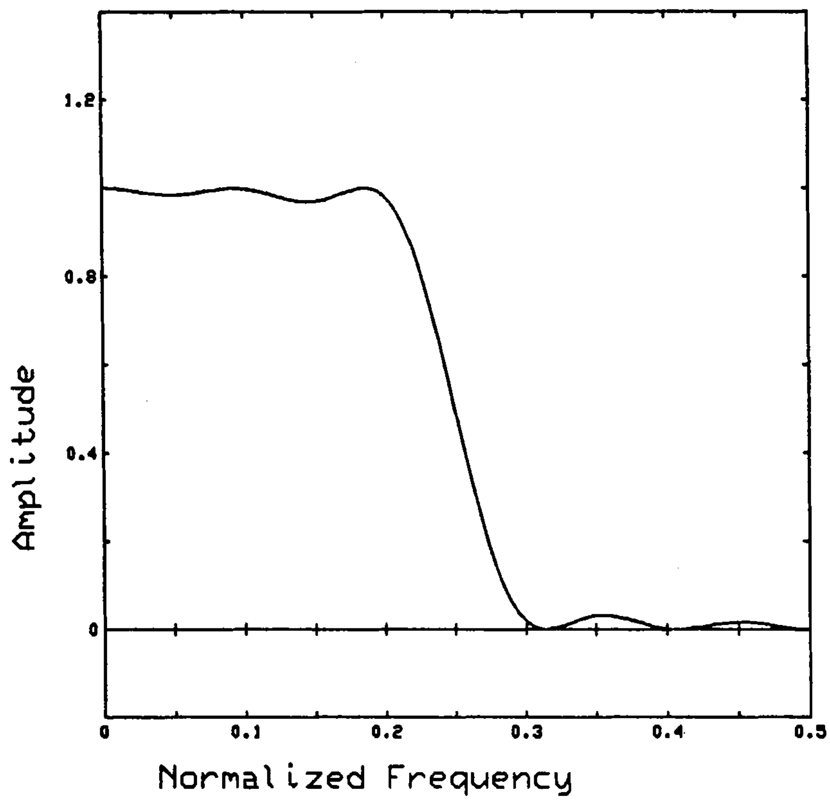

Fig. 5.4 Frequency response of an offset antisymmetric function

This is illustrated in Fig. 5.3.

The frequency response of $F_0(z)$, in terms of $V(\omega)$, is given by

$$F_0(e^{j\omega}) = V(\omega) + \frac{1}{2} \tag{5.36}$$

As illustrated in Fig. 5.4, the 1/2 offset causes the positive part of the antisymmetric function to move close to unity-gain line and the negative part close to the ω-axis (zero-gain line) which makes the bandpass and stopband ripple of $F_0(e^{j\omega})$ the same and the gain at $\omega = \pi/2$ equal to -6 dB (1/2).

The discussion in Section 5.5.1 shows that the response $F_0(z)$ can be decomposed into two time-reversed filters, if its frequency response curve does not cross the ω-

axis which implies that the frequency response curve must lie between 0 and the unity-gain line, i.e.

$$0 \leq F_0(e^{j\omega}) \leq 1 \tag{5.37}$$

This requires $V(\omega)$ to be defined as

$$-\frac{1}{2} \leq V(\omega) \leq \frac{1}{2} \tag{5.38}$$

5.5.4 Design of $F_0(z)$—Windowing

In the existing literature [16],[20], half-band filters, with the even numbered coefficients as specified by Eq. (5.32), are designed by using window design techniques. The idea behind these techniques is to design a window $w(n)$ that weights the coefficients of the ideal half-band filter. Both the frequency characteristics and the length of the resulting filter are determined by the shape of $w(n)$. Consider a typical finite impulse response filter $T(z)$ with coefficients $t(n)$ defined as

$$t(n) = w(n)\frac{\sin(\pi n/2)}{\pi n} \tag{5.39}$$

where

$$w(n) \begin{cases} \neq 0 & \text{for } -\dfrac{M-1}{2} \leq n \leq \dfrac{M-1}{2} \\ = 0 & \text{elsewhere} \end{cases}$$

It is possible to design a response, that can be decomposed into two time-reversed filters, out of any window design response $T(z)$ using the following procedure.

1. Obtain the antisymmetric (with respect to $\omega = \pi/2$) response $T_a(z)$ by allowing $t(0) = 0$.

2. Find the global maximum $T_{\max}$ of the function $T_a(e^{j\omega})$ for $0 \leq \omega \leq \frac{\pi}{2}$.

3. Form the antisymmetric response $V(z)$ with coefficients $v(n)$ equal to

$$v(n) = \frac{1}{2T_{\max}} t_a(n) \tag{5.40}$$

The normalization factor $\frac{1}{2T_{\max}}$ makes the global maximum of the frequency response $V(\omega)$ equal to 1/2 and the frequency response obey Eq. (5.38).

4. Obtain the decomposable response $F_0(z)$ with

$$f_0(n) = \begin{cases} \frac{1}{2} & \text{for } n = 0 \\ v(n) & \text{elsewhere} \end{cases} \tag{5.41}$$

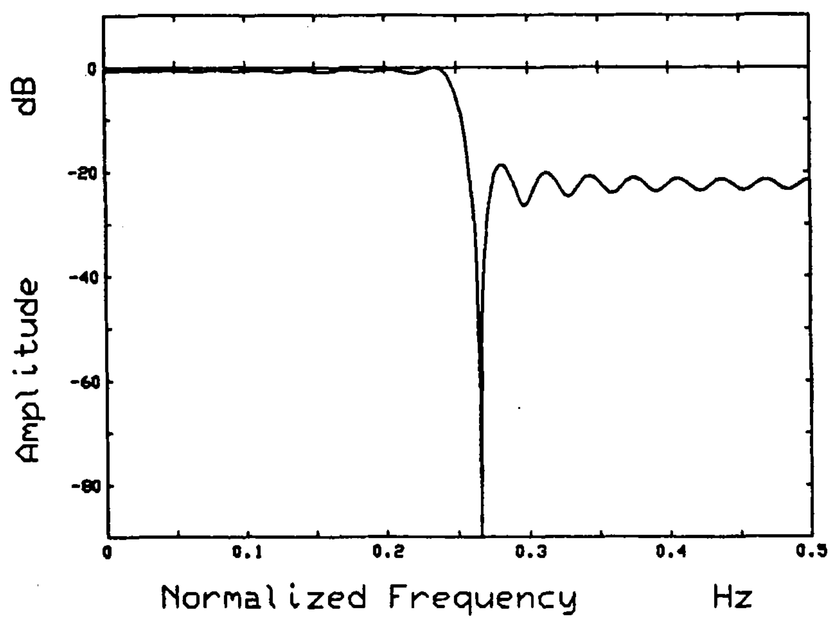

Fig. 5.5 Frequency characteristics of a decomposable response $F_0(z)$ obtained from a 63-tap rectangular response

Due to the normalization operation that is required to ensure that $F_0(z)$ is decomposable, the frequency characteristics of $F_0(z)$ depend on the values of the extrema of the antisymmetric response $T_a(z)$. The difference between $T_{\max}$ and the values of the other extrema establishes the ripple of both the passband and the stopband. For this reason, windows like the rectangular, Hamming, Kaiser etc. will not produce responses with good frequency characteristics, if they are used to obtain the antisymmetric response $T_a(z)$. As an example, consider the decomposable response $F_0(z)$ obtained from a 63-tap rectangular window response whose frequency characteristics are illustrated in Fig. 5.5. The big difference between the global maximum and the other extrema makes the frequency characteristics of the decomposable response very poor. The only window that can be used to obtain a decomposable response with good frequency characteristics is the Chebyshev window which results to an equiripple response. A program capable of designing Chebyshev windows can be found in [21].

5.5.5 Optimal (Minimax Error) Design of $F_0(z)$

Obviously, the response $T_a(z)$ that has the maximum difference between $T_{\max}$ and the other extrema in the region $0 \leq \omega \leq \frac{\pi}{2}$ minimized, will produce a decomposable response with minimum passband and stopband ripple. Due to its nature, the problem of designing a response $T_a(z)$ with such characteristics can be considered as an optimal Chebyshev approximation (minimax error) problem.

A computer program for designing the optimal Chebyshev approximation to the desired ideal frequency response of a linear phase filter was developed by McClellan, Parks and Rabiner [15]. This program which implements what is known as the

McClellan-Parks algorithm, can design either odd or even length filters provided that no constraints are imposed on the values of the filter coefficients. Due to the fact that the even numbered coefficients of $T_a(z)$ have specified values, the response cannot be designed directly. For this reason the design of a linear phase response with at least $N/2$ coefficients that are related only to the odd numbered coefficients of $T_a(z)$, is used as an intermediate step.

Two different responses, one with N and the other with $N-1$ coefficients that can be used as an intermediate step to the design of $T_a(z)$, are considered in this chapter. The first one, with N coefficients, can be imagined as the result of a sub-sampling operation that removes the even numbered coefficients of $T_a(z)$, followed by a time-shift operation to form a causal even length response with the odd numbered coefficients. Mathematically this operation is expressed as

$$u_1(n) = t_a(2n - N + 1) \tag{5.42}$$

where $u_1(n)$ is the nth coefficient of the intermediate step response with $n = 0, 1, \ldots, N-1$. The relationship between the z-transforms $U_1(z)$ and $T_a(z)$ is given by

$$U_1(z^2) = T_a(z) z^{-(N-1)} \tag{5.43}$$

We obtain the formula that translates the frequency characteristics of $T_a(z)$ into characteristics of $U_1(z)$ by evaluating the above relationship on the unit circle. For $z = e^{j\omega}$,

$$U_1(2\omega) = T_a(\omega) \tag{5.44}$$

where $U_1(\omega) = |U_1(e^{j\omega})|$ and $T_a(\omega) = |T_a(e^{j\omega})|$. After the design of $U_1(z)$, the coefficients of $T_a(z)$ can be determined by the formula

$$t_a(n) = \begin{cases} 0 & \text{for } n \text{ even} \\ u_1(\frac{n+N-1}{2}) & \text{for } n \text{ odd} \end{cases} \tag{5.45}$$

The second response $U_2(z)$ that can be used as an intermediate step to the design of $T_a(z)$, has $N-1$ coefficients which satisfy the equation

$$t_a(2n - N + 1) = u_2(n) + u_2(n-1) \tag{5.46}$$

with $u_1(n) \neq 0$ for $n = 0, 1, \ldots, N-2$. This corresponds to the following relationship between the z-transforms. u_2 ?

$$T_a(z) = z^{N+1}\left\{U_2(z^2) + z^{-2}U_2(z^2)\right\} \tag{5.47}$$

For $z = e^{j\omega}$, we obtain the formula that relates the frequency characteristics of $T_a(z)$ to those of $U_2(z)$,

$$U_2(2\omega) = \frac{1}{2\cos(\omega)}T_a(\omega) \tag{5.48}$$

where $U_2(\omega) = |U_2(e^{j\omega})|$. After the design of $U_2(z)$ the coefficients of $T_a(z)$ can be determined by the formula,

$$t_a(n) = \begin{cases} 0 & \text{for } n \text{ even} \\ u_2(\frac{n+N-1}{2}) + u_2(\frac{n+N-1}{2} - 1) & \text{for } n \text{ odd} \end{cases} \tag{5.49}$$

5.5.6 Extraction of the coefficients $h_0(n)$

As was mentioned earlier in this section, the design of the cascade filter response $F_0(z)$ is an intermediate step to the design of the lowpass half-band filter $H_0(z)$.

Referring to Eq. (5.14), the coefficients $f_0(n)$ of the cascade filter response are equal to

$$f_0(n) = f_0(-n) = \sum_{u=0}^{N-1} h_0(u)h_0(u-n) \tag{5.50}$$

for $n = 0, 1, \ldots, N-1$. For a given set of values $f_0(n)$, it is possible to determine the coefficients $h_0(n)$ by solving the N nonlinear equations derived from Eq. (5.50). Due to the fact that more than one set of values $h_0(n)$ can be found to satisfy the above set of equations, the problem can be better solved in the z-domain rather than the time domain.

Consider the z-transform of Eq. (5.50)

$$F_0(z) = H_0(z)H_0(z^{-1}) \tag{5.51}$$

and the relationship between $H_0(z)$ and $H_0(z^{-1})$ in terms of their zero-patterns described by Eq. (5.26) and Eq. (5.27). Assuming real valued coefficients $h_0(n)$, for every complex conjugate pair of zeros (z_m, z_m^*) in $H_0(z)$, there is a complex conjugate pair of zeros $(1/z_m, 1/z_m^*)$ in $H_0(z^{-1})$ and for every real zero z_r in $H_0(z)$ there is a real zero $1/z_r$ in $H_0(z^{-1})$. The number of different ways, the response $F_0(z)$ can be decomposed into two time-reversed filters, depends on the number of zeros that are not on the unit circle and is given by the formula

$$D_N = 2^{k+l} \tag{5.52}$$

where k and l represent the number of zero-groups of the form $(z_m, z_m^*, 1/z_m, 1/z_m^*)$ for $|z_m| \neq 1$ and $(z_r, 1/z_r)$ for $z_r \neq 1$ respectively.

The amplitude characteristics of the filter $H_0(z)$ are independent of the way the response $F_0(z)$ is decomposed, which affects only its phase characteristics. An

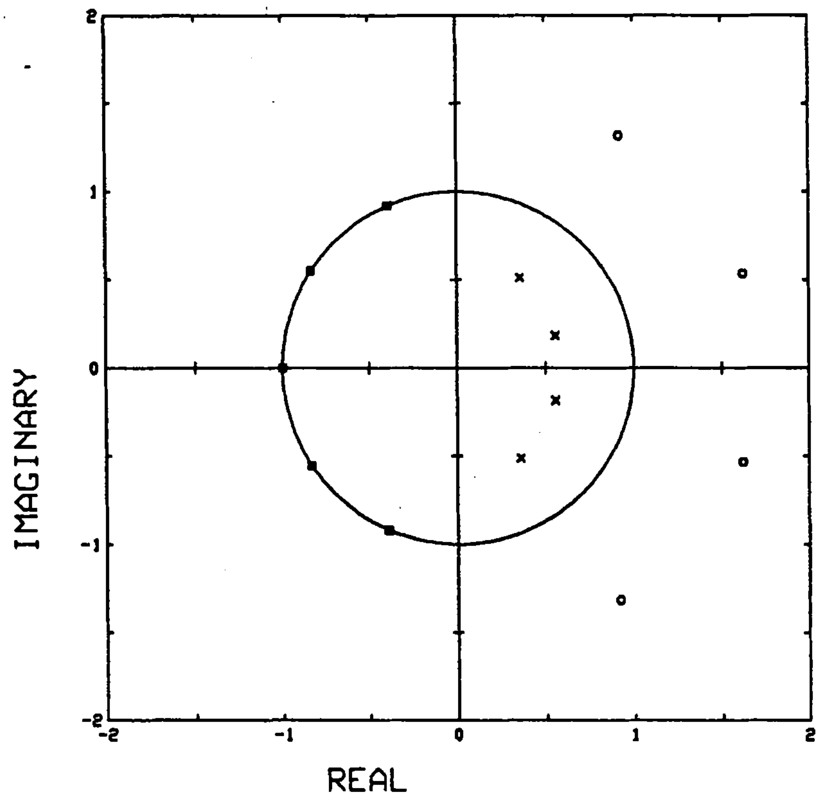

Fig. 5.6 Zero-plot for maximum/minimum phase filters

interesting way to decompose the response $F_0(z)$ is by allocating all the zeros inside the unit circle to the filter $H_0(z)$ and all the zeros outside the unit circle to its time-reversal $H_0(z^{-1})$ as illustrated in Fig. 5.6. This way makes $H_0(z)$ a minimum phase filter and $H_0(z^{-1})$ a maximum phase one. Obviously, the way $F_0(z)$ is decomposed is not critical since the subband system will still be reversible.

To determine the values of the coefficients $h_0(n)$ after the zeros are allocated to the filters, we first create a $N-1$-degree polynomial $K(z)$ such as

$$K(z) = \sum_{n=0}^{N-1} k_n z^n = \prod_{m=0}^{N-1} (z - z_m) \tag{5.53}$$

where z_m is the mth zero allocated to $H_0(z)$ and k_n is the nth coefficient of $K(z)$. The values of the coefficients k_n can be expressed in terms of the zeros z_m using the formulas:

$$
\begin{aligned}
k_{N-1} &= 1 \\
k_{N-2} &= -(z_1 + z_2 + \dots z_{N-1}) \\
k_{N-3} &= z_1 z_2 + z_1 z_3 + \dots z_1 z_{N-1} + z_2 z_3 + \dots \underbrace{z_{N_2}}_{N-2} z_{N-1} \\
k_{N-4} &= -(z_1 z_2 z_3 + z_1 z_2 z_4 + \dots\dots z_{N-3} z_{N-2} z_{N-1}) \\
\dots & \quad \dots \\
\dots & \quad \dots \\
k_0 &= -z_1 z_2 z_3 \dots z_{N-1}
\end{aligned}
\tag{5.54}
$$

Referring to Eq. (5.26), $H_0(z)$ can be expressed in terms of $K(z)$ by the formula

$$H_0(z) = G_a z^{-(N-1)} K(z) \tag{5.55}$$

The inverse z-transform of Eq. (5.55) determines the relationship between the coefficients $h_0(n)$ and k_n,

$$h_0(n) = G_a k_{n-N+1} \quad \text{for} \quad n = 0, 1, \dots, N-1. \tag{5.56}$$

The gain G_a can be determined by using at least one of the coefficients $f_0(n)$ of the cascade filter response $F_0(z)$ and the easiest way is to consider $f_0(N-1)$. Referring to Eq. (5.50) and Eq. (5.56), for $n = N-1$,

$$
\begin{aligned}
f_0(N-1) &= h_0(N-1) h_0(0) \\
&= {G_a}^2 k_0 k_{N-1}
\end{aligned}
\tag{5.57}
$$

Since $k_{N-1} = 1$,

$$G_a = \sqrt{\frac{f_0(N-1)}{k_0 k_{N-1}}} = \sqrt{\frac{f_0(N-1)}{k_0}} \tag{5.58}$$

and the values $h_0(n)$ can be found using Eq. (5.56).

The method to determine the values of $h_0(n)$ makes the assumption that the zeros of the cascade filter response $F_0(z)$ are known. Consider the $2N-2$ degree shifted polynomial $\vec{F}_0(z)$ defined as

$$\begin{aligned} \vec{F}_0(z) &= z^{N-1}F_0(z) \\ &= \sum_{n=0}^{2N-2} \vec{f}_0(n)z^n \end{aligned} \tag{5.59}$$

with $\vec{f}_0(n) = f_0(n-N+1)$. Except for trivial cases where analytical solutions can be applied, the problem of finding the zeros of the polynomial $\vec{F}_0(z)$ is solved using numerical methods. A zero-finding algorithm for polynomials with real coefficients that can be successfully used to determine the zeros of $\vec{F}_0(z)$, is included in the IMSL software package [22]. This algorithm iterates towards a zero using Laguerre's method which is cubically convergent for isolated zeros and linearly convergent for multiple zeros.

5.5.7 Reoptimization of the coefficients $h_0(n)$

In general, the values of the zeros of a polynomial that are obtained by using a numerical method, are approximations of the actual values. The "goodness" of the approximation depends not only on the type of arithmetic used (single or double precision) but also on bounds set for the acceptance of a specific value as a zero. Obviously, the error due to these approximations accumulates when the values of the coefficients $h_0(n)$ are computed, resulting to a filter that does not obey the conditions for a reversible subband system. To compensate for the accumulated error, the computed coefficients are adjusted by using an optimization algorithm

(Hooke and Jeaves method [17]) which attempts to minimize a single objective function over several variables which in this case are the coefficients $h_0(n)$.

To obtain an objective function that can best adjust the values of the coefficients $h_0(n)$, we first consider the error function $e(n)$ defined as

$$e(n) = |f_0(n) - h_0(n) * h_0(-n)| \quad \text{for} \quad n = -(N-1), \ldots, 0, \ldots, N-1 \qquad (5.60)$$

which obviously depends on the precision of the zero determination. We also define the functions E_e and E_o as

$$E_e = \sum_{n \neq 0}^{\text{even}} e(n) = \sum_{n \neq 0}^{\text{even}} |h_0(n) * h_0(-n)| \qquad (5.61.a)$$

$$E_o = e(0) + \sum_{n}^{\text{odd}} e(n) \qquad (5.61.b)$$

E_e is the overall error for the zero valued coefficients and its value is related to the distortion, the overall system response will suffer due to the nonperfect decomposition of the cascade filter response $F_0(z)$. E_o is the overall error for the nonzero coefficients and its value is related to the level of matching between the actual and the expected frequency characteristics of the filter $H_0(z)$.

The single metric E_r that is to be used as the objective function is constructed from E_o and E_e.

$$E_r = E_o + \alpha E_e \qquad (5.62)$$

where α is the weighting that denotes the emphasis given to the overall system distortion as opposed to the frequency characteristics of the filter $H_0(z)$.

5.5.8 Extraction of the Coefficients $h_1(n)$, $g_0(n)$ and $g_1(n)$

The coefficients of the filters $H_1(z)$, $G_0(z)$ and $G_1(z)$ can be obtained by considering the inverse z-transforms of Eq. (5.11). For N even,

$$h_1(n) = (-1)^{n+1} h_0(N-1-n) \tag{5.63.a}$$

$$g_0(n) = h_0(N-1-n) \tag{5.63.b}$$

$$g_1(n) = (-1)^n h_0(n) \tag{5.63.c}$$

5.5.9 Summary of the Filter Design Procedure

The procedure for designing the filters for the subband system by using the Parks-McClellan algorithm, is summarized into the following steps.

1. Choose between $U_1(z)$ and $U_2(z)$ the transformation response to be used and obtain its characteristics from the expected characteristics of $H_0(z)$.

2. Use the Parks-McClellan algorithm to design either $U_1(z)$ or $U_2(z)$.

3. Obtain the antisymmetric response $T_a(z)$ and estimate its global maximum $T_{\max}$.

4. Obtain the antisymmetric response $V(z)$ by normalizing the coefficients of $T_a(z)$ with $\dfrac{1}{2T_{\max}}$.

5. Obtain the cascade filter response $F_0(z)$ from $V(z)$.

6. Find the zeros of $F_0(z)$.

7. Allocate the zeros to the two time-reversed filters $H_0(z)$ and $H_0(z^{-1})$ and obtain their coefficients.

8. Reoptimize the values of the coefficients $h_0(n)$ by minimizing some error function.

9. Determine the coefficients of $H_1(z)$, $G_0(z)$ and $G_1(z)$.

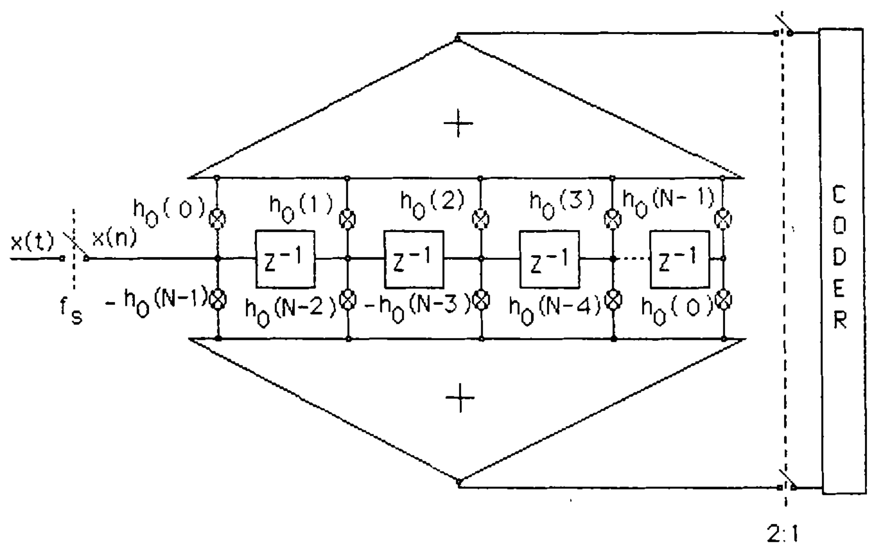

Fig. 5.7 Implementation of the Analysis Filter Bank

5.6 Implementation of the Subband System

Figures 5.7 and 5.8 give an implementation of the analysis and the reconstruction of the input signal respectively. Unlike the linear phase QMF filter banks, exact reconstruction filter banks are inefficient in terms of the computation load. The number of multiplications per channel to be performed for every second input

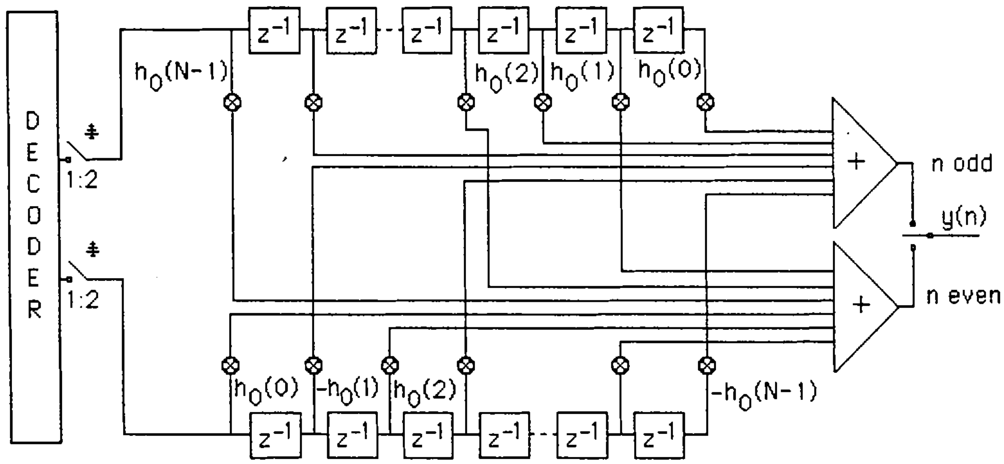

Fig. 5.8 Implementation of the Reconstruction Filter Bank

sample, is equal to the filter length N with $N-1$ additions almost twice the calculations required by a linear phase. Obviously, the inefficient implementation of the exact reconstruction filter banks is their main disadvantage over the linear phase QMF filter banks.

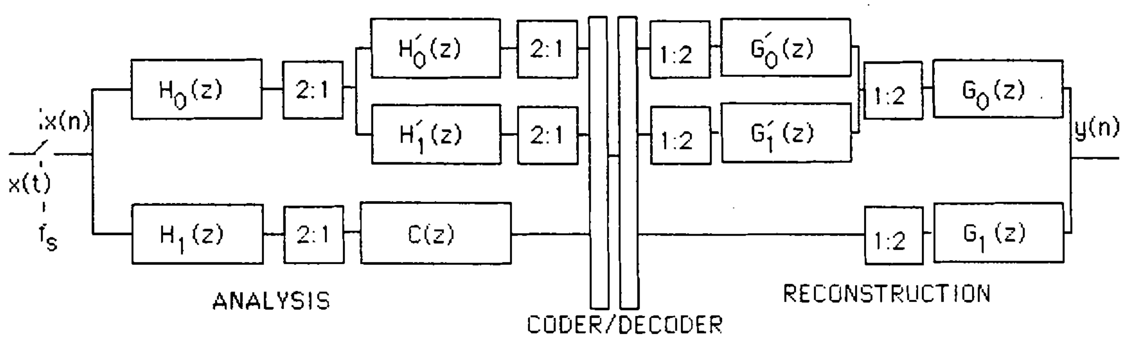

Fig. 5.9 Subband system with unequal width subbands

Consider the tree structure analysis/reconstruction subband system shown in Fig. 3.7 repeated here as Fig. 5.9. As it was argued in Chapter 3, the amplitude distortion accumulates when linear phase QMF filter banks are used which might be disturbing for a high quality subband system. Also, the band-splitting used, which results in unequal width subbands requires an equalization filter $C(z)$ equal to the overall response of a two band subband system

$$C(z) = \frac{1}{2}\left\{ H_0'^2(z) - H_0'^2(-z) \right\} \tag{5.64}$$

otherwise, the reconstructed signal will suffer from aliasing as well as amplitude distortion.

Exact reconstruction filter banks appear to have a better performance. Clearly, there is no amplitude distortion accumulation and since the overall response of a two band subband system is a pure delay, the equalization filter $C(z)$ is a pure delay. If $H_0(z)$ has N taps then

$$C(z) = z^{-2N-2} \tag{5.65}$$

An attractive way of splitting the signal into unequal width subbands could utilize both linear phase QMF and exact reconstruction filter banks. Consider again Fig. 5.9, it is possible to use linear phase QMF filters for the first splitting and exact reconstruction for the second one so that the equalization filter $C(z)$ will be a pure delay. By introducing this splitting scheme, we save computations due to the linear phase filters of the first splitting and the use a pure delay for equalization. Obviously, the overall system response will suffer some amplitude distortion but not as much as if all the filters were linear phase ones.

Chapter 6 Design Details for Exact Reconstruction Filter Banks

6.1 Introduction

The procedure for designing exact reconstruction filter banks for subband systems, discussed in Chapter 5, is based on the filter design algorithm by McClellan and Parks [15]. It appears that this algorithm, in its original form, can be used to design equiripple filters, a result of equal-weighted Chebyshev approximations. The algorithm requires some modifications, if it is to be used for the design of non-equiripple filters.

In this chapter, we discuss the McClellan-Parks algorithm and the way it can be modified for unequal-weighted approximations so that non-equiripple filters can be designed. We also discuss an alternative approach to the design of non-equiripple filters. Unlike the McClellan-Parks algorithm which designs optimum Chebyshev approximations without any manual intervention, this approach can be used to design filters which exactly satisfy a necessary but sufficient number of conditions. Manual intervention is required in order to establish the conditions for which the filter response has acceptable characteristics.

6.2 McClellan-Parks Algorithm

The McClellan-Parks algorithm designs the optimal Chebyshev approximation to the desired ideal frequency response for linear-phase FIR filters. This is done very efficiently by using the Remez exchange algorithm. A detailed analysis of this filter design method can be found in [20],[15] which are the main sources of information for the brief discussion to be followed.

Consider the Fourier transform of a linear-phase filter $H(e^{j\omega})$ which is defined as follows:

$$\begin{aligned} H(e^{j\omega}) &= \sum_{n=0}^{N-1} h(n)e^{-j\omega n} \\ &= H(\omega)e^{-j(\omega\frac{N-1}{2}-\frac{L\pi}{2})} \end{aligned} \tag{6.1}$$

where $H(\omega) = |H(e^{j\omega})|$ and $L = 0$ or 1. The linear-phase filters are divided according to the length N (even or odd) and according to the symmetry [positive ($L = 0$) or negative ($L = 1$)] of their impulse response, into four different types. For each type, the frequency response $H(\omega)$ can be expressed as follows:

Type 1: Positive Symmetry, odd length:

$$H(\omega) = \sum_{n=0}^{N_1} a(n)\cos(\omega n) \tag{6.2}$$

where $N_1 = (N-1)/2$.

Type 2: Positive symmetry, even length:

$$H(\omega) = \cos(\frac{\omega}{2}) \sum_{n=0}^{N_1-1} b(n)\cos(\omega n) \tag{6.3}$$

where $N_1 = N/2$.

Type 3: Negative symmetry, odd length:

$$H(\omega) = \sin(\omega) \sum_{n=0}^{N_1-1} c(n)\cos(\omega n) \tag{6.4}$$

where $N_1 = (N-1)/2$.

Type 4: Negative symmetry, even length:

$$H(\omega) = \sin(\frac{\omega}{2}) \sum_{n=0}^{N_1-1} d(n)\cos(\omega n) \tag{6.5}$$

where $N_1 = N/2$. The values of $a(n)$, $b(n)$, $c(n)$ and $d(n)$ can be expressed in terms of the values of the coefficients $h(n)$ and the expressions can be found in [15].

The above expressions can be used to combine the design of all four types of filters into one algorithm. This can be accomplished by expressing $H(\omega)$ as

$$H(\omega) = Q(\omega)P(\omega) \tag{6.6}$$

where $P(\omega)$ is a linear combination of cosine functions. The motivation of expressing the four type into a common form is that a single central computation routine based on the Remez exchange method can be used to calculate the best approximation in each of the four types. This is accomplished by modifying both the desired magnitude function and the weighting function to formulate a new approximation problem.

The original approximation problem can be stated as follows: given a desired magnitude response $D(\omega)$ and a positive weight function $W(\omega)$, both which are continuous on the compact subset of $[0, \pi]$ and given one of the four types of linear-phase filters, then one wishes to minimize the maximum absolute weighted error defined as

$$||E(\omega)|| = \max_{\omega \in F}\Big\{W(\omega)|D(\omega) - H(\omega)|\Big\} \tag{6.7}$$

over the set of coefficients of $H(\omega)$. The error function $E(\omega)$ can be written as

$$\begin{aligned} E(\omega) &= W(\omega)\Big\{D(\omega) - H(\omega)\Big\} \\ &= W(\omega)Q(\omega)\Big\{\frac{D(\omega)}{Q(\omega)} - P(\omega)\Big\} \end{aligned} \tag{6.8}$$

omitting the points where $Q(\omega) = 0$.

By defining

$$\hat{D}(\omega) = \frac{D(\omega)}{Q(\omega)} \tag{6.9.a}$$

$$\hat{W}(\omega) = W(\omega)Q(\omega) \tag{6.9.b}$$

we obtain the equivalent approximation problem to minimize the following function

$$||E(\omega)|| = \max_{\omega \in F'}\Big\{\hat{W}(\omega)|\hat{D}(\omega) - P(\omega)|\Big\} \tag{6.10}$$

over the set of coefficients of $P(\omega)$. F' is the new set that does not include the end-points where $Q(\omega) = 0$.

The design makes use of the *Alternation Theorem* which states that if $P(\omega)$ is a linear combination of cosine functions, i.e.

$$P(\omega) = \sum_{n=0}^{r-1} p(n)\cos(\omega n) \tag{6.11}$$

then a necessary and sufficient condition that $P(\omega)$ be the unique best weighted Chebyshev approximation to a continuous function $\hat{D}(\omega)$ on F' is that the error function $E(\omega)$ has at least $r+1$ extremal frequencies ω_i in F' such as

$$|E(\omega_i)| = \max_{\omega \in F'}|E(\omega)| = \delta \tag{6.12}$$

and

$$E(\omega_i) = -E(\omega_{i+1}) \ \text{ for } \ \omega_i < \omega_{i+1} \tag{6.13}$$

This theorem says that given a set of coefficients $p(n)$ $n = 0, 1 \ldots, r-1$ for $P(\omega)$ and a set of extremal frequencies ω_i $i = 0, 1 \ldots, r$, $P(\omega)$ is the optimum approximation if

$$\hat{W}(\omega_i)\left\{\hat{D}(\omega_i) - P(\omega_i)\right\} = (-1)^i \delta \quad i = 0, 1 \ldots, r \tag{6.14}$$

From the above set of equations we can express the optimum deviation δ as

$$\delta = \frac{\sum_{i=0}^{r} \alpha_i \hat{D}(\omega_i)}{\sum_{i=0}^{r} (-1)^i \frac{\alpha_i}{\hat{W}(\omega_i)}} \tag{6.15}$$

where

$$\alpha_i = \prod_{\substack{k=0 \\ k \neq i}}^{r} \frac{1}{(x_i - x_k)} \tag{6.16}$$

and

$$x_k = \cos(\omega_k) \tag{6.17}$$

Also, from the deviation δ and the extremal frequencies ω_i, using the Lagrange interpolation formula in its barycentric form we can express $P(\omega)$ as

$$P(\omega) = \frac{\sum_{i=0}^{r-1} (\frac{\beta_i}{x - x_i}) C_i}{\sum_{i=0}^{r-1} \frac{\beta_i}{(x - x_i)}} \tag{6.18}$$

where

$$\beta_i = \prod_{\substack{k=0 \\ k \neq i}}^{r-1} \frac{1}{(x_i - x_k)} \tag{6.19}$$

$$C_i = \hat{D}(\omega_i) - (-1)^i \frac{\delta}{\hat{W}(\omega_i)} \tag{6.20}$$

and

$$x = \cos(\omega) \tag{6.21}$$

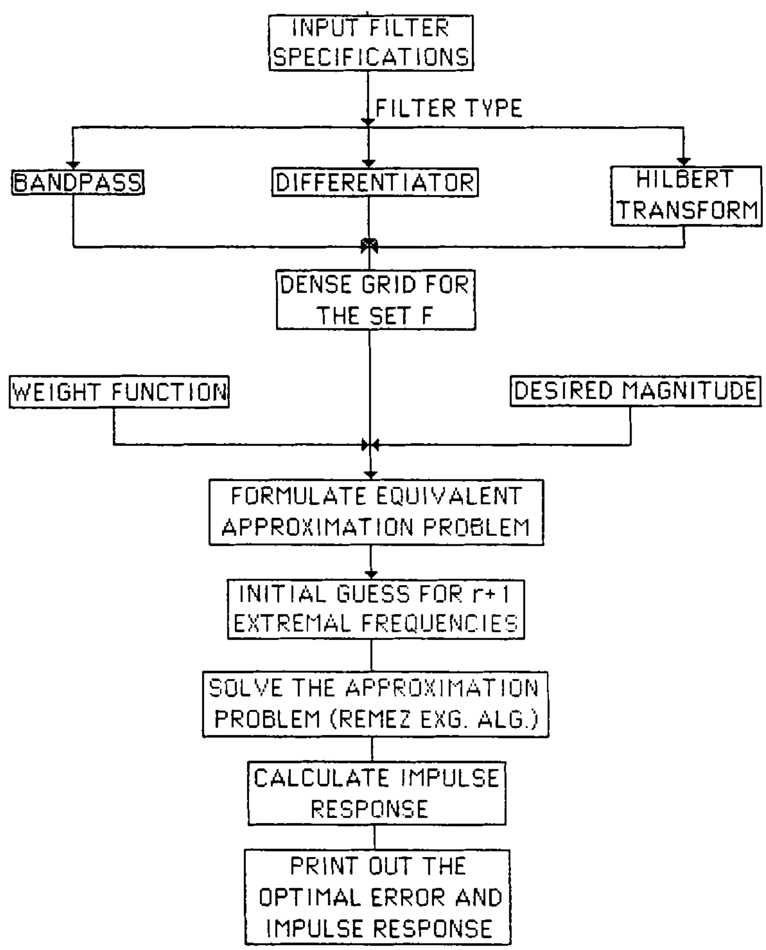

Fig. 6.1 Flowchart of the McClellan-Parks algorithm

A flowchart of the McClellan-Parks algorithm is shown in Fig. 6.1 and consists of the following four steps:

1. An input section in which the desired frequency response $D(\omega)$, the weighting function $W(\omega)$, and the filter length N is specified.

2. A formulation of the appropriate equivalent problem, i.e. formation of $\hat{D}(\omega)$, $\hat{W}(\omega)$ and $P(\omega)$.

3. Solution of the approximation problem using the Remez exchange algorithm.

4. Calculation of the filter impulse response.

The first step is the interface between the designer and the program where the specifications are inserted into the program. The second is the formulation af the equivalent problem already discussed.

As a third step, the Remez exchange algorithm is used to solve the approximation problem. The flowchart of this algorithm is shown in Fig. 6.2. First, the algorithm guesses the positions ω_i of the $r+1$ extrema in $P(\omega)$ and finds the optimum value of δ using Eq. (6.15). After calculating δ, the program interpolates $P(\omega)$ on the r points ω_i $i = 0, 1 \ldots, r-1$ using Eq. (6.18) and then calculates the error function $E(\omega)$. If $|E(\omega)| \leq \delta$ for all the frequencies in F', then the optimum approximation is found, otherwise if $|E(\omega)| > \delta$, the extremal of $E(\omega)$ are chosen as the new candidates for extremal frequencies and the procedure is repeated again. The new set of extremal frequencies will force δ to increase and finally converge to its upper bound.

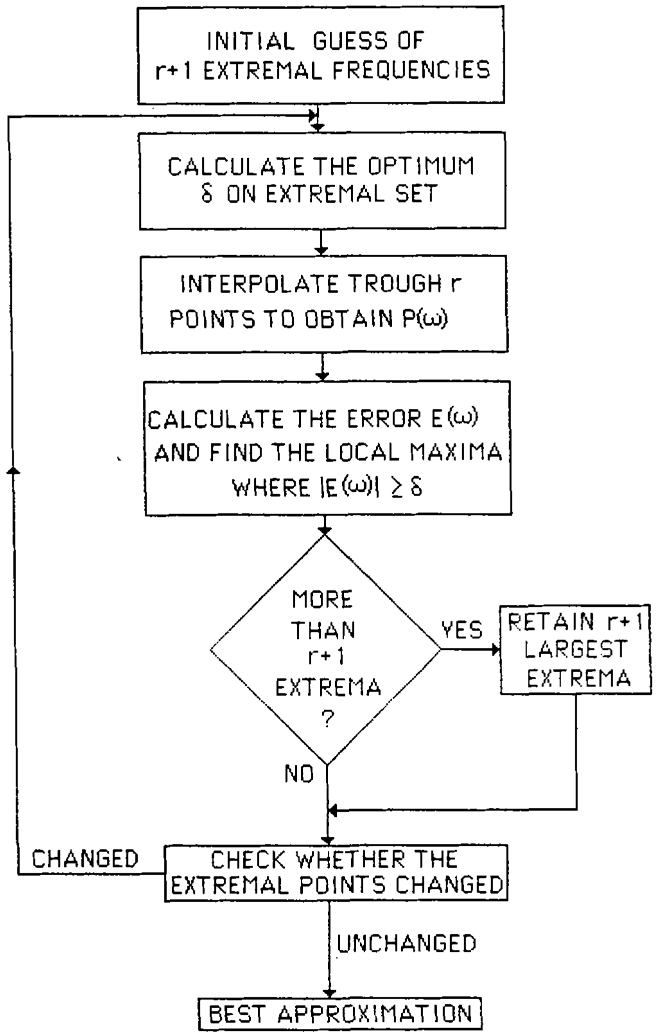

Fig. 6.2 Flowchart of the Remez exchange algorithm

6.3 Design of Antisymmetric Functions with McClellan-Parks Algorithm

As it was stated in the previous chapter, a zero-phase antisymmetric function $T_a(z)$ must satisfy

$$t_a(2n) = 0 \tag{6.22}$$

Due to its antisymmetric property, the problem of designing the Chebyshev approximation to its desired value, can be stated as the minimization of the absolute maximum error that is defined as

$$||E(\omega)|| = \max_{\omega \in F}\left\{W(\omega)|D(\omega) - T_a(\omega)|\right\} \tag{6.23}$$

where the desired-value function $D(\omega)$, the weighting function $W(\omega)$ and $T_a(\omega)$ are defined in the region F $[0, \frac{\pi}{2})$.

Since $T_a(z)$ cannot be designed directly by the algorithm, we form the equivalent problem using either the transformation $U_1(z)$ or $U_2(z)$.

For $U_1(z)$, the transformation formula is given by Eq. (5.44) with

$$U_1(2\omega) = T_a(\omega) \tag{6.24}$$

in the region $[0, \frac{\pi}{2}]$ and the equivalent approximation problem becomes the minimization of

$$||E_1(\omega)|| = \max_{\omega \in F_1}\left\{W_1(\omega)|D_1(\omega) - U_1(\omega)|\right\} \tag{6.25}$$

where

$$E_1(\omega) = E(\frac{\omega}{2}) \tag{6.26.a}$$

$$W_1(\omega) = W(\frac{\omega}{2}) \tag{6.26.b}$$

$$D_1(\omega) = D(\frac{\omega}{2}) \tag{6.26.c}$$

in the region F_1 $[0, \pi]$.

For $U_2(z)$, the transformation formula is given by Eq. (5.48) with

$$U_2(2\omega) = \frac{1}{2\cos(\omega)}T_a(\omega) \tag{6.27}$$

in the region $[0, \frac{\pi}{2})$ and the equivalent problem becomes the minimization of

$$||E_2(\omega)|| = \max_{\omega \in F_2}\left\{W_2(\omega)|D_2(\omega) - U_2(\omega)|\right\} \tag{6.28}$$

where

$$E_2(\omega) = E(\frac{\omega}{2}) \tag{6.29.a}$$

$$D_2(\omega) = \frac{1}{2\cos(\frac{\omega}{2})} D(\frac{\omega}{2}) \tag{6.29.b}$$

$$W_2(\omega) = 2\cos(\frac{\omega}{2}) W(\frac{\omega}{2}) \tag{6.29.c}$$

6.4 Design of Antisymmetric Functions for Exact Reconstruction Systems with McClellan-Parks Algorithm

As it was described in the previous chapter, the appropriate antisymmetric function $V(z)$ that can be used to derive the exact reconstruction filters must satisfy the equation

$$-\frac{1}{2} \leq V(\omega) \leq \frac{1}{2} \tag{6.30}$$

In general, the corresponding desired function $D(\omega)$ for the above antisymmetric response, is defined as

$$D(\omega) = \frac{1}{2} \tag{6.31}$$

in the region $0 \leq \omega \leq \omega_c$ with $\omega_c < \frac{\pi}{2}$ which corresponds to the passband and is left to be undefined in the region $\omega_c < \omega < \frac{\pi}{2}$ which corresponds to the transition band.

Due to the existence of the upper and lower bounds the approximation problem must be redefined so that the designed function $V(\omega)$ be tangent to the desired function $D(\omega)$ at any local maximum in the region $[0, \frac{\pi}{2})$, i.e.

$$W(\omega_i)\left\{D(\omega_i) - V(\omega_i)\right\} = \left\{1 - (-1)^{i+l}\right\}\delta \tag{6.32}$$

where ω_i are the extremal frequencies in $[0, \frac{\pi}{2})$ and $l = 0$ or 1 depending whether the first extremal is a maximum or a minimum.

This problem can be solved by using the original McClellan-Parks algorithm provided that the weighting is the same for all frequencies. Given a desired function $D(\omega)$ and the corresponding optimum approximation $V(\omega)$, it is easy to prove the linearity property which implies that the optimum approximation to $C_k D(\omega)$ where C_k is a constant, is $C_k V(\omega)$. Assuming that the weight function $W(\omega)$ is equal to unity, the above set of equations can be expressed as

$$(1 - 2\delta)D(\omega_i) - V(\omega_i) = (-1)^{i+l}\delta \tag{6.33}$$

provided that $D(\omega)$ is defined as in Eq. (6.31). Since δ is constant, an equivalent problem can be formed with $C_k D(\omega)$ as the desired function and $T_a(\omega)$ the optimum approximation to $C_k D(\omega)$ that can be solved with the McClellan-Parks algorithm using the transformations described in the previous section. The function $V(\omega)$ will be then determined by normalizing $T_a(\omega)$ with $1/2T_{\max}$ where $T_{\max} = \max_{\omega \in F}\{T_a(\omega)\}$.

If the weight $W(\omega)$ depends on the frequency, the McClellan-Parks algorithm can not design $V(\omega)$ to satisfy Eq. (6.32). One possible way of designing $V(\omega)$ is to modify the Remez exchange algorithm to solve for the equivalent problem that is to find the extremal frequencies ω_i to satisfy the set of equations

$$\hat{W}(\omega_i)\Big\{\hat{D}(\omega_i) - P(\omega_i)\Big\} = \Big\{1 - (-1)^{i+l}\Big\}\delta \tag{6.34}$$

Instead, we use a different method which is easier to implement, provided that the original Remez algorithm exists.

Consider Eq. (6.32) rewritten as follows

$$W(\omega_i)\Big\{D(\omega_i) - \frac{\delta}{W(\omega_i)} - V(\omega_i)\Big\} = (-1)^{i+l}\delta \tag{6.35}$$

and its equivalent as

$$\hat{W}(\omega_i)\Big\{\hat{D}(\omega_i) - \frac{\delta}{\hat{W}(\omega_i)} - P(\omega_i)\Big\} = (-1)^{i+l}\delta \tag{6.36}$$

If δ was known, we would have established a new problem with the same weight function $W(\omega)$ and a desired function $D'(\omega)$ equal to

$$D'(\omega) = D(\omega) - \frac{\delta}{W(\omega)} \tag{6.37}$$

which could be solved with the original Remez algorithm. Since $D'(\omega)$ is not known *a priori*, we modify the Remez algorithm so that the original desired function $D(\omega)$ can be adjusted and finally converge to $D'(\omega)$ the same time the algorithm iterates towards the optimum solution.

Consider the modified Remez exchange algorithm illustrated in Fig. 6.3. Every time the new deviation δ is calculated and the new extremal frequencies are obtained the desired value $\hat{D}'(\omega)$ is adjusted to

$$\hat{D}'(\omega) = \hat{D}(\omega) - \frac{\delta}{\hat{W}(\omega)} \tag{6.38}$$

where $\hat{D}(\omega)$ is the equivalent of the original desired function and $\hat{W}(\omega)$ is the equivalent weight function. For the modified algorithm, it is true that if the algorithm finally converges and exits the loop, the solution obtained will satisfy Eq. (6.32). In this case, the deviation δ does not necessarily increase to its upper bound throughout the process, it might oscillate about its optimum value before reaching its steady state.

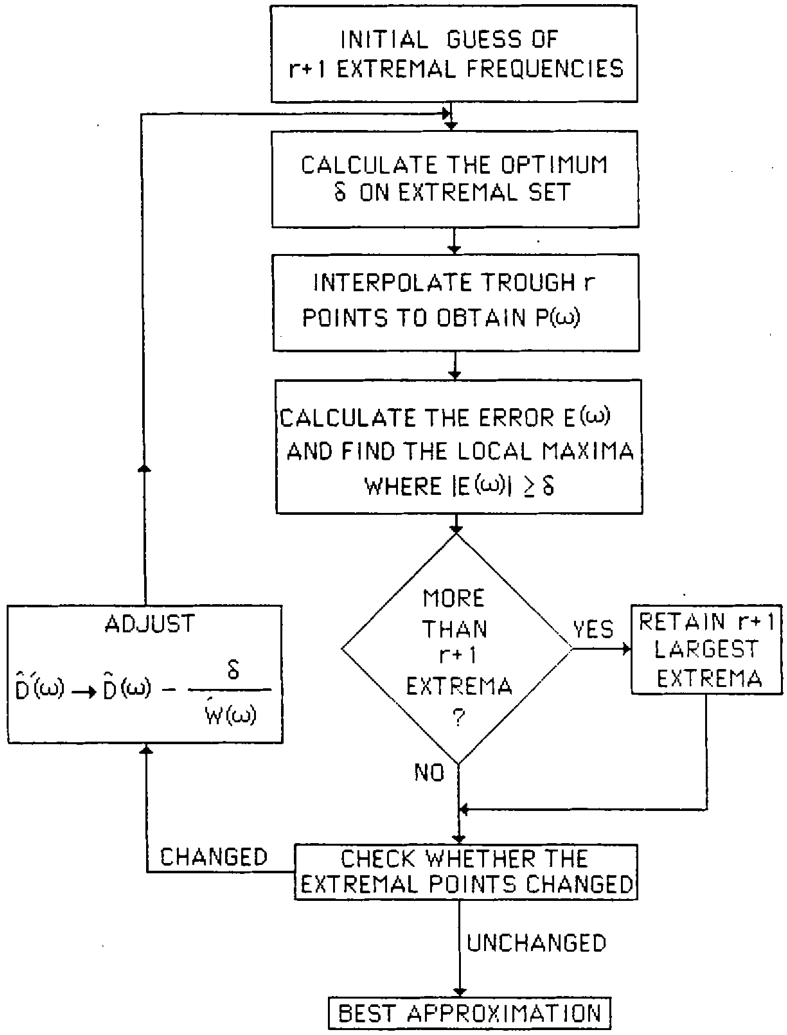

Fig. 6.3 Flowchart of the modified Remez exchange algorithm

In a subband coding system, a good isolation between the subbands is required in order to prevent the quantizing noise that is generated in a particular band to spread to the other bands. Obviously, the performance of the system in isolating the bands depends on the frequency characteristics of the analysis and the reconstruction filters. With the original McClellan-Parks algorithm only equiripple filters can be designed where as with the new algorithm that uses the modified Remez exchange algorithm, a designer can control the frequency characteristics of the filters

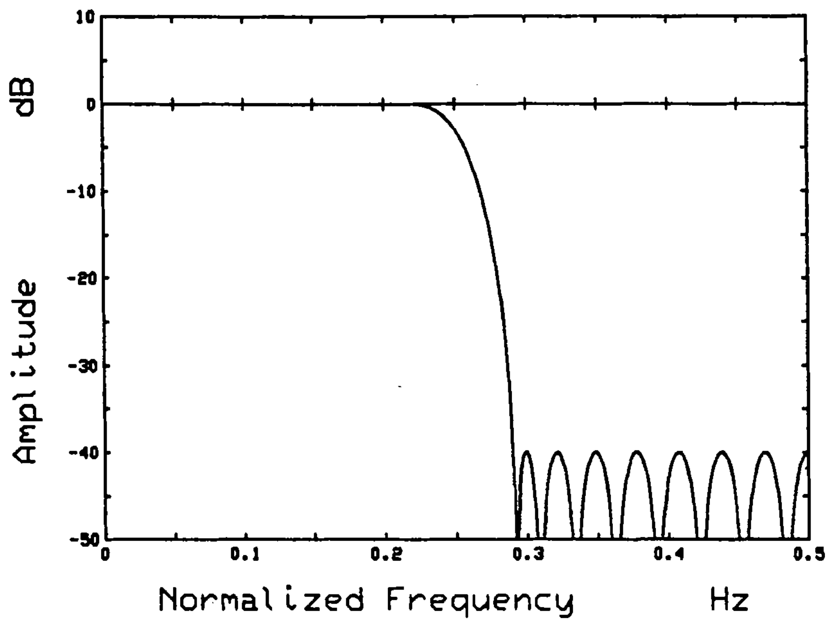

Fig. 6.4 32-tap equiripple filter designed by the modified Remez exchange algorithm

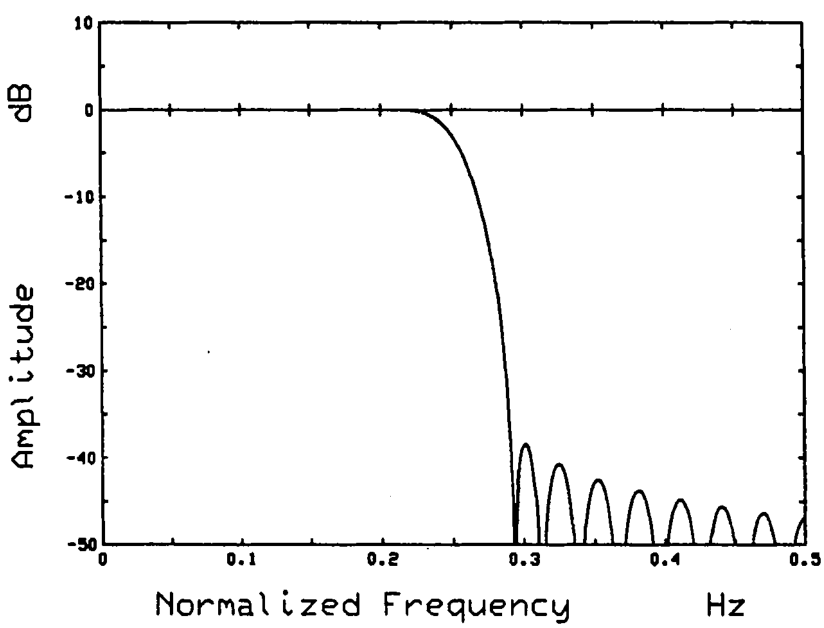

Fig. 6.5 32-tap non-equiripple filter designed by the modified Remez exchange algorithm

through the weighting function $W(\omega)$ and design filters that perform better than the equiripple ones in isolating the subbands. For example, consider the frequency characteristics of two lowpass filters shown in Fig. 6.4 and Fig. 6.5 that were designed using the modified Remez exchange algorithm. Both filters have the same number of coefficients ($N = 32$) and the same cutoff frequency ($\omega_c = 0.4\pi$). For the first filter shown in Fig. 6.4, the weighting function $W(\omega)$ was constant where as for the second filter shown in Fig. 6.5, the weighting function was the one given by the equation

$$W(\omega) = 10(1 - \frac{\omega}{\omega_c}) + 1 \tag{6.39}$$

Examining the frequency characteristics of the two filters, one should note that the stopband attenuation of the second filter is improved by up to 7 dB except for the very first lobe where the attenuation is decreased by approximately 2 dB. For some applications, this slight degradation of the attenuation performance in one part of the stopband will be permitted for the considerable improvement of the attenuation in the rest of the stopband.

6.5 An Alternative Approach to the Design of Antisymmetric Functions

In this section we present an alternative approach to the design of non-equiripple antisymmetric functions. Unlike the approach introduced in the previous section where the design of antisymmetric functions was done by a modified version of the McClellan-Parks algorithm without any need for manual intervention, the approach introduced in this section requires some manual intervention in order to obtain a function with ac eptable frequency characteristics. It was used before the modified version of the McClellan-Parks algorithm was developed, in order to improve the frequency characteristics of the equiripple functions which could be designed by the original version of the algorithm.

Referring to Eq. (5.33) and Eq. (5.34), the frequency response of an antisymmetric function $V(\omega)$ can be written in terms of its coefficients $v(n)$ as

$$V(\omega) = 2 \sum_{k=0}^{N/2-1} v(2k+1) \cos\Big\{(2k+1)\omega\Big\} \tag{6.40}$$

where N is the number of coefficients in $H_0(z)$. According to the above equation, the behaviour of $V(\omega)$ depends on the values of the $N/2$ coefficients $v(2k+1)$ for $k = 0, 1, \ldots, (N/2-1)$. This implies that $N/2$ independent conditions on the behaviour of $V(\omega)$ are necessary and sufficient to determine the values of these coefficients. Clearly, these conditions must not violate the basic requirement for the exact reconstruction filters given by Eq. (6.30).

We are interested on the antisymmetric functions which have all their local maxima that occur in the region $[0, \frac{\pi}{2})$ tangent to the line $\omega = \frac{1}{2}$. These functions have a total of $N/2$ extrema occurring in the region $[0, \frac{\pi}{2})$. Depending on whether $N/2$ is an even or odd number they have respectively $N/4$ maxima and $N/4$ minima or $(N+2)/4$ maxima and $(N-2)/4$ minima. The first extremum occurs at $\omega = 0$ and is either a maximum, if $N/2$ is an odd number, or a minimum, if $N/2$ is an even number. The last extremum is always a maximum.

Assuming that $N/2$ is an even number and that the frequencies at which the local maxima occur are ω_i, $i = 0, 1, \ldots, N/4$ with $0 < \omega_i < \omega_{i+1}$, we can write the following set of $N/4$ equations that indicate the occurrence of extrema at these frequencies.

$$\sum_{k=0}^{N/2-1} (2k+1)v(2k+1)\sin\Big\{(2k+1)\omega_i\Big\}=0 \tag{6.41}$$

for $i = 1, 2, \ldots, N/4$. To indicate that the above $N/4$ extrema are tangent to the line $\omega = \frac{1}{2}$, we form the following set of equations.

$$2\sum_{k=0}^{N/2-1} v(2k+1)\cos\Big\{(2k+1)\omega_i\Big\}=\frac{1}{2} \tag{6.42}$$

for $i = 1, 2, \ldots, N/4$.

Assuming that $N/2$ is an odd number and that the frequencies at which the local maxima occur are ω_i, $i = 1, 2, \ldots, (N+2)/4$ with $\omega_1 = 0$ and $\omega_i < \omega_{i+1}$, we can write a set of $(N-2)/4$ equations that indicate the occurrence of extrema at these frequencies.

$$\sum_{k=0}^{N/2-1} (2k+1)v(2k+1)\sin\Big\{(2k+1)\omega_i\Big\}=0 \tag{6.43}$$

for $i = 2, 3, \ldots, (N+2)/4$. Note that we do not need to write an equation for the extremum that occurs at $\omega = 0$. To indicate that the above $(N+2)/4$ extrema are tangent to the line $\omega = \frac{1}{2}$, we form the following set of $(N+2)/4$ equations.

$$2\sum_{k=0}^{N/2-1} v(2k+1)\cos\Big\{(2k+1)\omega_i\Big\}=\frac{1}{2} \tag{6.44}$$

for $i = 1, 2, \ldots, (N+2)/4$.

In both of the above cases, the total number of equations is $N/2$ and is equal to the number of unknown coefficients. This implies that it is possible to obtain the values of the coefficients by imposing conditions on the locations and values of the maxima and then solving the above described set of linear equations. We should note that the expected locations of the maxima must be carefully chosen since the above set of equations guarantees only the occurrence of extrema at the specified locations which can be either maxima or minima. Another important fact we must keep in mind, is that by increasing the distance between two consecutive maxima, the size of the ripple defined by these maxima will increase too.

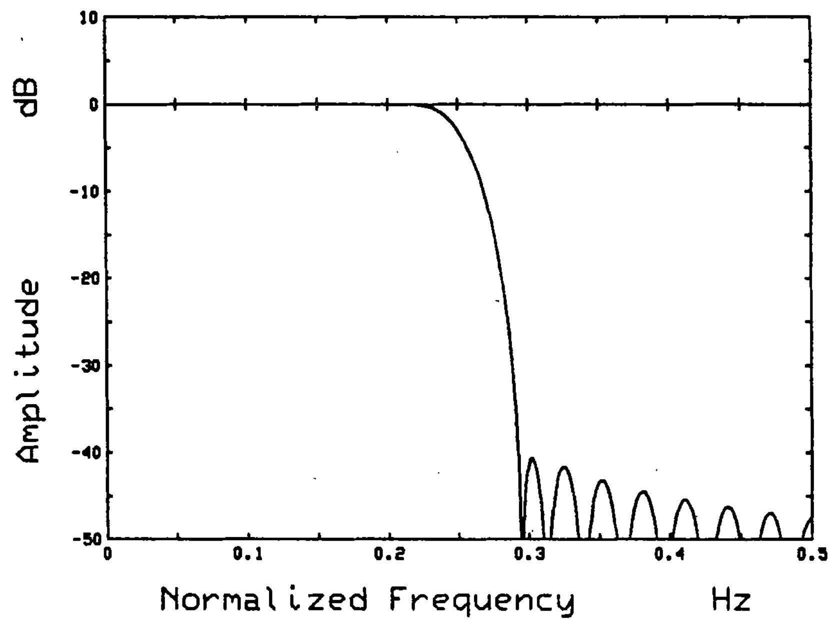

Fig. 6.6 32-tap filter designed by specifying the location of its maxima

One possible application of this approach is to modify the frequency characteristics of an existing antisymmetric function by changing the location of its maxima. Obviously, this approach implies a trial and error solution, if we are to design a function that is somehow better than the original one. As an example, consider the filter shown in Fig. 6.6 which was designed from the antisymmetric function that corresponds to the equiripple filter in Fig. 6.4 by changing the location of its maxima.

Chapter 7 Performance of Exact Reconstruction Filter Banks

7.1 Introduction

The major difference between linear phase QMF filters and time-reversed QMF filters is that time-reversed QMF filters, in the absence of individual channel coders, do not introduce any amplitude distortion to the response of a subband system. Minimization of amplitude distortion in the system response is always considered a major criterion for the design of linear phase QMF filters whereas for the design of time-reversed QMF filters it is taken for granted. The design of time-reversed QMF filters is based on the following three parameters:

1. The number of coefficients N.

2. The width of the transition band W_t.

3. The stopband attenuation A_s.

The number of filter coefficients N determines the overall delay caused by the system as well as the number of computations required to implement the system. Both factors are important for real time applications. The width of the transition W_t as well as the stopband attenuation A_s, determine the leakage between the subbands which is always considered an important factor in the presence of the individual channel coders. The stopband attenuation A_s also determines the passband ripple since the two, on a linear scale, complement each other.

The design of time-reversed filters discussed in Chapter 5 and Chapter 6 is done by specifying the number of filter coefficients N, the sampling frequency f_s, and the cutoff frequency f_c. The radial cutoff frequency ω_c is given by

$$\omega_c = 2\pi \frac{f_c}{f_s} \tag{7.1}$$

The desired value function $D(\omega)$ and the weighting function $W(\omega)$ are then specified in the region $0 \leq \omega \leq \omega_c$ with $\omega_c < \frac{\pi}{2}$. For a lowpass filter, the region $0 \leq \omega \leq \omega_c$ is defined to be the passband, the region $\omega_c < \omega < \pi - \omega_c$ the transition band and the region $\pi - \omega_c \leq \omega \leq \pi$ the stopband. According to this definition, the passband and stopband are the regions where the ripple is minimized whereas the transition band is the region where the response is not controlled. The width of the transition band W_t, in terms of ω_c, is given by

$$W_t = \pi - 2\omega_c \tag{7.2}$$

The above three criteria for the design of time-reversed QMF filters, always depend on each other and only two of them can be specified at a time. The third is left to be defined in terms of the specified ones. In the implementation of the filter design procedure, for a given weighting function $W(\omega)$, the stopband attenuation A_s is left to be determined as a function of the number of coefficients N and the width of the transition band W_t. This implies that filters with constraints on their stopband attenuation must be designed by trial and error unless a relationship between A_s, W_t and N is developed.

In this chapter, we consider the performance of time-reversed filters in terms of the stopband attenuation A_s as a function of the the weighting $W(\omega)$, the number of filter coefficients N and the width of the transition band W_t. We include performance charts for three different weighting functions which enable the designer to relate the filter design parameters and make tradeoffs between them. We finally discuss the performance of the time-reversed filters in subband systems, when implemented with finite precision arithmetic.

7.2 Equiripple Time-Reversed Filters

The performance of time-reversed QMF filters with equiripple characteristics is illustrated in Fig. 7.1. Referring to Fig. 7.1.a, it appears that for a given number of coefficients N, the stopband attenuation A_s increases almost linearly with the width of the transition band W_t. Figure 7.1.b shows that for a given value of W_t, a similar relationship occurs between A_s and N. These observations indicate that the behaviour of the stopband attenuation A_s as a function of N and W_t can be

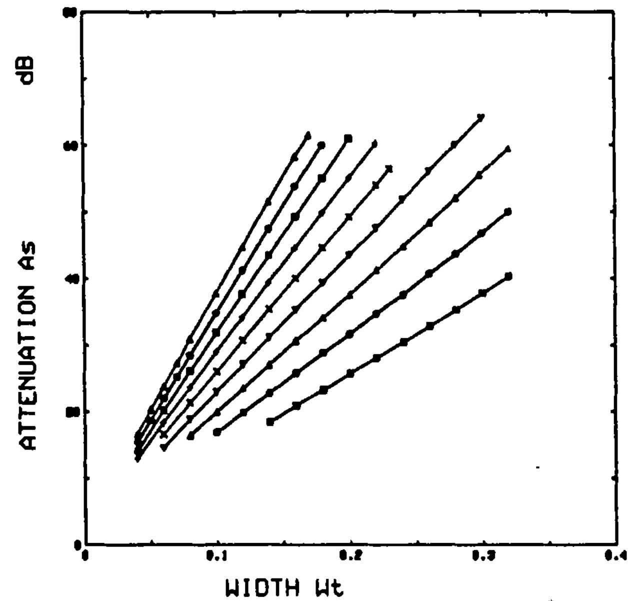

a) Stopband attenuation A_s versus width of transition band W_t (normalized by π ($f_{\max}$)): counterclockwise $N = 16, 20, 24, \ldots, 48$

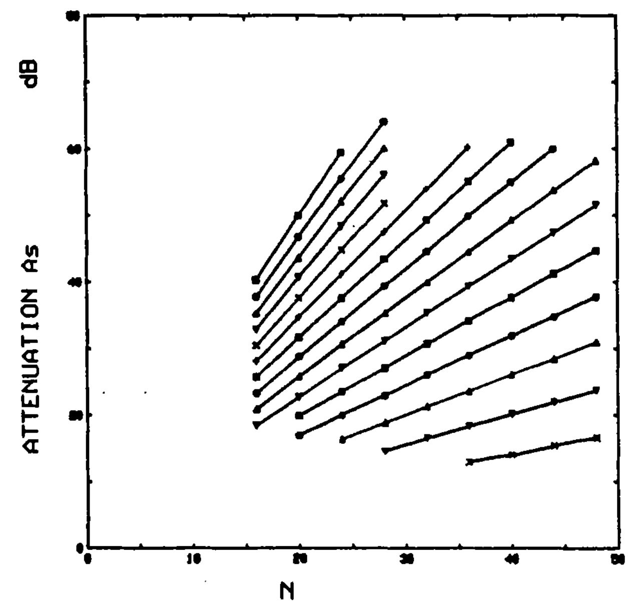

b) Stopband Attenuation A_s versus number of coefficients N: counterclockwise $W_t = 0.04\pi, 0.06\pi, 0.08\pi, \ldots, 0.32\pi$

Fig. 7.1 Performance charts for equiripple time-reversed QMF filters approximated by a formula of the form

$$A_s = m_1 W_t N + m_2 W_t + m_3 N + m_4 \tag{7.3}$$

where $m_1, \ldots, m_4$ are constants. Minimization of the mean square error gives

$$A_s = 7.169 W_t N + 5.355 W_t + 0.028 N + 1.491 \tag{7.4}$$

where A_s is in dB's, N takes even values and W_t is normalized with respect to π ($f_{\max}$). This yields an absolute maximum approximation error of of less than 0.5 dB.

7.3 Non-Equiripple Time-Reversed Filters

The performance of time-reversed filters with non-equiripple characteristics have been considered for two different weighting functions $W(\omega)$. The first weighting function is given by

$$W(\omega) = 10(1 - \frac{\omega}{\omega_c}) + 1 \quad \text{for } 0 \leq \omega \leq \frac{\pi}{2} \tag{7.5}$$

This function yields a difference of 10.4 dB between the stopband attenuation at $\omega = \pi$ and at $\omega = \pi - \omega_c$. The performance of the filters is shown in Fig. 7.2 where the maximum stopband attenuation A_s which occurs at $\omega = \pi$, is considered. Figure 7.2.a shows the relationship between the stopband attenuation A_s and the width of the transition band W_t for different number of coefficients N. Figure 7.2.b shows the relationship between the stopband attenuation A_s and the number of coefficients N for different values of the width W_t.

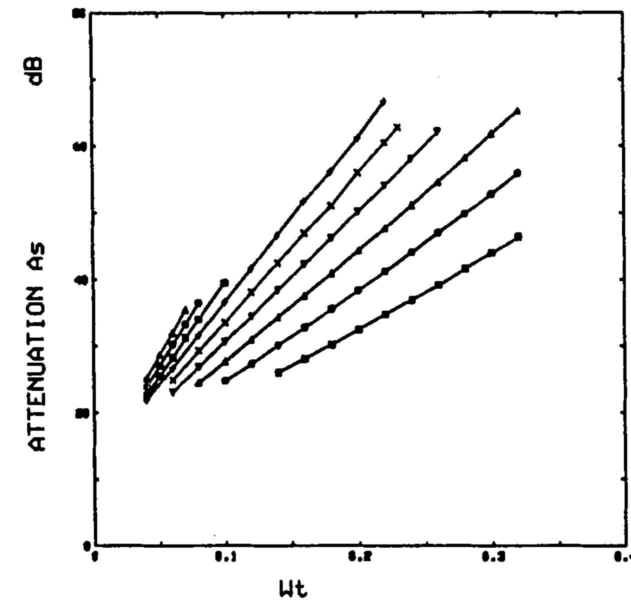

a) Maximum stopband Attenuation A_s versus width of transition band W_t (normalized by π ($f_{\max}$)): counterclockwise $N = 16, 20, 24, \ldots, 48$

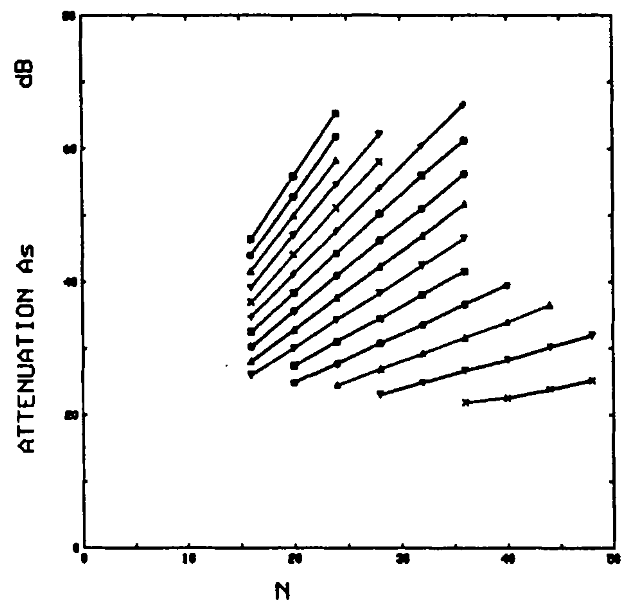

b) Maximum stopband attenuation A_s versus number of coefficients N: counterclockwise $W_t = 0.04\pi, 0.06\pi, 0.08\pi, \ldots, 0.32\pi$

Fig. 7.2 Performance charts for non-equiripple time-reversed QMF filters obtained by using Eq. (7.5)

A formula of the form given by Eq. (7.3) can be used to approximate the relationship between A_s, N and W_t. Minimization of the mean square error gives

$$A_s = 7.001 W_t N + 0.323 W_t + 0.050 N + 9.518 \tag{7.6}$$

This formula yields an absolute maximum approximation error of less than 0.8 dB.

The second weighting function that have been used is given by

$$W(\omega) = 50(1 - \frac{\omega}{\omega_c}) + 1 \quad \text{for } 0 \leq \omega \leq \frac{\pi}{2} \tag{7.7}$$

This function yields a difference of 17.1 dB between the stopband attenuation at $\omega = \pi$ and at $\omega = \pi - \omega_c$. In a similar way as to the previous example, Fig. 7.3 shows the performance of the designed filters. A similar formula to Eq. (7.3) that relates the stopband attenuation A_s to N and W_t, is also obtained.

$$A_s = 6.829 W_t N - 4.875 W_t + 0.021 N + 15.240 \tag{7.8}$$

This formula yields an absolute maximum approximation error of less than 1.0 dB.

7.4 The Effect of Weighting on Filter Designs

Figure 7.4 shows the performance of equal-length time-reversed filters designed with the three different weighting functions discussed in the previous sections. Each weighting function is represented by two curves that correspond to the maximum and minimum attenuation except for the equal-weighting (equiripple) one that is represented by a single curve. The inner curve corresponds to equiripple filters, the next two curves correspond to filters designed with the weighting given by

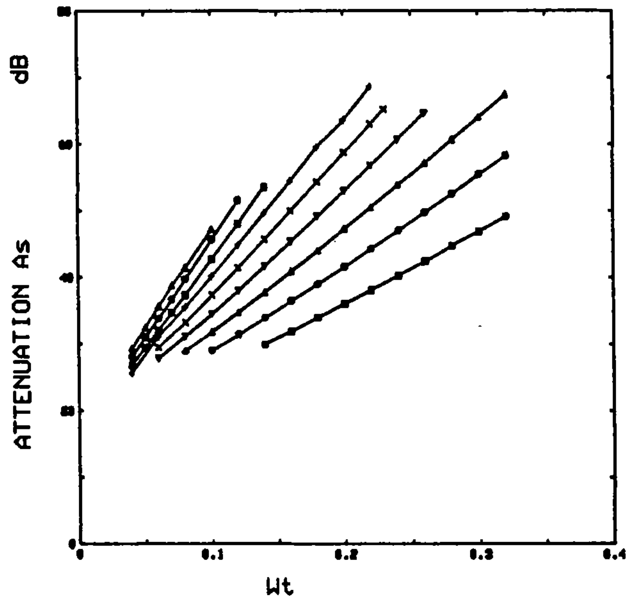

a) Maximum stopband attenuation A_s versus width of transition band W_t (normalized by π ($f_{\max}$)): counterclockwise $N = 16, 20, 24, \ldots, 48$

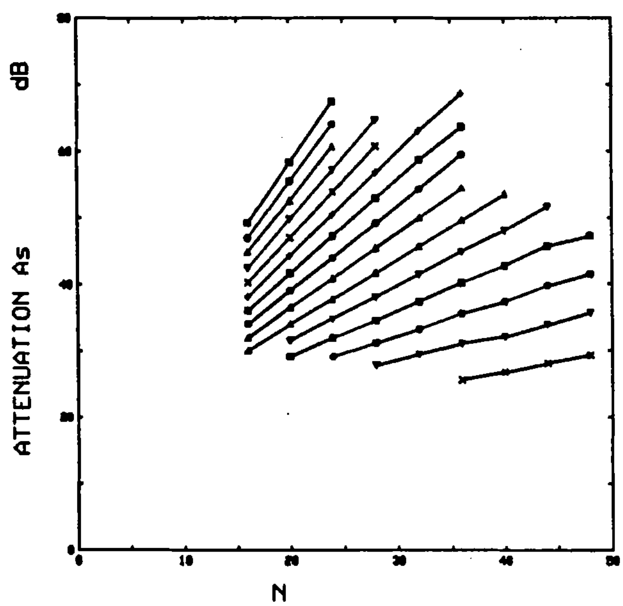

b) Maximum stopband attenuation A_s versus number of coefficients N: counterclockwise $W_t = 0.04\pi, 0.06\pi, 0.08\pi, \ldots, 0.32\pi$

Fig. 7.3 Performance charts for non-equiripple time-reversed QMF filters obtained by using Eq. (7.7)

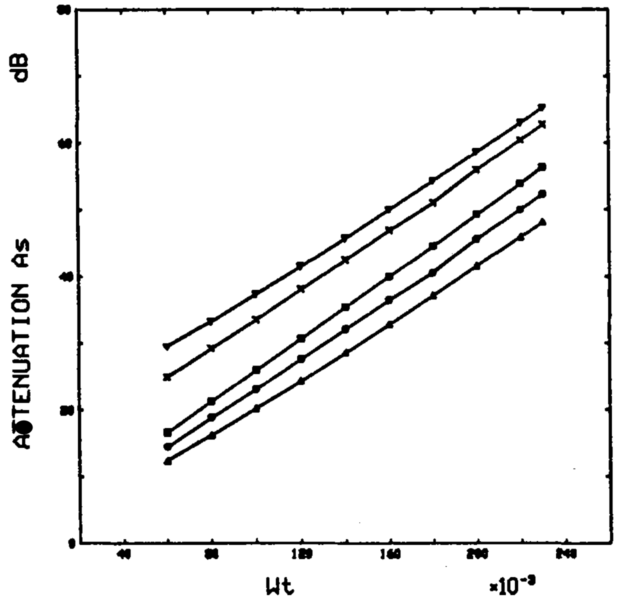

a) Maximum and Minimum attenuation A_s versus width of transition band W_t (normalized by π ($f_{\max}$)) for $N = 32$

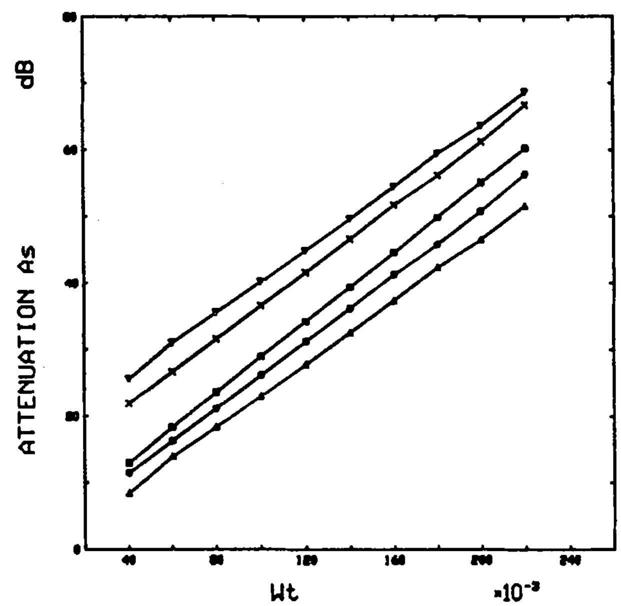

b) Maximum and Minimum attenuation A_s versus width of transition band W_t (normalized by π ($f_{\max}$))for $N = 36$

Fig. 7.4 Performance charts of equal-length time-reversed QMF filters with different weightings

Eq. (7.5), and the outermost curves correspond to filters designed with the weighting given by Eq. (7.7). The maximum and minimum attenuation curves diverge from the equiripple curve as the weighting function diverges from the equal-weighting function.

The performance of the filters designed with a particular weighting function is examined in terms of the relative positions of the corresponding maximum and minimum attenuation curves with respect to the equiripple curve. For a given width W_t, the distance between the equiripple curve and the maximum attenuation curve corresponds to the improvement in the stopband attenuation characteristics whereas the distance between the equiripple curve and the minimum attenuation curve corresponds to the price that must be paid for this improvement. Figure 7.4 shows that for small values of W_t, the equiripple curve lies close to the minimum attenuation curves. The distance between these curves increases as W_t increases. On the other hand, the distance between the maximum attenuation curve and the equiripple curve decreases as W_t increases. This implies that for filters with narrow transition bands, unequal weighting functions can be used to improve the stopband attenuation characteristics whereas for filters with wide transition bands equiripple designs are more attractive.

The performance of time-reversed QMF filters designed with different weightings as a function of the number of coefficients N, is shown in Fig. 7.5. As in the previous figure, the inner curve corresponds to equiripple filters, the next two curves correspond to filters designed with the weighting given by Eq. (7.5) and the out-

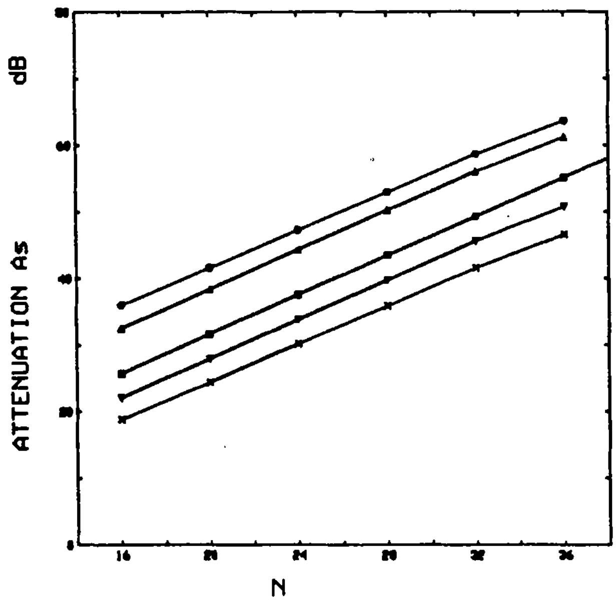

a) Maximum and minimum attenuation A_s versus number of coefficients N for $W_t = 0.20\pi$

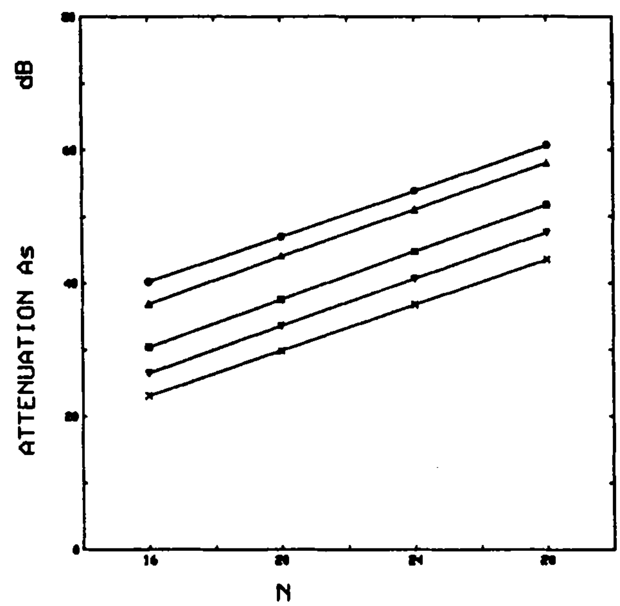

b) Maximum and minimum attenuation A_s versus number of coefficients N for $W_t = 0.24\pi$

Fig. 7.5 Performance charts of equal-width W_t time-reversed QMF filters with different weightings ermost curves correspond to filters designed with the weighting given by Eq. (7.7). The curves appear to be parallel to each other which implies that the weighting one must use to improve the characteristics of the filters, does not depend on the number of coefficients N.

7.5 Performance of Time-Reversed QMF Filters in subband Systems

The performance of time-reversed QMF filters in subband systems have been examined by computer simulation using single precision floating point arithmetic. A number of filters summarized in Appendix A, have been designed and tested in the absence of individual channel coders.

With frequency selective input signals, the alias-free condition was examined. It was found that with single precision floating point arithmetic, the aliasing introduced by the systems is negligible. The exact reconstruction condition was examined with allpass input signals. It was found that the amplitude distortion introduced by the systems is also negligible (not more than 0.0004 dB).

Chapter 8 Conclusions

The intention of this work was to discuss different filter families that deal with the issues involved in the design of subband coding systems. Redundant information have been always considered a first priority issue in the design of subband coding systems. For this reason, only filters that belong to the general family of fractional-band filters were considered. Specifically, linear phase QMF filters, IIR-QMF filters, and Pseudo-QMF filters were briefly discussed whereas nonlinear phase time-reversed QMF filters were given more emphasis.

Linear phase QMF filters can be used to remove aliasing and phase distortion. They introduce amplitude distortion which can be controlled and minimized with special filter design techniques. Their implementation can be accomplished in a very efficient way by taking advantage of certain similarities between the filter coefficients. They are mainly designed for two band subband systems but they can be also used in tree structures (or the equivalent parallel structures) for multiband systems.

IIR-QMF filters can be designed to remove aliasing and amplitude distortion but they introduce phase distortion. The level of the phase distortion is sometimes severe even for speech signals and limits their applications. It is suggested that they should be used for the outermost stages of tree-structured multiband systems to reduce delay, computational load with only a moderate phase distortion. Their implementation can be also accomplished in a very efficient way due to some similarities between the filter coefficients.

Pseudo-QMF filters represent a different category of filters that can be used for multiband systems. They are designed to remove the aliasing due to adjacent bands only and they introduce amplitude distortion. Their main advantages are that they can be implemented very efficiently and that they can be used for an arbitrary number of equal-bandwidth bands whereas with tree structures, the number of equal-bandwidth bands is constrained to powers of 2.

Nonlinear phase time-reversed QMF filters were given more emphasis in this study. Theoretically these filters can be designed to remove aliasing, phase as well as amplitude distortion. The original study, had developed the conditions for noncausal time-reversed QMF filters whereas in this study we examined the case with causal filters. Based on the results we obtained, we then developed a filter design procedure which uses the McClellan-Parks algorithm to design optimum weighted Chebyshev approximations. The performance charts of the designed filters were presented in the previous chapter and can be used to help the designer to choose the appropriate values for the filter design parameters. Also, a number of filter design examples are presented in Appendix A.

Nonlinear phase time-reversed QMF filters, when implemented with single precision arithmetic, introduce amplitude distortion which is negligible. The fact that amplitude distortion is not a design parameter makes the design of these filters easier than the design of linear phase QMF filter where amplitude distortion is considered an important design parameter. Also, time-reversed filters can be used in non-symmetric tree-structures without any need for adding compensation filters.

The main disadvantage of time-reversed QMF filters over linear phase QMF filters is the implementation complexity. It appears that with time-reversed QMF more memory to store the values of the filter coefficients and more number of computations are required than with linear phase QMF filters.

The performance of time-reversed QMF filters is still to be examined and compared with the performance of other filters in the presence of individual channel coders. There are some questions as to whether coding algorithms are sensitive to the nonlinear phase of the analysis filter bank. This is left for future research.

Appendix A Filter Design Examples

Example 1

Specifications: $N = 16$, $W_t = 0.32\pi$ ($\omega_c = 0.34\pi$), $A_s = 40.3$ dB

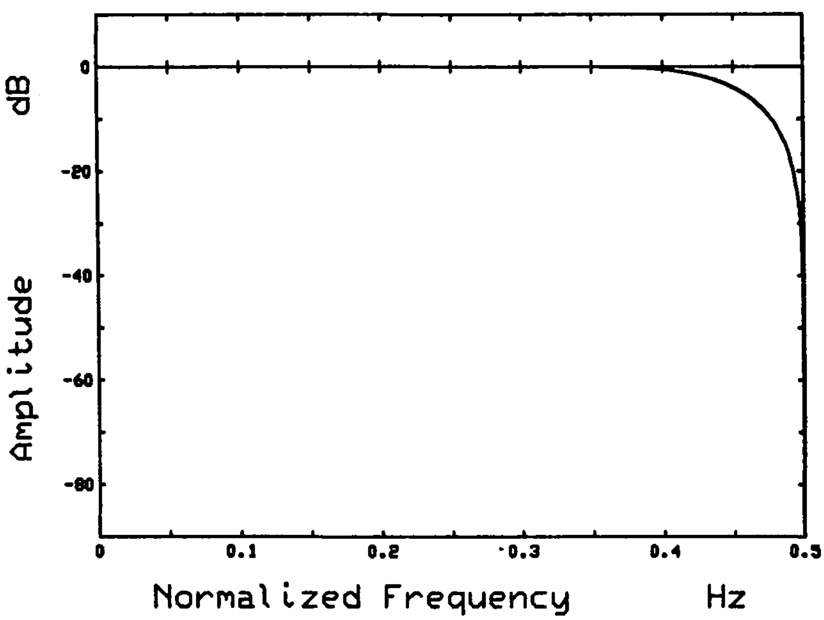

Fig. 1.a Transformation $U_1(\omega)$

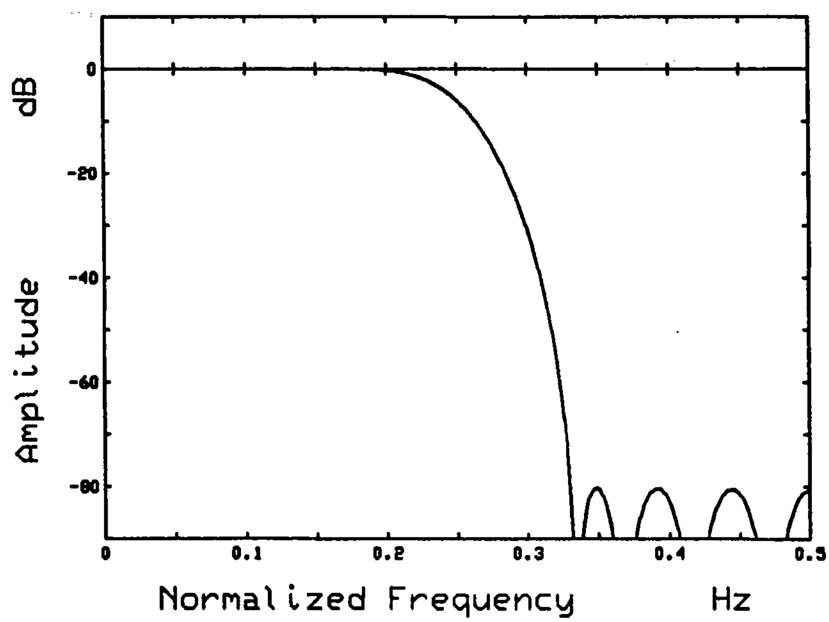

Fig. 1.b Cascade filter response $F_0(\omega)$

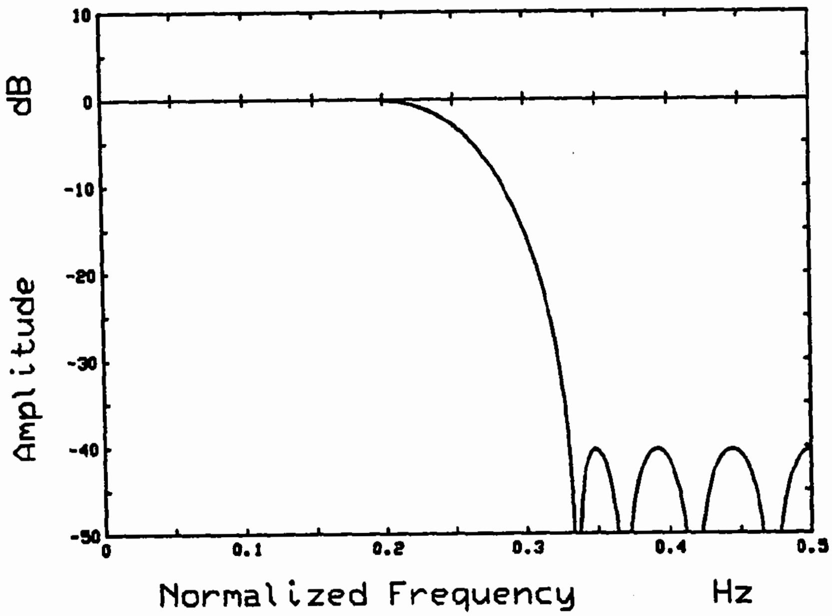

Fig. 1.c Lowpass filter response $H_0(\omega)$

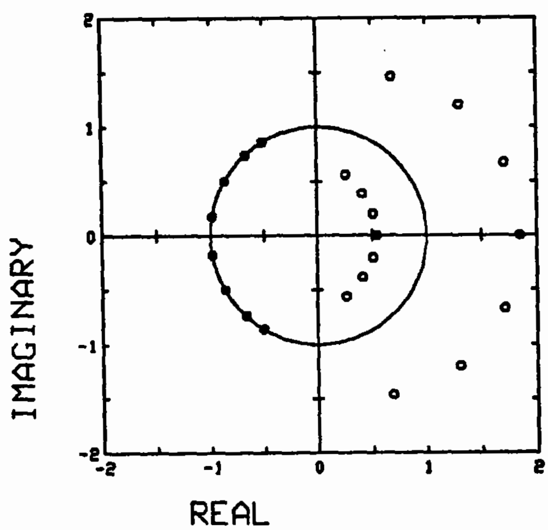

Fig. 1.d Location of zeros for $F_0(z)$

Filter Coefficients $h_0(n)$			
$h_0(0)$	$-2.4568239 \times 10^{-3}$	$h_0(8)$	7.5558924×10^{-2}
$h_0(1)$	7.7433910×10^{-3}	$h_0(9)$	7.9240207×10^{-2}
$h_0(2)$	$-3.3250626 \times 10^{-3}$	$h_0(10)$	$-1.2992087 \times 10^{-1}$
$h_0(3)$	$-1.6363097 \times 10^{-2}$	$h_0(11)$	$-1.5892358 \times 10^{-1}$
$h_0(4)$	1.5070384×10^{-2}	$h_0(12)$	1.8932747×10^{-1}
$h_0(5)$	2.9669048×10^{-2}	$h_0(13)$	4.8802894×10^{-1}
$h_0(6)$	$-3.8191988 \times 10^{-2}$	$h_0(14)$	3.8909860×10^{-1}
$h_0(7)$	$-4.8055219 \times 10^{-2}$	$h_0(15)$	1.2345324×10^{-1}

Example 2

Specifications: $N = 20$, $W_t = 0.26\pi$ $(\omega_c = 0.37\pi)$, $A_s = 40.7$ dB

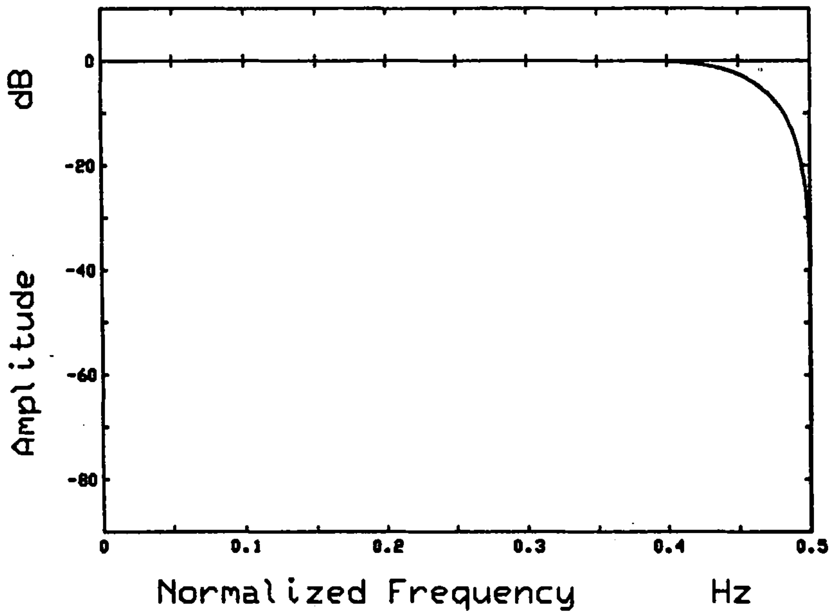

Fig. 2.a Transformation $U_1(\omega)$

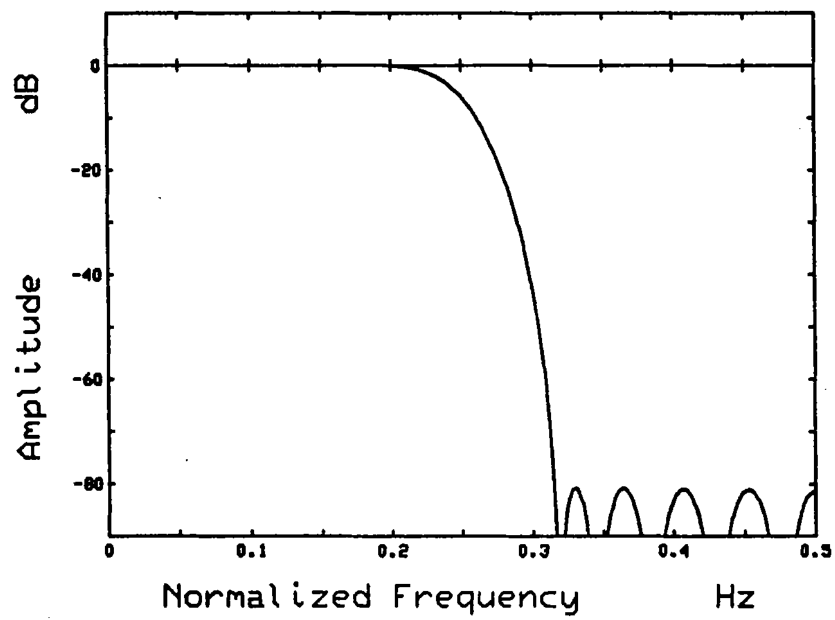

Fig. 2.b Cascade filter response $F_0(\omega)$

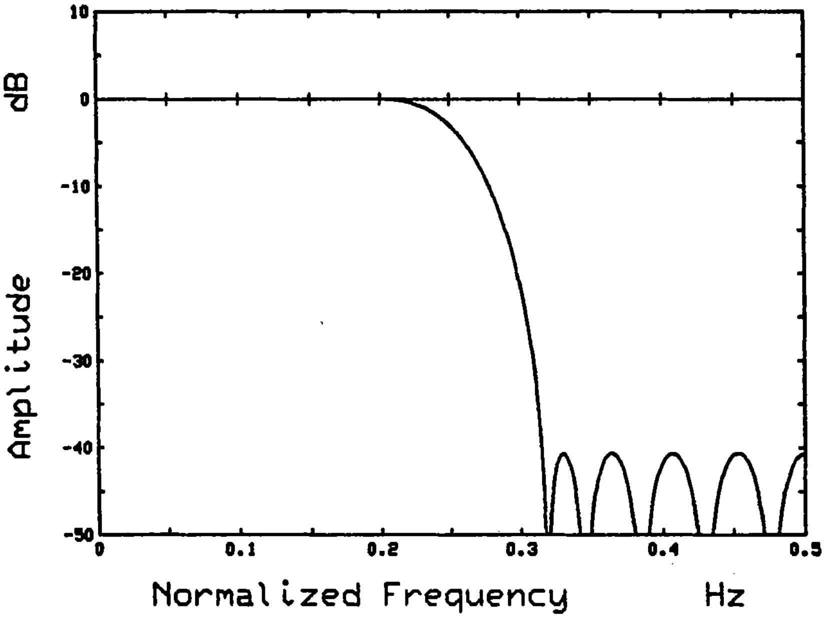

Fig. 2.c Lowpass filter response $H_0(\omega)$

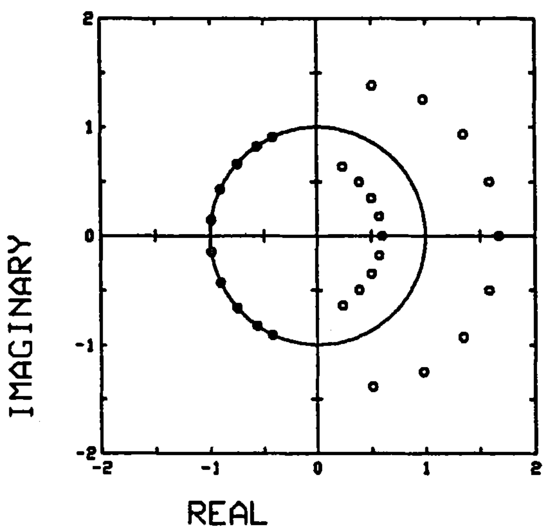

Fig. 2.d Location of zeros for $F_0(z)$

Filter Coefficients $h_0(n)$			
$h_0(0)$	$-1.6137630 \times 10^{-3}$	$h_0(10)$	$-7.0854503 \times 10^{-2}$
$h_0(1)$	5.2556542×10^{-3}	$h_0(11)$	$-2.6432023 \times 10^{-2}$
$h_0(2)$	$-3.6302538 \times 10^{-3}$	$h_0(12)$	1.1091515×10^{-1}
$h_0(3)$	$-7.8721885 \times 10^{-3}$	$h_0(13)$	4.6765399×10^{-2}
$h_0(4)$	1.0614178×10^{-2}	$h_0(14)$	$-1.6981213 \times 10^{-1}$
$h_0(5)$	1.1864857×10^{-2}	$h_0(15)$	$-1.2225752 \times 10^{-1}$
$h_0(6)$	$-2.3272125 \times 10^{-2}$	$h_0(16)$	2.4470898×10^{-1}
$h_0(7)$	$-1.5707261 \times 10^{-2}$	$h_0(17)$	4.8420979×10^{-1}
$h_0(8)$	4.2772560×10^{-2}	$h_0(18)$	3.5551248×10^{-1}
$h_0(9)$	1.9628653×10^{-2}	$h_0(19)$	1.0916105×10^{-1}

Example 3

Specifications: $N = 28, W_t = 0.20\pi \ (\omega_c = 0.40\pi),\ A_s = 43.5$ dB

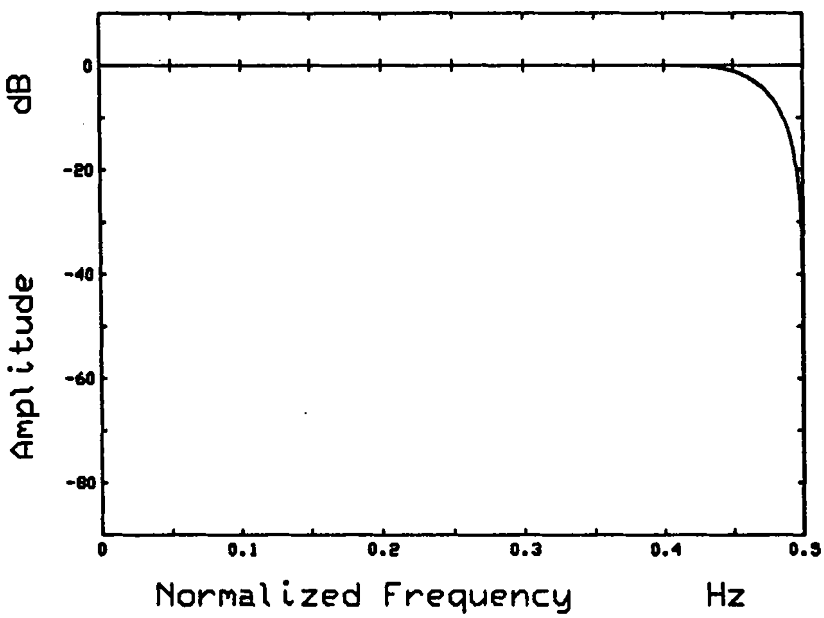

Fig. 3.a Transformation $U_1(\omega)$

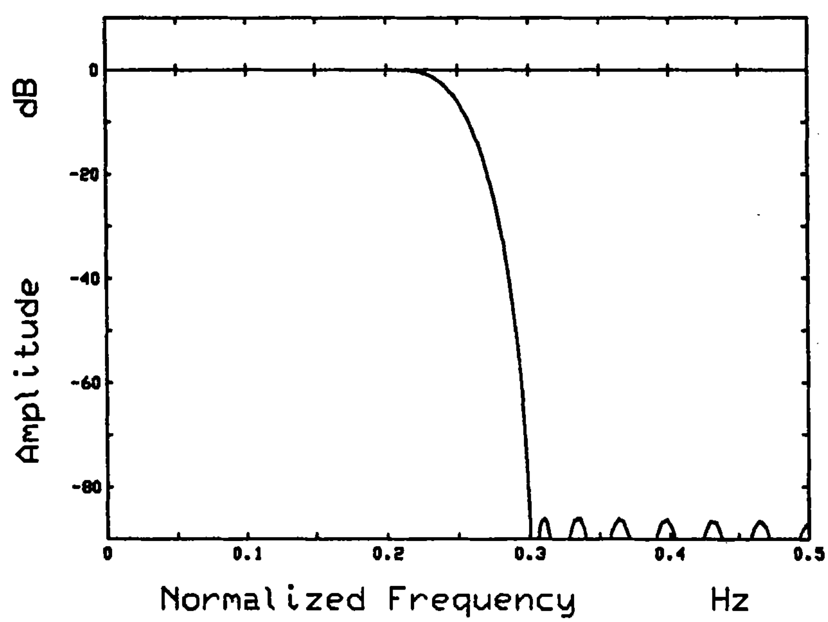

Fig. 3.b Cascade filter response $F_0(\omega)$

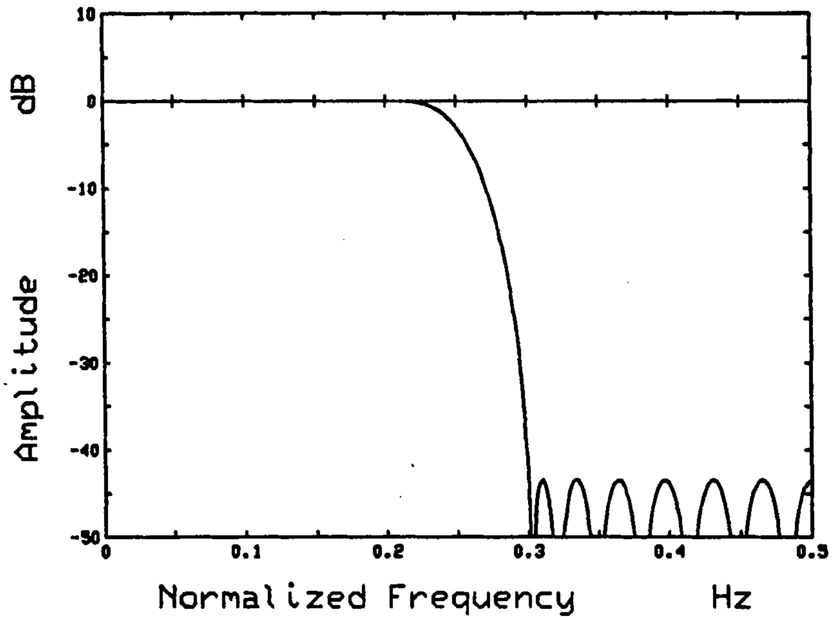

Fig. 3.c Lowpass filter response $H_0(\omega)$

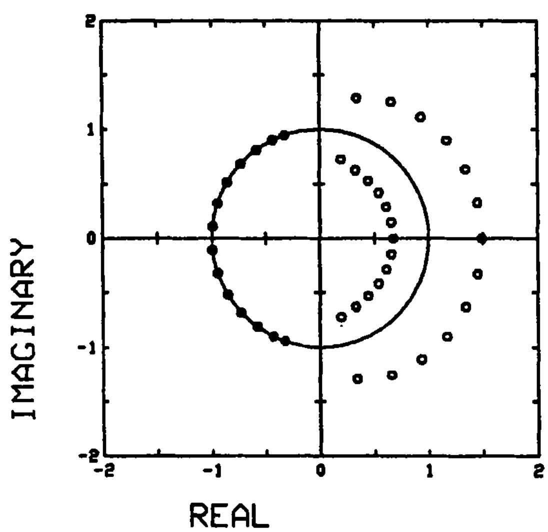

Fig. 3.d Location of zeros for $F_0(z)$

Filter Coefficients $h_0(n)$			
$h_0(0)$	$-7.2860471 \times 10^{-4}$	$h_0(14)$	$-4.7025927 \times 10^{-2}$
$h_0(1)$	2.5676430×10^{-3}	$h_0(15)$	2.2027747×10^{-2}
$h_0(2)$	$-2.6707777 \times 10^{-3}$	$h_0(16)$	6.4726825×10^{-2}
$h_0(3)$	$-1.8825047 \times 10^{-3}$	$h_0(17)$	$-3.1041048 \times 10^{-2}$
$h_0(4)$	5.1714213×10^{-3}	$h_0(18)$	$-9.0293864 \times 10^{-2}$
$h_0(5)$	1.6434580×10^{-3}	$h_0(19)$	3.7392810×10^{-2}
$h_0(6)$	$-9.4797027 \times 10^{-3}$	$h_0(20)$	1.3112887×10^{-1}
$h_0(7)$	$-3.4609742 \times 10^{-4}$	$h_0(21)$	$-2.9666099 \times 10^{-2}$
$h_0(8)$	1.5544902×10^{-2}	$h_0(22)$	$-2.0292738 \times 10^{-1}$
$h_0(9)$	$-2.4525657 \times 10^{-3}$	$h_0(23)$	$-4.0378380 \times 10^{-2}$
$h_0(10)$	$-2.3547147 \times 10^{-2}$	$h_0(24)$	3.2225308×10^{-1}
$h_0(11)$	7.0853804×10^{-3}	$h_0(25)$	4.6675440×10^{-1}
$h_0(12)$	3.3811825×10^{-2}	$h_0(26)$	3.0067835×10^{-1}
$h_0(13)$	$-1.3690738 \times 10^{-2}$	$h_0(27)$	8.5321710×10^{-2}

Example 4

Specifications: $N = 32$, $W_t = 0.18\pi$ $(\omega_c = 0.41\pi)$, $A_s = 44.6$ dB

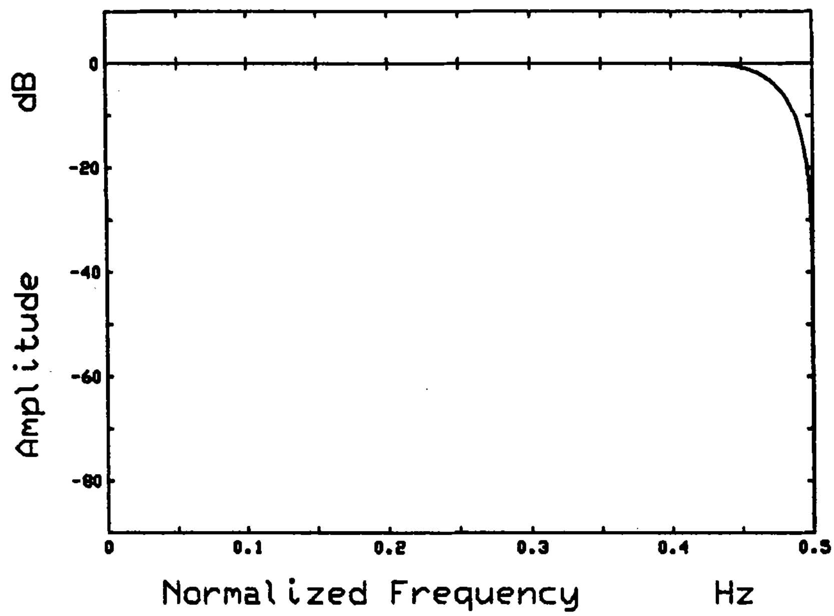

Fig. 4.a Transformation $U_1(\omega)$

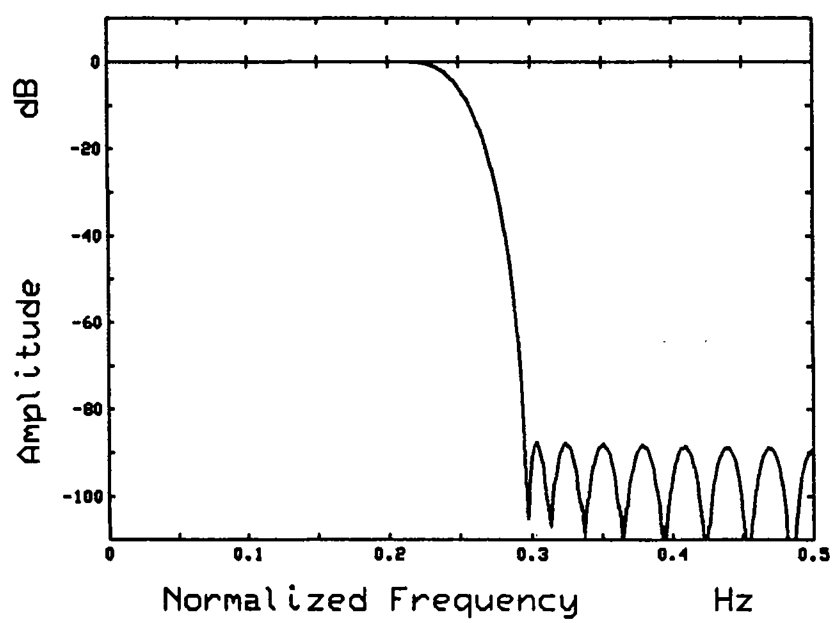

Fig. 4.b Cascade filter response $F_0(\omega)$

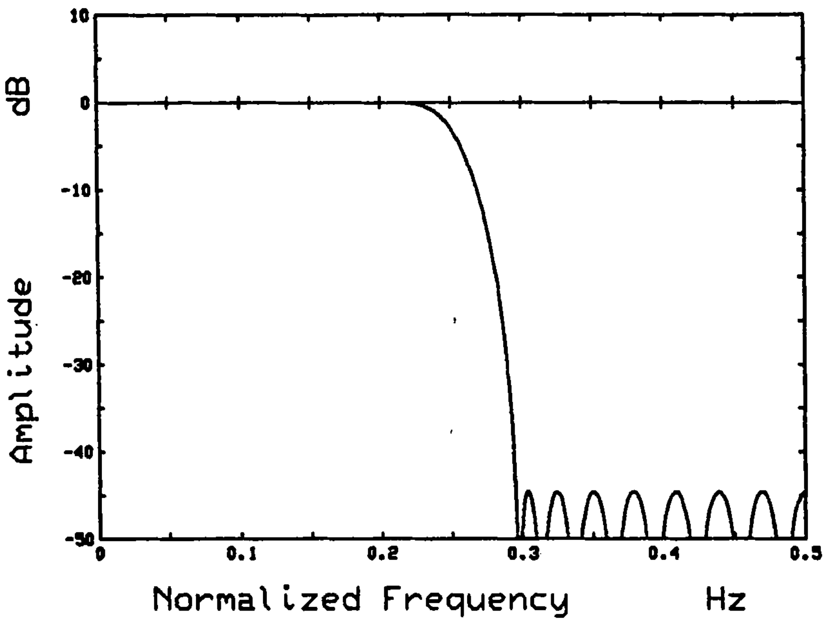

Fig. 4.c Lowpass filter response $H_0(\omega)$

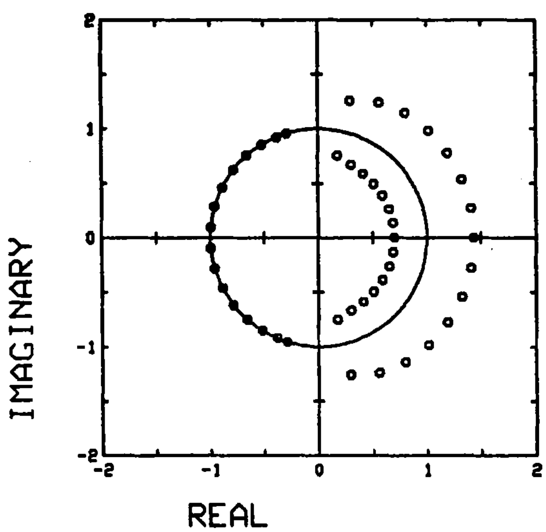

Fig. 4.d Location of zeros for $F_0(z)$

Filter Coefficients $h_0(n)$			
$h_0(0)$	$-5.3710731 \times 10^{-4}$	$h_0(16)$	3.4545094×10^{-2}
$h_0(1)$	1.9473078×10^{-3}	$h_0(17)$	$-3.0846441 \times 10^{-2}$
$h_0(2)$	$-2.2650216 \times 10^{-3}$	$h_0(18)$	$-4.5249908 \times 10^{-2}$
$h_0(3)$	$-8.5122197 \times 10^{-4}$	$h_0(19)$	4.2021264×10^{-2}
$h_0(4)$	3.7368814×10^{-3}	$h_0(20)$	6.0482559×10^{-2}
$h_0(5)$	2.6636234×10^{-4}	$h_0(21)$	$-5.4073220 \times 10^{-2}$
$h_0(6)$	$-6.3519167 \times 10^{-3}$	$h_0(22)$	$-8.4412175 \times 10^{-2}$
$h_0(7)$	1.1881181×10^{-3}	$h_0(23)$	6.4137047×10^{-2}
$h_0(8)$	9.8824208×10^{-3}	$h_0(24)$	1.2598691×10^{-1}
$h_0(9)$	$-3.8266083 \times 10^{-3}$	$h_0(25)$	$-6.1184811 \times 10^{-2}$
$h_0(10)$	$-1.4334622 \times 10^{-2}$	$h_0(26)$	$-2.0451131 \times 10^{-1}$
$h_0(11)$	7.9251356×10^{-3}	$h_0(27)$	$-5.1571207 \times 10^{-3}$
$h_0(12)$	1.9773092×10^{-2}	$h_0(28)$	3.4555070×10^{-1}
$h_0(13)$	$-1.3715463 \times 10^{-2}$	$h_0(29)$	4.5620578×10^{-1}
$h_0(14)$	$-2.6367123 \times 10^{-2}$	$h_0(30)$	2.8113172×10^{-1}
$h_0(15)$	2.1344582×10^{-2}	$h_0(31)$	7.7541920×10^{-2}

Example 5

Specifications: $N = 36, W_t = 0.18\pi$ $(\omega_c = 0.41\pi)$, $A_s = 49.9$ dB

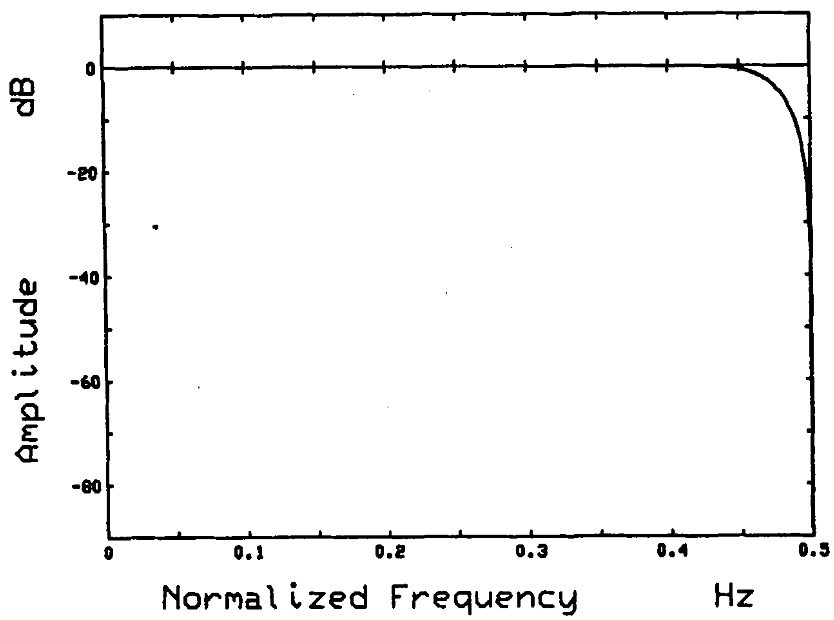

Fig. 5.a Transformation $U_1(\omega)$

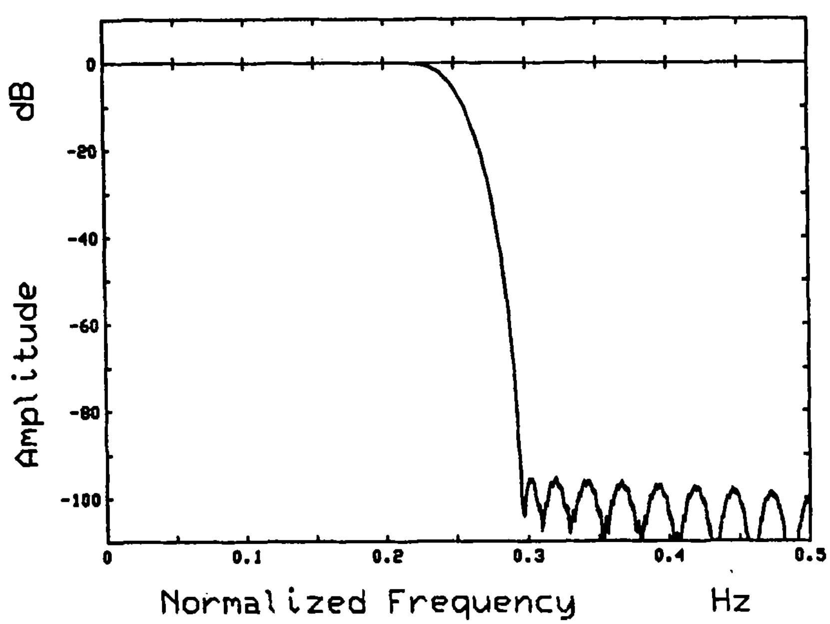

Fig. 5.b Cascade filter response $F_0(\omega)$

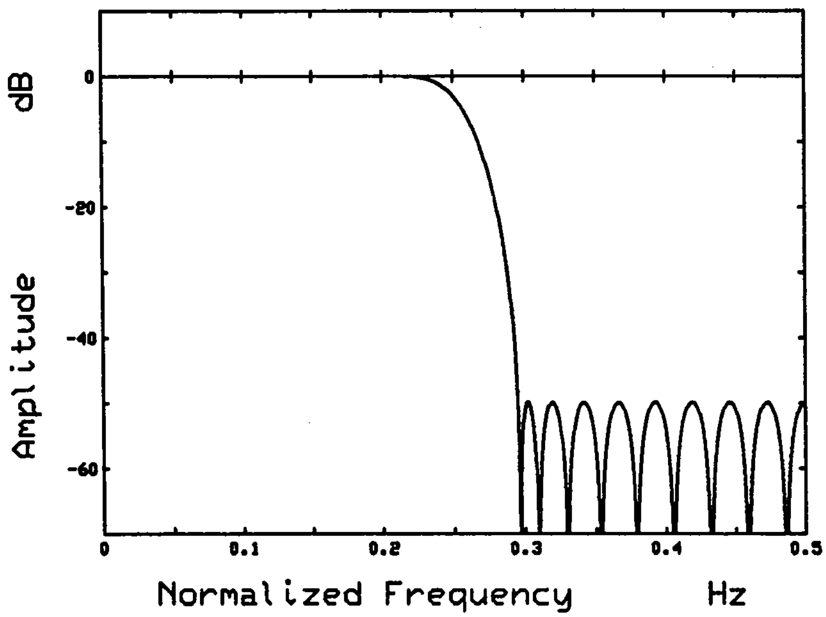

Fig. 5.c Lowpass filter response $H_0(\omega)$

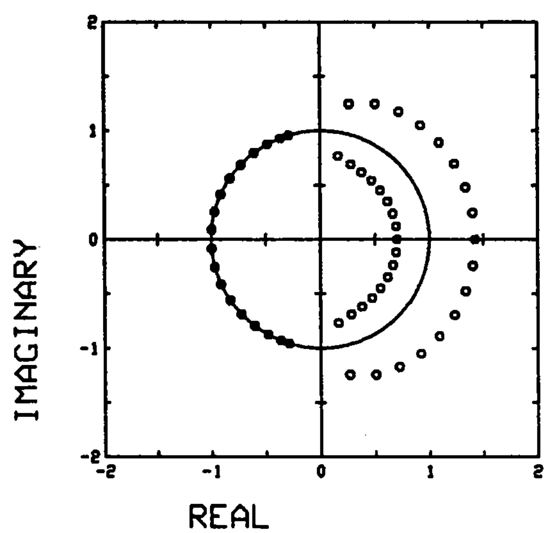

Fig. 5.d Location of zeros for $F_0(z)$

Filter Coefficients $h_0(n)$			
$h_0(0)$	$-2.4442594 \times 10^{-4}$	$h_0(18)$	$-1.8116239 \times 10^{-2}$
$h_0(1)$	9.7763551×10^{-4}	$h_0(19)$	3.8264161×10^{-2}
$h_0(2)$	$-1.3247344 \times 10^{-3}$	$h_0(20)$	2.2176880×10^{-2}
$h_0(3)$	$-1.8084289 \times 10^{-4}$	$h_0(21)$	$-5.1039602 \times 10^{-2}$
$h_0(4)$	2.1186199×10^{-3}	$h_0(22)$	$-2.8359718 \times 10^{-2}$
$h_0(5)$	$-4.5704954 \times 10^{-4}$	$h_0(23)$	6.6388087×10^{-2}
$h_0(6)$	$-3.5143911 \times 10^{-3}$	$h_0(24)$	3.9132345×10^{-2}
$h_0(7)$	1.8135055×10^{-3}	$h_0(25)$	$-8.4439800 \times 10^{-2}$
$h_0(8)$	5.3058083×10^{-3}	$h_0(26)$	$-5.9751918 \times 10^{-2}$
$h_0(9)$	$-4.1411899 \times 10^{-3}$	$h_0(27)$	1.0392658×10^{-1}
$h_0(10)$	$-7.4101387 \times 10^{-3}$	$h_0(28)$	1.0204371×10^{-1}
$h_0(11)$	7.6820769×10^{-3}	$h_0(29)$	$-1.1590637 \times 10^{-1}$
$h_0(12)$	9.7511367×10^{-3}	$h_0(30)$	$-1.9402676 \times 10^{-1}$
$h_0(13)$	$-1.2666428 \times 10^{-2}$	$h_0(31)$	6.7619589×10^{-2}
$h_0(14)$	$-1.2271208 \times 10^{-2}$	$h_0(32)$	3.8864864×10^{-1}
$h_0(15)$	1.9298215×10^{-2}	$h_0(33)$	4.3241451×10^{-1}
$h_0(16)$	1.4992901×10^{-2}	$h_0(34)$	2.3924112×10^{-1}
$h_0(17)$	$-2.7764358 \times 10^{-2}$	$h_0(35)$	5.9814475×10^{-2}

Example 6

Specifications: $N = 40$, $W_t = 0.16\pi$ $(\omega_c = 0.42\pi)$, $A_s = 49.3$ dB

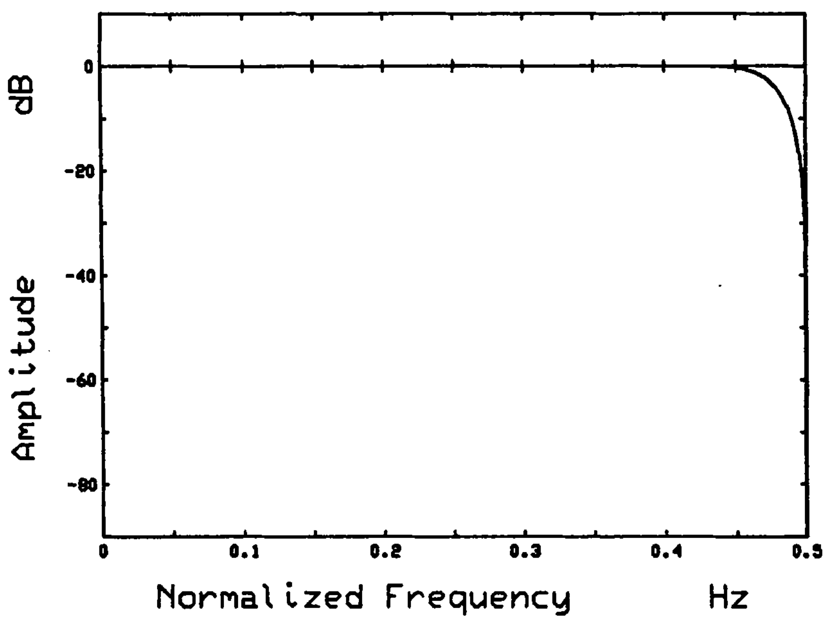

Fig. 6.a Transformation $U_1(\omega)$

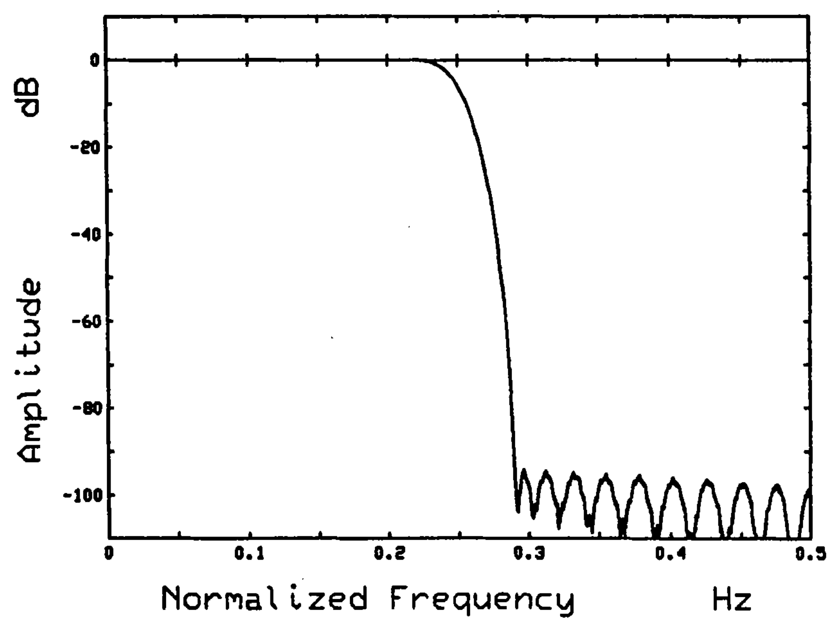

Fig. 6.b Cascade filter response $F_0(\omega)$

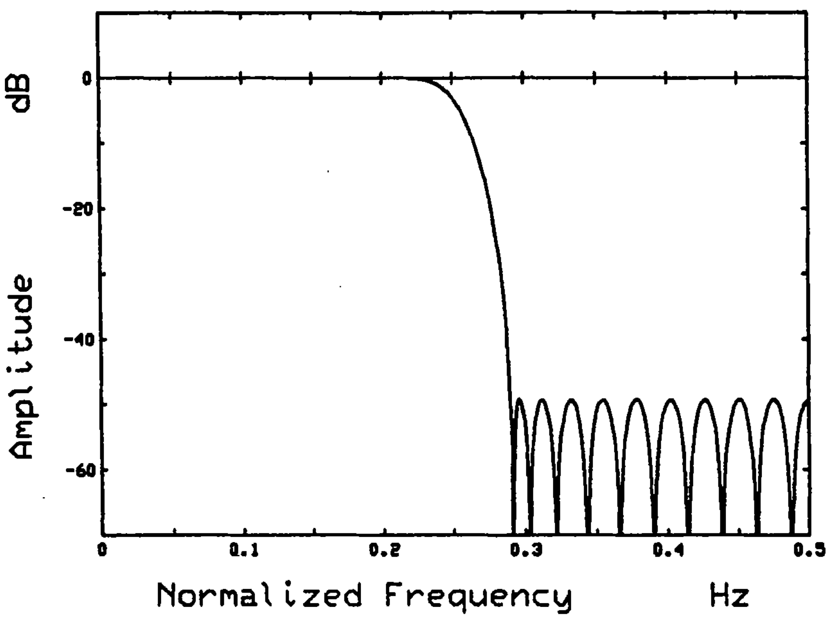

Fig. 6.c Lowpass filter response $H_0(\omega)$

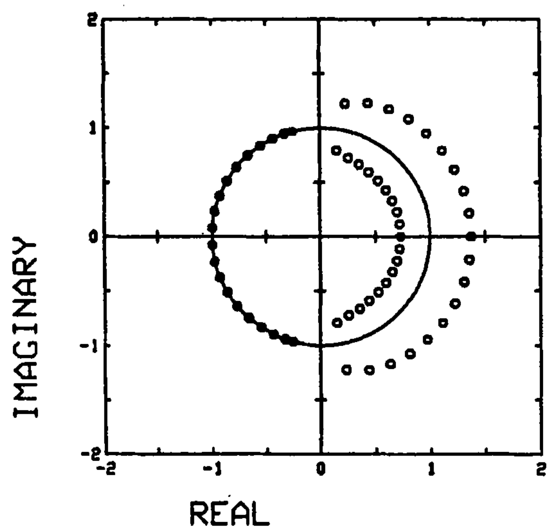

Fig. 6.d Location of zeros for $F_0(z)$

Filter Coefficients $h_0(n)$					
$h_0(0)$	$-2.3086526 \times 10^{-4}$	$h_0(14)$	$-7.2698213 \times 10^{-3}$	$h_0(28)$	2.8699825×10^{-2}
$h_0(1)$	9.1815069×10^{-4}	$h_0(15)$	1.4421455×10^{-2}	$h_0(29)$	$-9.3164397 \times 10^{-2}$
$h_0(2)$	$-1.2978541 \times 10^{-3}$	$h_0(16)$	8.3442479×10^{-3}	$h_0(30)$	$-4.8960860 \times 10^{-2}$
$h_0(3)$	5.9548996×10^{-5}	$h_0(17)$	$-2.0303947 \times 10^{-2}$	$h_0(31)$	1.1370748×10^{-1}
$h_0(4)$	1.7176449×10^{-3}	$h_0(18)$	$-9.3354935 \times 10^{-3}$	$h_0(32)$	9.2139292×10^{-2}
$h_0(5)$	$-6.4571793 \times 10^{-4}$	$h_0(19)$	2.7534293×10^{-2}	$h_0(33)$	$-1.2768251 \times 10^{-1}$
$h_0(6)$	$-2.6061193 \times 10^{-3}$	$h_0(20)$	1.0367244×10^{-2}	$h_0(34)$	$-1.8765785 \times 10^{-1}$
$h_0(7)$	1.7619275×10^{-3}	$h_0(21)$	$-3.6283557 \times 10^{-2}$	$h_0(35)$	8.1374077×10^{-2}
$h_0(8)$	3.6916335×10^{-3}	$h_0(22)$	$-1.1759273 \times 10^{-2}$	$h_0(36)$	3.9149793×10^{-1}
$h_0(9)$	$-3.5569607 \times 10^{-3}$	$h_0(23)$	4.6801248×10^{-2}	$h_0(37)$	4.2607965×10^{-1}
$h_0(10)$	$-4.8833349 \times 10^{-3}$	$h_0(24)$	1.4179933×10^{-2}	$h_0(38)$	2.3448949×10^{-1}
$h_0(11)$	6.1748615×10^{-3}	$h_0(25)$	$-5.9462474 \times 10^{-2}$	$h_0(39)$	5.8961397×10^{-2}
$h_0(12)$	6.1004341×10^{-3}	$h_0(26)$	$-1.8948330 \times 10^{-2}$		
$h_0(13)$	$-9.7532649 \times 10^{-3}$	$h_0(27)$	7.4774981×10^{-2}		

Example 7

Specifications: $N = 44$, $W_t = 0.12\pi$ $(\omega_c = 0.44\pi)$, $A_s = 41.2$ dB

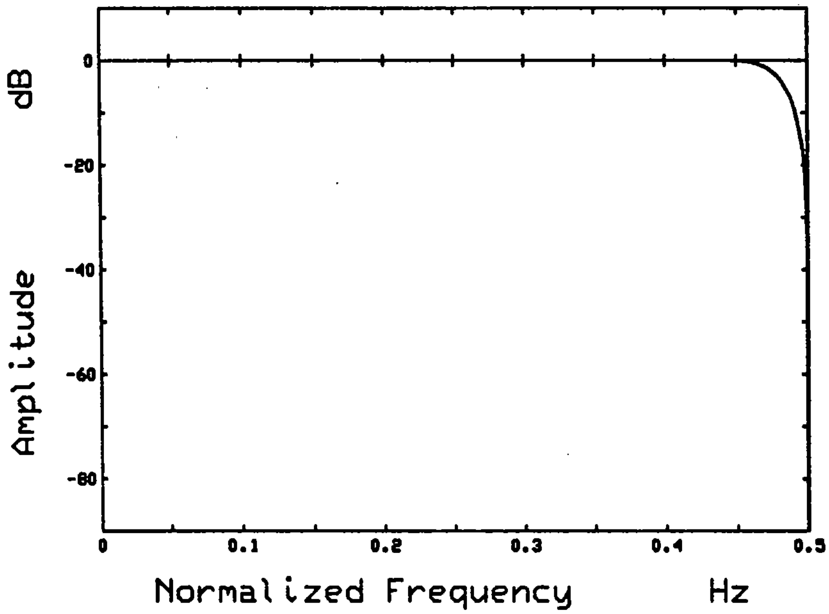

Fig. 7.a Transformation $U_1(\omega)$

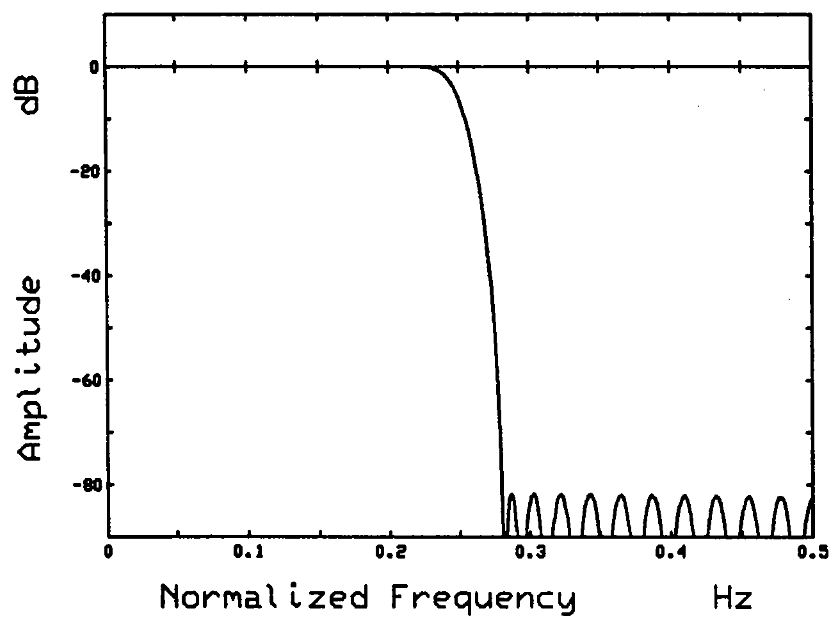

Fig. 7.b Cascade filter response $F_0(\omega)$

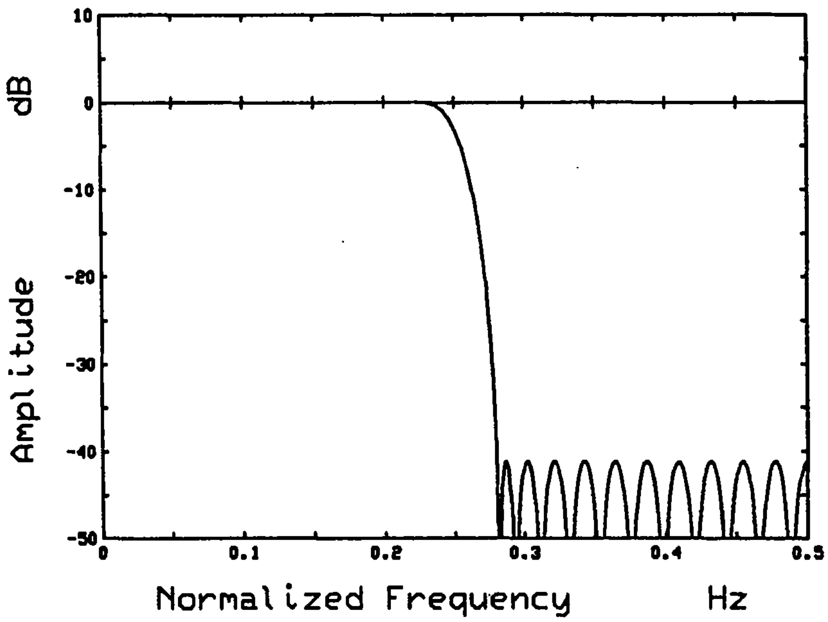

Fig. 7.c Lowpass filter response $H_0(\omega)$

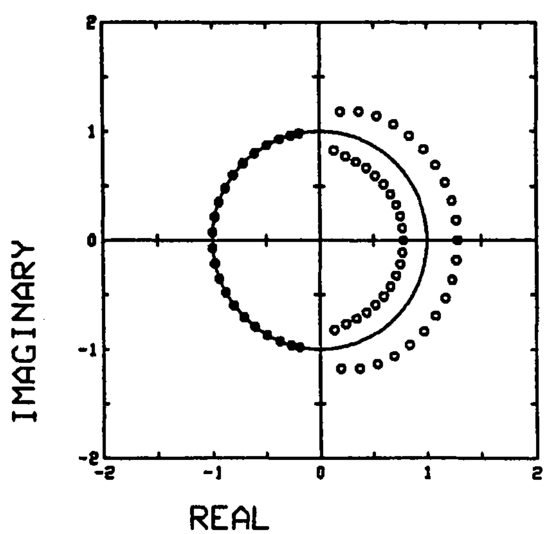

Fig. 7.d Location of zeros for $F_0(z)$

Filter Coefficients $h_0(n)$					
$h_0(0)$	$-6.1415490 \times 10^{-4}$	$h_0(15)$	1.0479063×10^{-2}	$h_0(30)$	$-3.4839403 \times 10^{-2}$
$h_0(1)$	2.1040762×10^{-3}	$h_0(16)$	9.5065421×10^{-3}	$h_0(31)$	6.5074827×10^{-2}
$h_0(2)$	$-2.6822930 \times 10^{-3}$	$h_0(17)$	$-1.4184692 \times 10^{-2}$	$h_0(32)$	4.8710973×10^{-2}
$h_0(3)$	3.1346121×10^{-4}	$h_0(18)$	$-1.1060999 \times 10^{-2}$	$h_0(33)$	$-7.6195154 \times 10^{-2}$
$h_0(4)$	2.5162461×10^{-3}	$h_0(19)$	1.8614777×10^{-2}	$h_0(34)$	$-7.2715456 \times 10^{-2}$
$h_0(5)$	$-8.5758610 \times 10^{-4}$	$h_0(20)$	1.2798494×10^{-2}	$h_0(35)$	8.5038791×10^{-2}
$h_0(6)$	$-3.2713846 \times 10^{-3}$	$h_0(21)$	$-2.3836883 \times 10^{-2}$	$h_0(36)$	1.1633678×10^{-1}
$h_0(7)$	1.7760460×10^{-3}	$h_0(22)$	$-1.4854553 \times 10^{-2}$	$h_0(37)$	$-7.9981688 \times 10^{-2}$
$h_0(8)$	4.2859913×10^{-3}	$h_0(23)$	2.9931175×10^{-2}	$h_0(38)$	$-1.9899331 \times 10^{-1}$
$h_0(9)$	$-3.1459878 \times 10^{-3}$	$h_0(24)$	1.7474414×10^{-2}	$h_0(39)$	8.7423516×10^{-3}
$h_0(10)$	$-5.4456808 \times 10^{-3}$	$h_0(25)$	$-3.6997181 \times 10^{-2}$	$h_0(40)$	3.4270108×10^{-1}
$h_0(11)$	5.0169386×10^{-3}	$h_0(26)$	$-2.1088175 \times 10^{-2}$	$h_0(41)$	4.4699708×10^{-1}
$h_0(12)$	6.7106990×10^{-3}	$h_0(27)$	4.5157811×10^{-2}	$h_0(42)$	2.8178366×10^{-1}
$h_0(13)$	$-7.4425047 \times 10^{-3}$	$h_0(28)$	2.6438249×10^{-2}	$h_0(43)$	8.2249303×10^{-2}
$h_0(14)$	$-8.0641521 \times 10^{-3}$	$h_0(29)$	$-5.4525372 \times 10^{-2}$		

Example 8

Specifications: $N = 48$, $W_t = 0.10\pi$ $(\omega_c = 0.45\pi)$, $A_s = 37.8$ dB

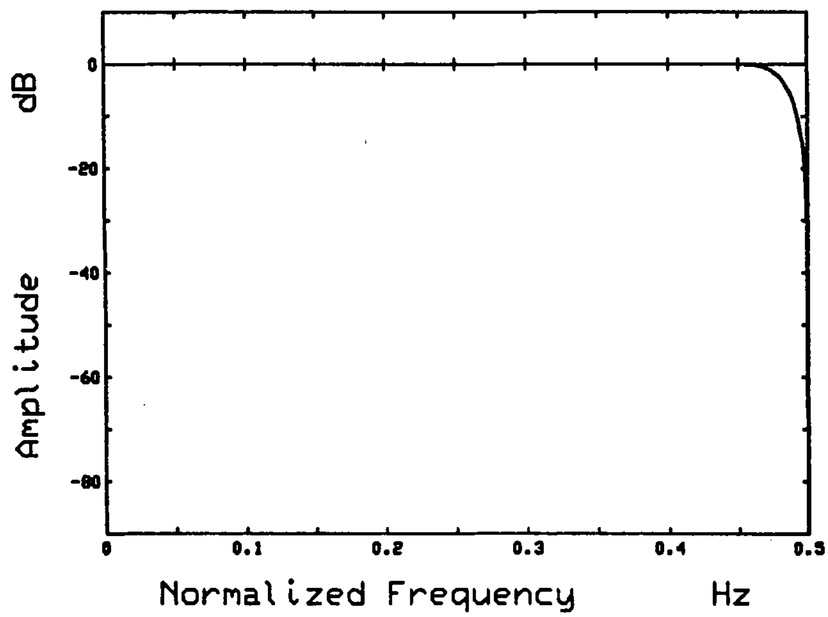

Fig. 8.a Transformation $U_1(\omega)$

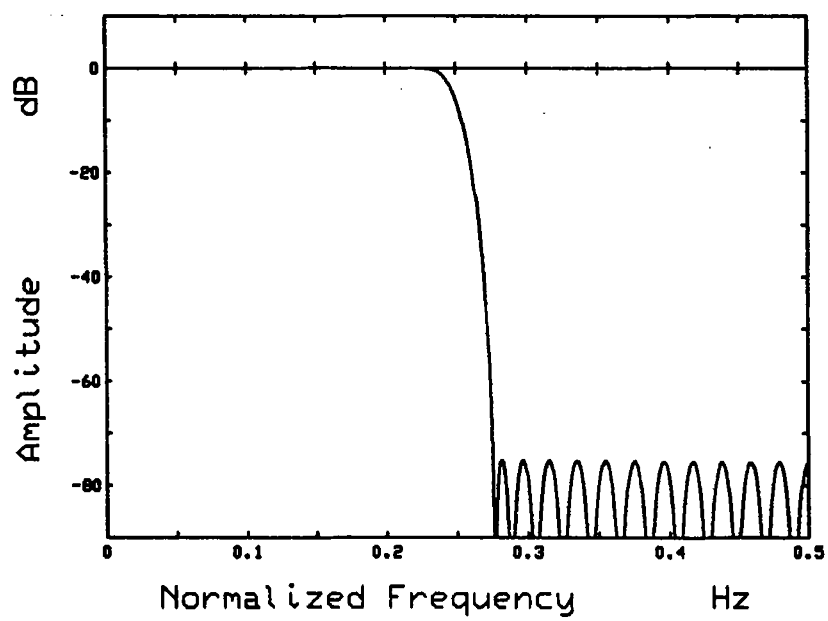

Fig. 8.b Cascade filter response $F_0(\omega)$

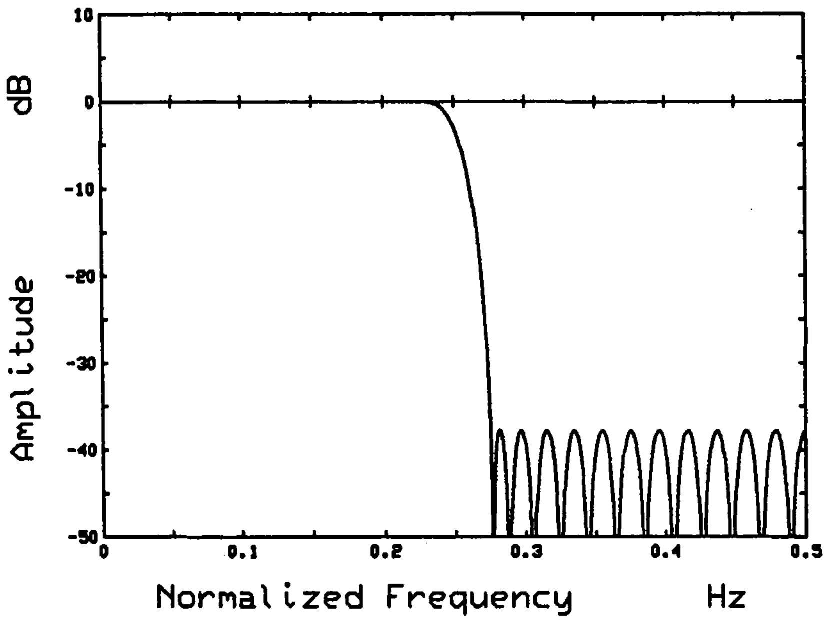

Fig. 8.c Lowpass filter response $H_0(\omega)$

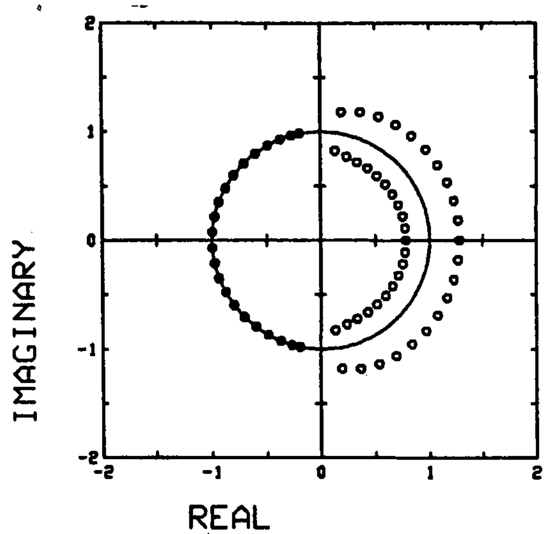

Fig. 8.d Location of zeros for $F_0(z)$

Filter Coefficients $h_0(n)$					
$h_0(0)$	$-9.3663795 \times 10^{-4}$	$h_0(16)$	8.3560298×10^{-3}	$h_0(32)$	3.0502315×10^{-2}
$h_0(1)$	2.9863652×10^{-3}	$h_0(17)$	$-1.0920380 \times 10^{-2}$	$h_0(33)$	$-5.2383247 \times 10^{-2}$
$h_0(2)$	$-3.6598413 \times 10^{-3}$	$h_0(18)$	$-9.6259657 \times 10^{-3}$	$h_0(34)$	$-3.9991417 \times 10^{-2}$
$h_0(3)$	6.1039758×10^{-4}	$h_0(19)$	1.4007157×10^{-2}	$h_0(35)$	6.0562867×10^{-2}
$h_0(4)$	2.8399023×10^{-3}	$h_0(20)$	1.1024600×10^{-2}	$h_0(36)$	5.4982452×10^{-2}
$h_0(5)$	$-1.0717413 \times 10^{-3}$	$h_0(21)$	$-1.7594401 \times 10^{-2}$	$h_0(37)$	$-6.8282004 \times 10^{-2}$
$h_0(6)$	$-3.3276526 \times 10^{-3}$	$h_0(22)$	$-1.2609239 \times 10^{-2}$	$h_0(38)$	$-7.9687104 \times 10^{-2}$
$h_0(7)$	1.8037720×10^{-3}	$h_0(23)$	2.1718589×10^{-2}	$h_0(39)$	7.2054100×10^{-2}
$h_0(8)$	4.1218737×10^{-3}	$h_0(24)$	1.4490403×10^{-2}	$h_0(40)$	1.2225877×10^{-1}
$h_0(9)$	$-2.8765154 \times 10^{-3}$	$h_0(25)$	$-2.6432564 \times 10^{-2}$	$h_0(41)$	$-5.9508945 \times 10^{-2}$
$h_0(10)$	$-5.0528302 \times 10^{-3}$	$h_0(26)$	$-1.6840173 \times 10^{-2}$	$h_0(42)$	$-1.9807374 \times 10^{-1}$
$h_0(11)$	4.3007350×10^{-3}	$h_0(27)$	3.1795770×10^{-2}	$h_0(43)$	$-1.9941113 \times 10^{-2}$
$h_0(12)$	6.0755710×10^{-3}	$h_0(28)$	1.9940336×10^{-2}	$h_0(44)$	3.1706219×10^{-1}
$h_0(13)$	$-6.0970426 \times 10^{-3}$	$h_0(29)$	$-3.7878976 \times 10^{-2}$	$h_0(45)$	4.5145224×10^{-1}
$h_0(14)$	$-7.1766387 \times 10^{-3}$	$h_0(30)$	$-2.4242959 \times 10^{-2}$	$h_0(46)$	3.0308776×10^{-1}
$h_0(15)$	8.2933598×10^{-3}	$h_0(31)$	4.4740744×10^{-2}	$h_0(47)$	9.5059871×10^{-2}

Example 9

Specifications: $N = 24$, $W_t = 0.24\pi$ $(\omega_c = 0.38\pi)$, $A_s = 45.5$ dB

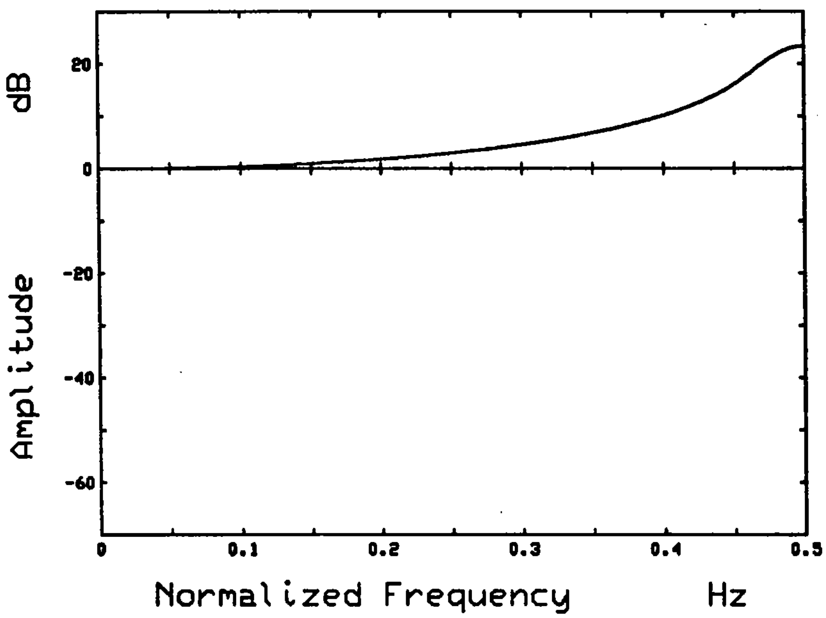

Fig. 9.a Transformation $U_2(\omega)$

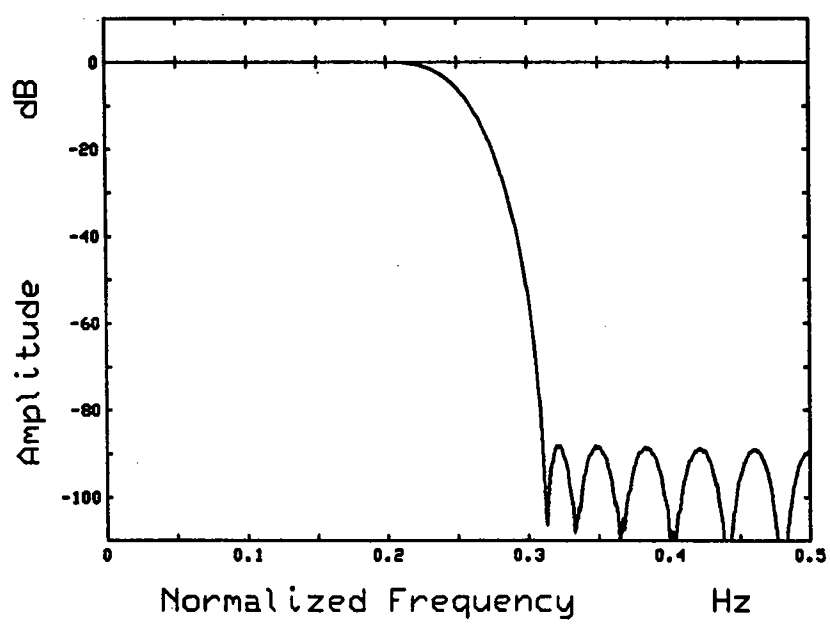

Fig. 9.b Cascade filter response $F_0(\omega)$

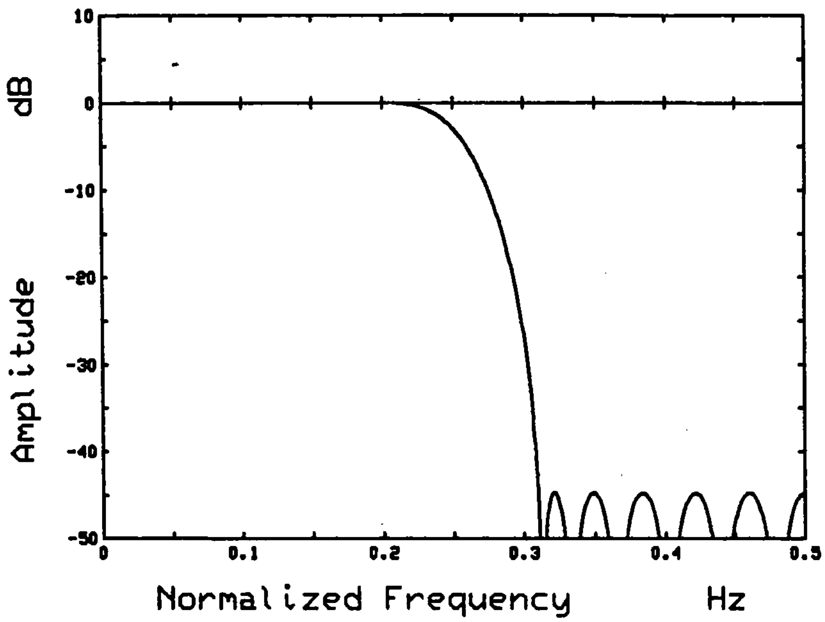

Fig. 9.c Lowpass filter response $H_0(\omega)$

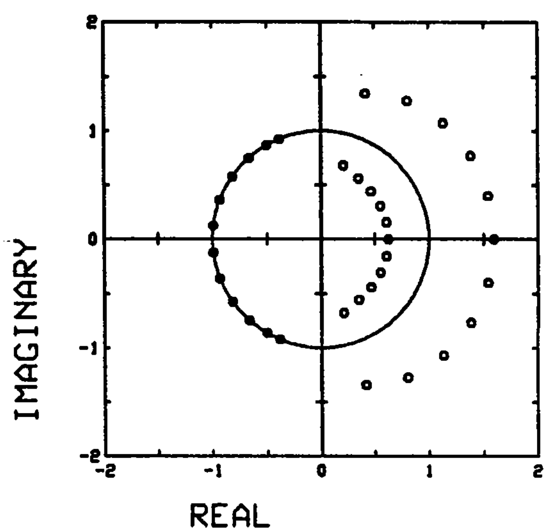

Fig. 9.d Location of zeros for $F_0(z)$

Filter Coefficients $h_0(n)$			
$h_0(0)$	$-7.9020460 \times 10^{-4}$	$h_0(12)$	5.9408557×10^{-2}
$h_0(1)$	2.8202763×10^{-3}	$h_0(13)$	$-1.0391766 \times 10^{-2}$
$h_0(2)$	$-2.6051287 \times 10^{-3}$	$h_0(14)$	$-8.7393443 \times 10^{-2}$
$h_0(3)$	$-3.3192672 \times 10^{-3}$	$h_0(15)$	1.4860508×10^{-2}
$h_0(4)$	6.6480095×10^{-3}	$h_0(16)$	1.2935981×10^{-1}
$h_0(5)$	3.9761381×10^{-3}	$h_0(17)$	$-6.1599145 \times 10^{-3}$
$h_0(6)$	$-1.3779881 \times 10^{-2}$	$h_0(18)$	$-1.9902807 \times 10^{-1}$
$h_0(7)$	$-3.3314504 \times 10^{-3}$	$h_0(19)$	$-6.2562463 \times 10^{-2}$
$h_0(8)$	2.4441894×10^{-2}	$h_0(20)$	3.1025604×10^{-1}
$h_0(9)$	7.2121970×10^{-4}	$h_0(21)$	4.7533920×10^{-1}
$h_0(10)$	$-3.9278350 \times 10^{-2}$	$h_0(22)$	3.0986651×10^{-1}
$h_0(11)$	4.1048378×10^{-3}	$h_0(23)$	8.6820366×10^{-2}

Example 10

Specifications: $N = 32$, $W_t = 0.20\pi$ $(\omega_c = 0.40\pi)$, $A_s > 47.3$ dB,

$$W(\omega) = 10(1 - \frac{\omega}{\omega_c}) + 1$$

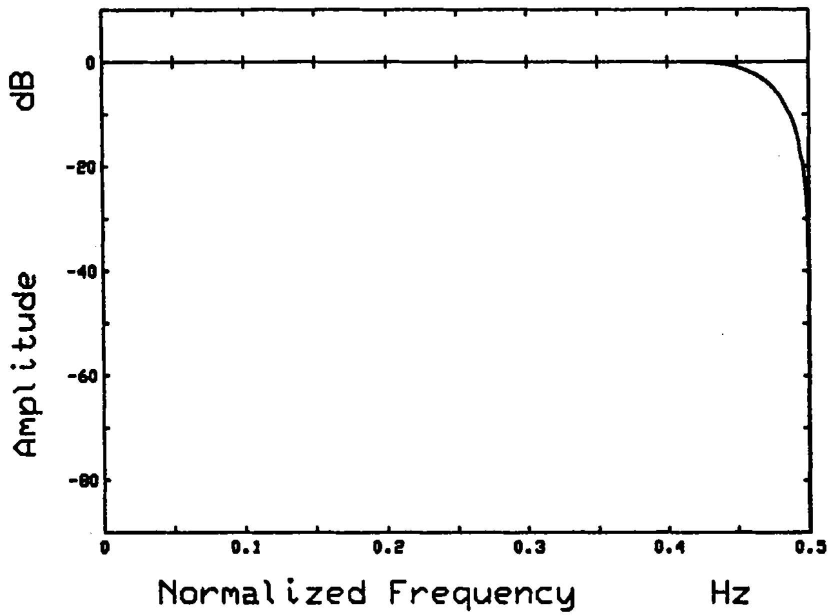

Fig. 10.a Transformation $U_1(\omega)$

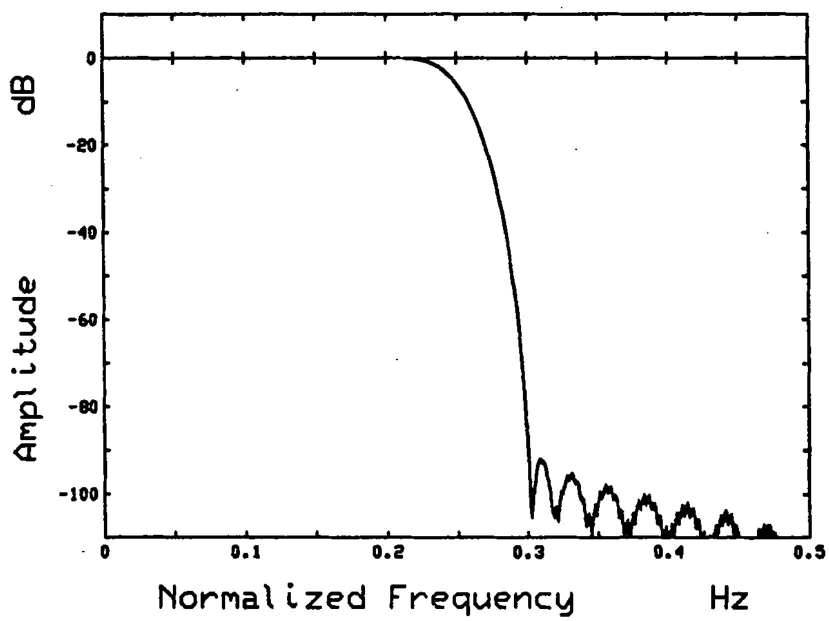

Fig. 10.b Cascade filter response $F_0(\omega)$

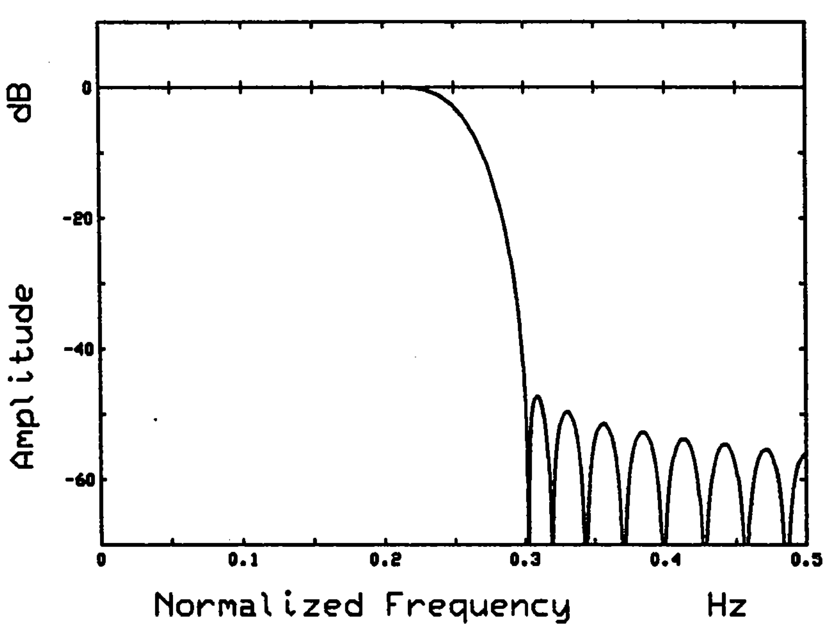

Fig. 10.c Lowpass filter response $H_0(\omega)$

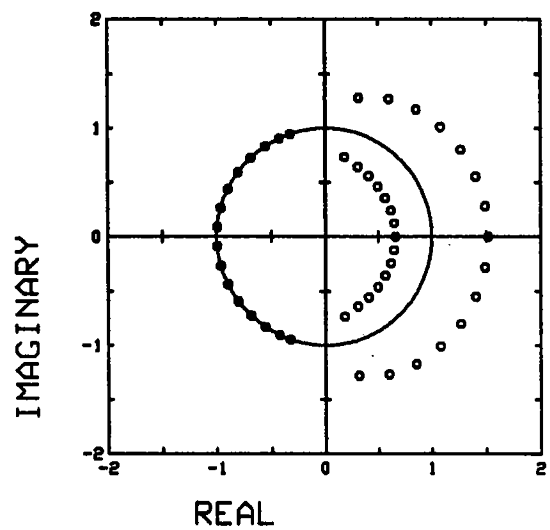

Fig. 10.d Location of zeros for $F_0(z)$

Filter Coefficients $h_0(n)$			
$h_0(0)$	$-1.9802146 \times 10^{-4}$	$h_0(16)$	2.5490951×10^{-2}
$h_0(1)$	8.3553734×10^{-4}	$h_0(17)$	$-4.0948277 \times 10^{-2}$
$h_0(2)$	$-1.0703507 \times 10^{-3}$	$h_0(18)$	$-3.2934935 \times 10^{-2}$
$h_0(3)$	$-6.2068184 \times 10^{-4}$	$h_0(19)$	5.6929716×10^{-2}
$h_0(4)$	2.5984128×10^{-3}	$h_0(20)$	4.4416378×10^{-2}
$h_0(5)$	$-1.9073494 \times 10^{-4}$	$h_0(21)$	$-7.6031651 \times 10^{-2}$
$h_0(6)$	$-4.7424695 \times 10^{-3}$	$h_0(22)$	$-6.4909314 \times 10^{-2}$
$h_0(7)$	1.9864790×10^{-3}	$h_0(23)$	9.7030488×10^{-2}
$h_0(8)$	7.6145262×10^{-3}	$h_0(24)$	1.0609029×10^{-1}
$h_0(9)$	$-5.2883471 \times 10^{-3}$	$h_0(25)$	$-1.1158435 \times 10^{-1}$
$h_0(10)$	$-1.1111137 \times 10^{-2}$	$h_0(26)$	$-1.9664023 \times 10^{-1}$
$h_0(11)$	1.0485538×10^{-2}	$h_0(27)$	6.8340757×10^{-2}
$h_0(12)$	1.5195449×10^{-2}	$h_0(28)$	3.9550438×10^{-1}
$h_0(13)$	$-1.7970346 \times 10^{-2}$	$h_0(29)$	4.3437744×10^{-1}
$h_0(14)$	$-1.9880649 \times 10^{-2}$	$h_0(30)$	2.3378359×10^{-1}
$h_0(15)$	2.8033857×10^{-2}	$h_0(31)$	5.5406466×10^{-2}

Example 11

Specifications: $N = 32$, $W_t = 0.20\pi$ ($\omega_c = 0.40\pi$), $A_s > 46.5$ dB,

$W(\omega) = 50(1 - \dfrac{\omega}{\omega_c}) + 1$

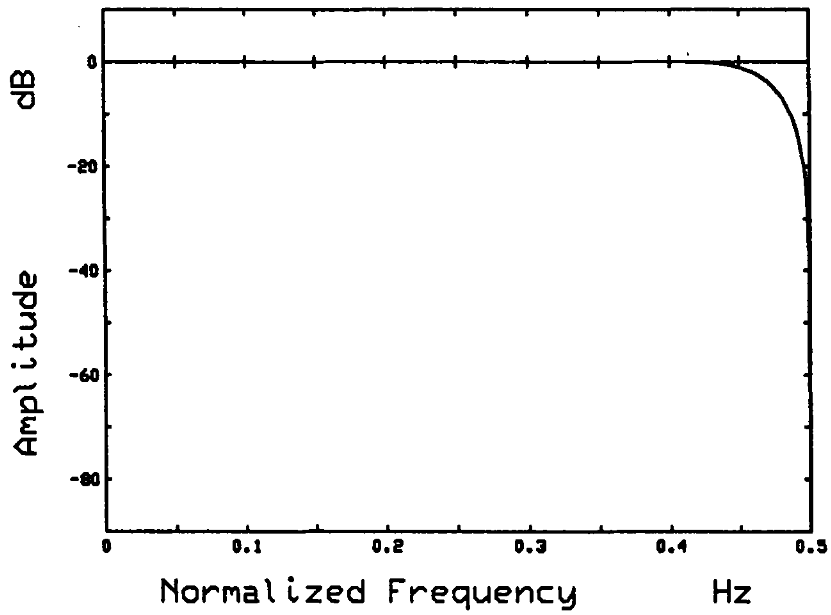

Fig. 11.a Transformation $U_1(\omega)$

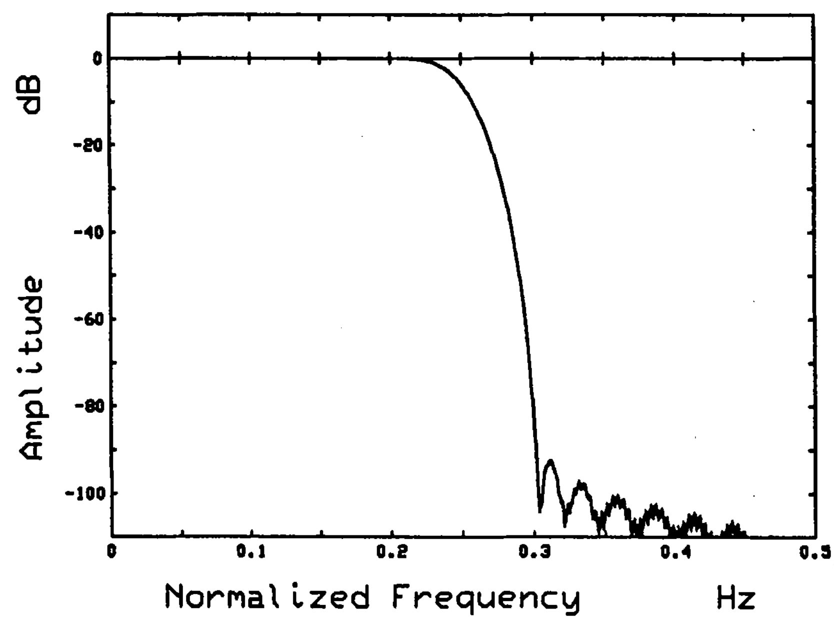

Fig. 11.b Cascade filter response $F_0(\omega)$

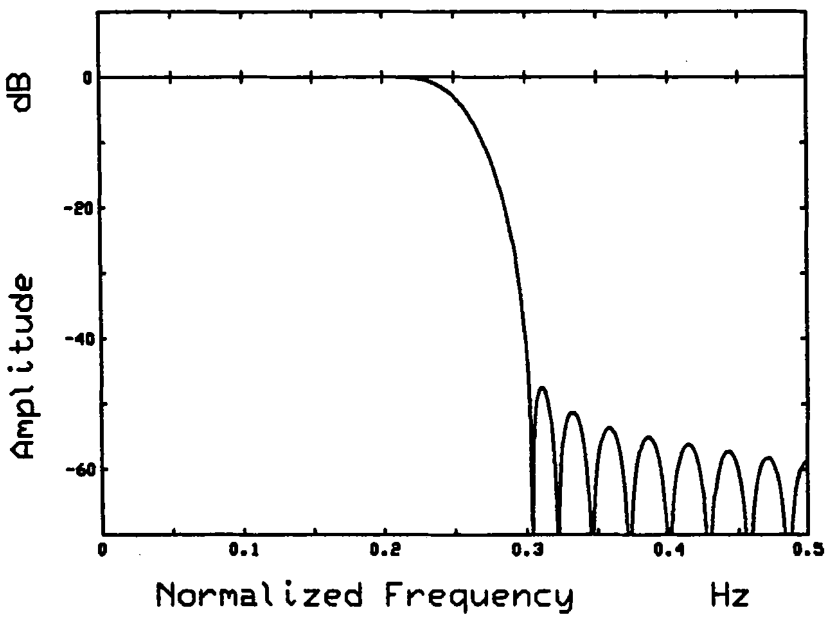

Fig. 11.c Lowpass filter response $H_0(\omega)$

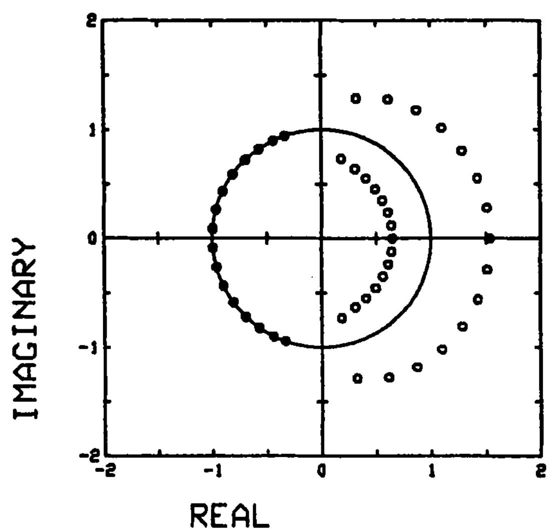

Fig. 11.d Location of zeros for $F_0(z)$

Filter Coefficients $h_0(n)$			
$h_0(0)$	$-1.5312975 \times 10^{-4}$	$h_0(16)$	2.2880311×10^{-2}
$h_0(1)$	6.6978350×10^{-4}	$h_0(17)$	$-4.2931926 \times 10^{-2}$
$h_0(2)$	$-8.8295739 \times 10^{-4}$	$h_0(18)$	$-2.9261366 \times 10^{-2}$
$h_0(3)$	$-5.4392343 \times 10^{-4}$	$h_0(19)$	5.9967310×10^{-2}
$h_0(4)$	2.3153856×10^{-3}	$h_0(20)$	3.9447068×10^{-2}
$h_0(5)$	$-2.3681951 \times 10^{-4}$	$h_0(21)$	$-8.0694261 \times 10^{-2}$
$h_0(6)$	$-4.3528162 \times 10^{-3}$	$h_0(22)$	$-5.8580119 \times 10^{-2}$
$h_0(7)$	2.0675369×10^{-3}	$h_0(23)$	1.0441966×10^{-1}
$h_0(8)$	7.0570086×10^{-3}	$h_0(24)$	9.8963318×10^{-2}
$h_0(9)$	$-5.4771776 \times 10^{-3}$	$h_0(25)$	$-1.2375410 \times 10^{-1}$
$h_0(10)$	$-1.0299011 \times 10^{-2}$	$h_0(26)$	$-1.9178752 \times 10^{-1}$
$h_0(11)$	1.0894241×10^{-2}	$h_0(27)$	8.7783152×10^{-2}
$h_0(12)$	1.3981563×10^{-2}	$h_0(28)$	4.0593320×10^{-1}
$h_0(13)$	$-1.8721858 \times 10^{-2}$	$h_0(29)$	4.2703872×10^{-1}
$h_0(14)$	$-1.8084960 \times 10^{-2}$	$h_0(30)$	2.2223798×10^{-1}
$h_0(15)$	2.9295748×10^{-2}	$h_0(31)$	5.0809297×10^{-2}

References

[1] R. E. Crochiere, S. A. Webber, and J. L. Flanagan, "Digital coding of speech in sub-bands," *Bell System Technical Journal*, vol. 55, pp. 1069–1085, October 1976.

[2] A. Papoulis, "Generalized sampling expansion," in *Signal Analysis*, McGraw–Hill Co. N. Y., 1977, pp. 193–196.

[3] P. Kabal, "Sub-sampling and interpolation," in *Appendix A*, *Technical Report No. 81-08*, INRS–Telecommunications , October 1981, pp. 60-82.

[4] R. E. Crochiere, "On the design of sub-band coders for low-bit rate speech communication," *Bell System Technical Journal*, vol. 56, pp. 747–770, May–June 1977.

[5] A. Croisier, D. Esteban, and C. Galand, "Perfect channel splitting by use of interpolation /decimation/tree decomposition techniques," presented at the Int. Conf. Inform. Sci. Syst., Patras,Greece, 1976.

[6] J. D. Johnston, "A filter family designed for use in quadrature mirror filter banks," in *Proceedings IEEE International Conference on Acoustics, Speech, and Signal Processing*, April 1980, pp. 291–294.

[7] V. K. Jain and R. E. Crochiere, "Quadrature mirror filter design in the time domain," *IEEE Transactions on Acoustics, Speech, and Signal Processing*, vol. ASSP-32, No. 2, pp. 353–361, April 1984.

[8] J. H. Rothweiler, "Polyphase quadrature filters—A new subband coding technique," in *Proceedings IEEE International Conference on Acoustics, Speech, and Signal Processing*, 1983, pp. 1280–1283.

[9] H. Nussbaumer, "Pseudo QMF filter bank," *IBM Technical Disclosure Bulletin*, vol. 24, No. 6, pp. 3081–3087, November 1981.

[10] H. Nussbaumer and M. Vetterli, "Computationally efficient QMF filter banks," in *Proceedings IEEE International Conference on Acoustics, Speech, and Signal Processing*, 1984, pp. 11.3.1–11.3.4.

[11] H. Nussbaumer and C. Galand, "Parallel filter banks using complex quadrature mirror filters (CQMF)," in *Signal Processing II: Theories and Applications*, Elsevier Science Publishers B. V. (North Holland), Eurasip, 1983, pp. 69–72.

[12] T. P. Barnwell, "Subband coder design incorporating recursive quadrature filters and optimum ADPCM coders," *IEEE Transactions on Acoustics,*

Speech, and Signal Processing, vol. ASSP-30, No. 5, pp. 751–765, October 1982.

[13] D. Esteban and C. Galand, "Application of quadrature mirror filters to split band voice coding schemes," in *Proceedings IEEE International Conference on Acoustics, Speech, and Signal Processing*, May 1977, pp. 191–195.

[14] J. T. Smith and T. P. Barnwell, "A procedure for designing exact reconstruction filter banks for tree structured subband coders," in *Proceedings IEEE International Conference on Acoustics, Speech, and Signal Processing*, March 1984, pp. 27.1.1–27.1.4.

[15] J. H. McClellan, T. W. Parks, and L. R. Rabiner, "A computer program for designing optimum FIR linear phase digital filters," *IEEE Trans. Audio Electroacoust.*, vol. AU-21, pp. 506–526, December 1973.

[16] A. V. Oppenheim and R. W. Schafer, *Digital Signal Processing*. Prentice–Hall Inc., Englewood Cliffs, N. J., 1975.

[17] R. Hooke and T. Jeaves, "Direct search solution of numerical and statistical problems," *J. Ass. Comp. Mach.*, vol. 8, pp. 212–229, April 1961.

[18] D. Esteban and C. Galand, "16 Kbps real time QMF sub-band coding implementation," in *Proceedings IEEE International Conference on Acoustics, Speech, and Signal Processing*, 1980, pp. 332–335.

[19] C. Galand and H. Nussbaumer, "New quadrature mirror filter structures," *IEEE Transactions on Acoustics, Speech, and Signal Processing*, vol. ASSP-32, No. 3, pp. 522–531, June 1984.

[20] L. Rabiner and B. Gold, *Theory and Application of Digital Signal Processing*. Prentice–Hall Inc., Englewood Cliffs, N. J., 1974.

[21] L. R. Rabiner, C. A. McGonegal and D. Paul, "FIR windowed filter design program— WINDOW," in *Programs for Digital Signal Processing*, Digital Signal Processing Committee IEEE Acoustics, Speech and Signal Processing Society, 1979, pp. 5.2-1–5.2-17.

[22] IMSL Inc., "Zeros and extrema," in *IMSL reference manual*, vol. 4, Chapter Z, IMSL Inc. Texas, 1982, pp. ZPOLR-1–ZPOLR-2.